X-751-70-428
PREPRINT

MILLIMETER-WAVE PROPAGATION EXPERIMENTS UTILIZING THE ATS-5 SATELLITE

PAPERS FROM THE FALL 1970 URSI MEETING COLUMBUS, OHIO

NOVEMBER 1970

GSFC
GODDARD SPACE FLIGHT CENTER
GREENBELT, MARYLAND

07

X-751-70-428

MILLIMETER-WAVE PROPAGATION EXPERIMENTS UTILIZING THE ATS-5 SATELLITE

Papers from the Fall 1970 URSI Meeting
Columbus, Ohio

compiled by
Louis J. Ippolito
NASA Goddard Space Flight Center
Greenbelt, Maryland

November 1970

Goddard Space Flight Center
Greenbelt, Maryland

MILLIMETER-WAVE PROPAGATION EXPERIMENTS UTILIZING THE ATS-5 SATELLITE

PREFACE

A special session at the 1970 U.S.A. Fall Meeting of the URSI (International Scientific Radio Union), held in Columbus, Ohio, was devoted to the Millimeter Wave Propagation Experiment associated with the Applications Technology Satellite (ATS-5).

Papers were presented by representatives of six of the participating stations and they provided the first data on propagation characteristics of earth-space links at frequencies above 15 GHz. The papers present a comprehensive survey of the 32 and 15 GHz transmissions to and from the ATS-5 satellite and the related radiometric, radar, and meteorological studies.

The results of these measurements by the various groups involved provided the first data on the transmission characteristics of a coherent source at these short wavelengths through the entire atmosphere and received simultaneously at sites widely separated geographically.

For these reasons, it is felt that the collection of these papers into a single volume is timely and significant.

A. W. Straiton
The University of Texas
Austin, Texas
(Session Chairman)

A. A. Ksienski
The Ohio State University
Columbus, Ohio
(Session Organizer)

ACKNOWLEDGMENTS

The cooperation and assistance of the contributing authors in the timely preparation of the papers presented in this document is greatefully appreciated.

Louis J. Ippolito
Principal Investigator
ATS-5 Millimeter Wave Experiment
NASA Goddard Space Flight Center
Greenbelt, Maryland

CONTENTS

NOTE: A brief description of the overall ATS-5 millimeter wave experiment configuration, ground network and spacecraft hardware is presented in Section 1 of the first paper.

PROPAGATION STATISTICS FOR 15 AND 32 GHz EARTH-SPACE TRANSMISSIONS FROM THE APPLICATIONS TECHNOLOGY SATELLITE (ATS-5)

Louis J. Ippolito
NASA/Goddard Space Flight Center
Greenbelt, Maryland

1. INTRODUCTION

The recent history of radio communication has been characterized by a continual extension to higher and higher frequency bands to support the increasing data handling requirements of an expanding technology.

The frequency bands between 10 and 300 GHz, commonly called "millimeter waves," offer a promising area for reducing the overcrowded situation in the lower bands. In addition to relieving spectrum crowding, millimeter wave systems offer extremely wide bandwidth capabilities, high gain-small aperture antenna characteristics, and reduced size and weight of components.

The first three "windows" in the electromagnetic spectrum above 10 GHz where water vapor and oxygen absorption are low occur at frequencies below 19 GHz, at 35 GHz, and at 94 GHz. It is in these bands that the greatest potential for earth-space applications exist, but propagation data is required by the systems designer before performance characteristics can be predicted and evaluated.

A Millimeter Wave Propagation Experiment was launched aboard the Applications Technology Satellite (ATS-5), on August 12, 1969, and is providing the first propagation measurements from an orbiting satellite in the Ku (12.5 to 18 GHz) and Ka (26.5 to 40 GHz) frequency bands. The prime objective of this experiment is to provide sufficient information on the propagation characteristics of the Earth's atmosphere so that this relatively unexplored and unused portion of the electromagnetic spectrum can be most effectively utilized for communications and data handling applications.

The ATS-5 Millimeter Wave Experiment is providing amplitude and phase measurements on two independent test links at 15.3 GHz (satellite-to-earth) and at 31.65 GHz (earth-to-satellite) during measured and defined meteorological conditions. Several stations in the continental U.S. and Canada have been operating with the satellite transmission since October 1969.

This paper will briefly describe the overall experiment configuration and present data results from the first 10 months of measurements made at the NASA/GSFC station, located at Rosman, North Carolina.

Results from other participating stations are reported in other papers of this Special Session and in the literature (Ref. 4, 5, 6, 7).

Experiment Configuration

The test signal for both the uplink and downlink consists of a carrier and two sidebands equally displaced on either side of the carrier. For the uplink, the sidebands can be set at one of the discrete values ±1.0, ±10 or ±50 MHz from the 31.65 GHz carrier. For the downlink, the sidebands can be set to ±0.1, ±1.0, ±10 or ±50 MHz from the 15.3 GHz carrier.

Downlink measurements of carrier amplitude, upper and lower sideband amplitude, and relative sideband phase are recorded at the participating sites on magnetic tape and paper charts. Uplink measurements are performed on-board the satellite and telemetered to an ATS tracking station (Rosman, N. C. or Mojave, Calif.) for reduction and processing.

NASA operationally supports five stations which provide a representative sample of the predominate weather profiles in the continental U.S. These stations are:

1. The NASA/GSFC Transportable Station located at Rosman, North Carolina, (receive and transmit capability).
2. The Naval Electronics Laboratory Center (NELC), La Posta, Calif. (receive capability).

3, 4. Ohio State University (OSU), Columbus, Ohio (two receive sites on variable base line for spatial diversity tests).

5. University of Texas, (U of T), Austin, Texas (receive capability).

In addition, a number of independent experimenters are participating in downlink measurements with the ATS-5 satellite. Table 1 lists all of the stations presently equipped to operate with the ATS-5 Millimeter Wave Experiment, in order of increasing elevation angle. A number of pairs of stations are available for diversity evaluation with baselines of 2 to 27 miles in length. The OSU mobile is designed for variable baseline measurements described in another paper in this session.

Figure 1 presents the basic components of the ATS-5 Millimeter Wave Propagation Experiment. The spacecraft hardware consists of the 31.65 GHz receiver-signal processor, the main 15.3 GHz transmitter, and a 15.3 GHz "back-up" CW transmitter, all interfacing with the ATS-5 Spacecraft telemetry and command subsystems.

The NASA Rosman MMW station has both a receive and transmit capability, the other participating stations operate with the 15.3 GHz downlink only. Satellite telemetry, tracking and command is accomplished from either of two NASA STADAN stations, located at Rosman, North Carolina and Mojave, California. Overall experiment management is provided by the Communications R&D Branch of Goddard's Communications and Navigation Division. Satellite and ground station interface is coordinated by the ATS Project Office through its Operations and Control Center (ATSOCC).

The Millimeter Wave Experiment flight package, built by Martin Marietta Corp., consists of four major systems; the primary 15.3 GHz transmitter, the backup 15.3 GHz transmitter (beacon), the 31.65 GHz receiver and the signal processor. The antennas for both the uplink and the downlink are linearly polarized conical horns with a full earth coverage field of view (20°, 3 db beamwidth, 19.1 db boresight gain). The horns are orthogonally aligned on the spacecraft to provide polarization isolation between the uplink and downlink.

Figure 2 shows the ATS-5 Millimeter Wave Experiment flight hardware package, which consists of the main transmitter, receiver, and signal processor. The backup transmitter is a separate package with its own antenna and is identical to the main transmitter except that it does not have a modulation capability. All of the antennas are located in the center portion of the spacecraft in the earth-viewing direction, as shown in Figure 3.

The 31.65 GHz receiver utilizes a balanced mixer front end with a 17 db maximum noise figure. Maximum received signal level (in CW) is -85 dbm and minimum sensitivity is -120 dbm.

The receiver phase locks on the carrier with an aided track and search circuit with a ±5 kHz minimum pull in range over a ±320 kHz band.

The carrier amplitude, upper and lower sideband amplitudes, relative sideband phases, and VCO error voltage are produced in the signal processor and relayed to earth through the ATS-5 telemetry systems.

Downlink transmitter power is 250 MW (unmodulated) and 70 MW per line (modulated), with a frequency stability of ±4 PPM per year. Thermal stability is ±3 PPM over the temperature range +4 to +38°.

The 30.6 GHz LO and the 15.3 GHz transmit carrier are both generated from a common solid-state source which starts with a 106.25 MHz crystal oscillator. The downlink modulation is accomplished at 5.1 GHz by a varactor phase modulator with the modulation index set to provide equal level carrier and first sidebands at the 15.3 GHz transmit frequency.

Detailed descriptions of the spacecraft hardware are given in references 2 and 3.

Satellite Spin Effects

The ATS-5 Spacecraft was designed for geosynchronous operation at 108° West Longitude, employing a gravity gradient 3-axis stabilization system. It was successfully launched from Cape Kennedy, Florida, on August 12, 1969 onboard an Atlas-Centaur launch vehicle. During the transfer orbit phase, however, an excessive amount of fuel was expended in maintaining stabilization. The satellite was then injected to synchronous velocity at the first apogee point, rather than the second, as originally planned. The injection maneuver caused the vehicle to end up in a flat spin over the Indian Ocean with the apogee motor still attached.

The satellite drifted slowly westward with the motor attached until late in September when an attempt was made to release the apogee motor and place the vehicle at its 108° West Longitude parking position. The motor was successfully released but the spacecraft ended up with a spin in the reverse direction from that required to despin it with a yo-yo despin mechanism. The spin rate (about 76 rpm) was considered too high to safely deploy the gravity gradient stabilization booms. The satellite is still in this spin condition. Techniques to stop the spin and deploy the booms are presently under study, but full gravity gradient stabilization appears unlikely. Present plans call for operation in the spin condition until July of 1971 before any attempts will be considered to modify the spacecraft's condition.

The significant effect of the satellite spin on the analysis of the propagation data is the elimination of a continuous record of amplitude and phase measurements. Signal variations which occur at rates greater than about 0.5 Hz are not detectable because of the spin-modulated data format. Long-term fading, fade rates, fade duration, probability densities and distributions are not effected by the spin-condition, and all of the planned computer-generated printouts are available for analysis.

Other special tests, such as site diversity measurements, radiometric and radar correlations, etc., are not impeded by the spin condition, except that

fluctuations of the satellite signals at rates greater than about 0.5 Hz cannot be detected, hence, detailed scintillation studies are not available.

Seven stations commenced downlink operations in late September 1969 and the uplink was first utilized in December 1969. Total operational hours for the ATS-5 Millimeter Wave Experiment through September 1, 1970 are: main transmitter, 1805 hours, back-up transmitter 304 hours, and uplink 127 hours.

Rosman Station Configuration

The NASA station, located near Rosman, North Carolina, utilizes a dual frequency feed system to permit simultaneous operation of both the uplink and the downlink with a 15 foot Cassegrain antenna system. The feed system consists of a fin (or pin) loaded aperture which allows independent beam shaping at the 15.3 and 31.65 GHz frequencies.

The antenna system includes a program-autotrack capability for continuous satellite tracking. The spin condition of the ATS-5 satellite prevents the utilization of the conical scan autotrack system, but program track has functioned adequately with updates generated from the satellite orbital parameters.

Figure 4 shows the Rosman station with the main 15 foot antenna system, equipment trailer, and radiometer and radar pedestals.

The Rosman station includes the following supporting meteorological measurements:

1. Integrated on-beam radar returns and RHI presentations.
2. Radiometer temperature, on-beam, at Ka and Ku-bands.
3. The outputs of 10 tipping rain buckets, placed under the beam.
4. Wind Speed
5. Wind Direction
6. Ambient Temperature
7. Dew Point Temperature
8. Atmospheric Pressure
9. Cloud Cover Photos
10. Weather Class

Figure 5 shows the NASA Rosman station block diagram for recording the propagation and meteorological data. All major data is recorded on the 14 channel magnetic tape and on strip charts for back-up. In addition a number of status functions are recorded on the tape to provide information for the data reduction program.

Following the recording process, data tapes are mailed on a weekly basis to the Goddard Space Flight Center for data reduction and processing. At this point the analog tape contents are digitized and re-recorded on digital magnetic tape.

The 15.3 GHz ground receiver is similar in design to the 31.65 GHz spacecraft receiver, but some improvements have been possible due to the lower RF frequency and because the ground system is not power and weight limited as is the spacecraft equipment.

A significant difference is the inclusion of an RF amplifier at 15.3 GHz resulting in a front end signal sideband noise figure of 7 db (max.). The RF amplifier is a single stage TDA employing a GaSb tunnel diode with a gain of 17 db and a 3 db bandwidth of 600 MHz. The temperature of the amplifier is stabilized at 65°C with a proportionally controlled heater. Some of the major receiver performance characteristics are listed below:

Frequency Stability: ±1 part in 10^8 per 0.1 sec (max.)
±3 PPM per year

PLL Search Range: ±300 kHz

Minimum Sensitivity (Hold-in Threshold): -145 dbm

Amplitude Measurement Range: 32 db

Absolute Amplitude Measurement Error: ±1 db max.

Phase Measurement Error: ±2.5° at maximum signal level.
1° per db down to 20 db below max. signal level.

A complete calibration and test set provides test signals to calibrate amplitude and phase in all modes of operation over the full range of expected levels.

The uplink transmitter for the ATS-5 Millimeter Wave Experiment, built by the Hughes Research Laboratories (HRL), consists of a 31.65 GHz klystron signal source, a varactor upconverter modulator, and a traveling wave tube (TWT) power amplifier system. The overall block diagram of the transmitter is shown in Figure 6. The 31.65 GHz frequency stabilized output of the klystron

is delivered to a varactor frequency upconverter which is capable of AM, FM, or PM modulation with bandwidths of hundreds of megahertz. The sideband programmer provides automatic or manual selection of 1 MHz, 10 MHz, or 50 MHz sidebands for the transmitted signal.

The stabilized klystron output is directed through a waveguide switch to either the modulation mode (path 2) or high power CW mode (path 1). In the modulation mode, the signal is fed through a ferrite circulator to the upconverter where the sideband modulation is produced. In the high power CW mode, the signal is fed through a variable attenuator directly to the output port to the power amplifier.

The TWT is a coupled cavity structure with a 450 MHz 3 db bandwidth. It has a saturated output power of over 1000 watts (CW) but is normally operated at 100 watts during clear weather conditions. The higher power capability provides an additional margin for CW propagation measurements through deep fades.

The measured fade margins available at 15.3 GHz are 15 db with the main transmitter, and 24 db with the back-up transmitter. The reduced margin with the main transmitter is due to a 9 db power degradation which occurred in February 1970. The signal has remained stable since then, and no further degradations have been observed. The full prelaunch power (250 MW) is available on the back-up transmitter for periods of up to 2 hours in duration. Both transmitters are available on call by the participating stations on a 24 hour per day, 7 day per week basis.

The measured uplink fade margin is 30 db with the transmitter in the CW mode.

2. PROPAGATION MEASUREMENTS

This section presents a summary of a number of high precipitation events recorded at Rosman with both the downlink and uplink. Later sections will cover attenuation statistics and compare measured attenuation with predictions from ground measured rainfall rate and sky temperature.

The time plots of 15.3 GHz downlink carrier attenuation, 16 GHz sky temperature, 15.6 GHz radar backscatter, and three rainfall rates are shown for five weather events in Figures 7 through 11.

The carrier attenuation is referenced to the measured clear weather level at the Rosman station (0 db). The values given are corrected to ±.5 db for transmitted power variations, daily spacecraft movement, and receiver calibration changes. Periods of manual antenna adjustment are shown on two of the plots by "connected arrows," and signal variations during these periods should be disregarded. The antenna system was in a program track mode during the other runs and manual adjustment was not required.

For day 92, two fades of 13.9 db and 10.3 db were observed, and the sky temperature tracked quite well. The radar peaked about 4 minutes before the first fade, and about 3 minutes before the second. (The jumps of backscatter level on the time plot during the first peak are gain step changes made to keep the signal level below 5 volts.) The rainfall rate, however, peaked two minutes after the first fade was observed and about two minutes before the second.

Day 142 consisted of a heavy thunderstorm combined with large hail and moderate winds. The attenuation level reached a maximum of 8.8 db at 2014 GMT and the hail did not noticeably affect the signal, even though it appeared to compromise about 50% of the precipitation during the peak period (2003 to 2009 GMT). The sky temperature again tracked well during the storm reaching a peak of 239°K at 2014 GMT. The radar was not operational.

On day 155 (Figure 9), a moderate rain occurred from 1400 to 1430 GMT which caused the sky temperature to increase but had little effect on the satellite attenuation. A heavy burst of rain commenced at about 1435 GMT, and the signal level dropped 11 db in four minutes until it dropped out at 15 db. The sky temperature also rose sharply and peaked at 260°K for about six minutes.

The back-up transmitter was energized at 144130 GMT, the antenna was peaked, and the signal measured 13 db attenuation at 14446 GMT. The signal level then began to increase and the attenuation was 5 db at 1449 GMT and 2 db at 1500 GMT.

A second period of rain occurred on day 155 (Figure 10) with a peak of 8 db attenuation at 1711 GMT.

The heaviest rain observed on the downlink occurred on day 156 (Figure 11). The signal dropped sharply at 1740 GMT and lock was lost at 174350 GMT. The sky temperature also rose sharply during this period and "peaked out" for about 3 minutes, from 1743 to 1746 GMT. Rain rates as high as 76.2 mm/hr were recorded on the rain gauges during the storms.

The radar backscatter did not show good correlation with measured attenuation or rainfall during any of the storm periods presented.

Time plots for two uplink periods are shown in Figures 12 and 13. On day 167 a peak attenuation of 18 db occurred at 31.65 GHz. The corresponding 15.3 GHz attenuation was 7.7 db, with rainfall rates as high as 75 mm/hr recorded on the ground.

The time plot for day 202 (Figure 13) shows a prolonged fade which lasted for 11 minutes with three peaks of 13 db, 12 db, and 14 db. Also shown on the figure is the difference, in db, between the carrier and the 50 MHz sideband amplitudes during the storm. The variations are within the total link measurement accuracy for the major portion of the run. A comparison of sideband difference for a number of periods with both attenuation and clear weather conditions indicates the same range of variations, hence the fluctuations do not appear to be a propagation effect.

The first peak of attenuation occurred with no rainfall recorded on the ground. The last two peaks of attenuation correspond to the two peaks observed on the ground and height averaged rainfall rates, which are discussed further in the next section.

3. ATTENUATION AND RAINFALL RATE

The rainfall rate, or rain intensity as monitored by ground located rain gauges is the most popular measurement available in propagation studies, in part because of the ease of making the measurement and also because of the extent of rain statistics available from weather bureau records. Good correlations of attenuation with rain gauge measurements have been demonstrated for terrestrial millimeter wave links (References 8, 9, 10, 11 among many others), but the extension to earth-satellite links has yet to be demonstrated.

The attenuation of millimeter wave energy due to rain is dependent on drop size distribution and rain intensity. Gunn and East (Reference 12) proposed the use of an empirical expression of the form

$$A = a R^b \qquad (1)$$

to relate the attenuation to the rainfall rate. A is the attenuation in db/km and R is the rainfall rate in mm/hr. The parameters a and b are frequency dependent constants.

A number of authors have developed values of the parameters a and b based on theoretical and experimental data at a number of frequencies. The initial values of a and b utilized on the ATS-5 Experiment were determined by comparing the results available in the literature and selecting representative values for the two frequencies of interest (Reference 3).

The resulting relations are:

$$A\left(\frac{db}{km}\right) = 0.035 R^{1.155} \quad @ \ 15.3 \ GHz \tag{2}$$

$$A\left(\frac{db}{km}\right) = 0.2 R^{1.0} \quad @ \ 31.65 \ GHz \tag{3}$$

The total path attenuations at 15.3 GHz and 31.65 GHz predicted from the above relations are plotted in Figures 14 and 15 for various path lengths, L. The 3.57 Km and 4.8 Km lengths correspond to the geometric ground and slant-path distances for the rain gauge network at Rosman.

The rain gauge network consists of 10 "tipping-bucket" gauges located on a ground line the azimuth direction of the ATS-5 satellite. Figure 16 shows the dimensions of the network.

The near rainfall rate, R_1 (0), is the rate as given by the nearest gauge, located directly in front of the antenna.

The ground average rainfall rate, $\bar{R}(0)$, is

$$\bar{R}(0) = \sum_{n=1}^{N} \frac{R_n(0)}{N} \tag{4}$$

where N is the number of buckets in valid operation at the time of measurement and $R_n(0)$ is the reading of the n'th bucket, in mm/hr.

The height average rainfall rate, $\bar{R}(h)$, is

$$\bar{R}(h) = \frac{1}{10} \sum_{n=1}^{10} \left(1 - \frac{h_n}{H}\right) R_n(0) \tag{5}$$

where h_n and H are defined in Figure 16.

The rainfall rates $R_n(0)$, in mm/hr, are determined by dividing the water accumulated per tip (0.254 mm) by the time (in hours) between adjacent tips. This results in rain rate values which increase in resolution as the rate increases, and gives essentially instantaneous readings for rates above 20 mm/hr.

A direct second by second or minute by minute comparison of measured attenuation with predicted attenuation would yield very little useful data, as seen from the time plots (Figures 7 through 13). Rain rate variations often do not occur in time coincidence with the attenuation increases.

A more meaningful approach is to compare distinct "peaks" of attenuation with corresponding peaks of rainfall rate which occur near the time of occurrence of the attenuation peak. For example, on day 92, the 13.9 db attenuation peak at 1201 GMT is compared with the 45 mm/hr peak for $R_1(0)$ at 1203 GMT, the 39 mm/hr peak for $\bar{R}(0)$ at 1204 GMT, and the 28 mm/hr peak for $\bar{R}(h)$ at 1204 GMT.

The results of peak 15.3 GHz attenuation and peak rainfall rate comparisons for eight storm occurrences are presented in Figure 17. The curves on each plot show the predicted attenuation for the given path length L.

The first interesting characteristic is the reduction in dispersion of the points when averaging techniques are employed. The reduction in dispersion is most pronounced for $\bar{R}(h)$. The best fit prediction curve for $\bar{R}(h)$ is for a slant path of 7.1 km, shown by the dotted line. The corresponding ground length for that slant path is 5.3 Km, shown by the dotted line in the $\bar{R}(0)$ plot. An accurate measurement of an actual "path length" for each storm is difficult, if not impossible to attain, since the definition of what constitutes a true path length is itself a subject for debate.

Similar results occur for 31.65 GHz peak attenuation plots, as shown in Figure 18. For the three storms presented, the prediction curve for $\bar{R}(h)$ with L = 4.8 km, the geometric path length, gives the best fit. The point dispersion is again significantly reduced by height averaging.

4. Attenuation and Sky Temperature

The prediction of millimeter wave earth-space attenuation from sky temperature measurements with a small aperture radiometer would be an extremely useful tool in evaluating potential ground station locations for reliability and diversity characteristics. The increased beamwidth resulting from the small aperture radiometer encloses a much larger volume of space than the satellite earth station antenna, however, and this may produce discrepancies between the

measured attenuation and that predicted from the sky temperature. The intent of the sky temperature measurements program at Rosman is to compare small aperture sky temperature with measured attenuation and evaluate the prediction characteristics over a large number of storm occurrences.

The radiometers are in use at Rosman, one at 16 GHz and the second at 35 GHz. Both employ Dicke type systems, with a mechanical modulator at 16 GHz and a ferrite modulator at 35 GHz. The operating characteristics of the radiometers are listed in Table 2. Both antennas are pointed in the satellite direction and have significantly large beamwidths than the 15 foot antenna system (0.3° @ 15.3 GHz).

The prediction of atmospheric attenuation from sky temperature measurements can be accomplished for the case of gaseous absorption with no scattering from the relation

$$T_s = \left(1 - \frac{1}{\alpha_T}\right) T_m \tag{6}$$

where

T_s = emission temperature of the sky, in °K

T_m = the mean absorption temperature of the atmosphere in °K

α_T = atmospheric attenuation factor.

The calculation of attenuation from the above relation is generally limited to clear sky or thin cloud conditions, since the assumptions in the derivation are not valid for appreciable condensed water absorption or scattering in the path.[13]

The mean absorption temperature of the path, T_m, is essentially independent of frequency and is related to the surface temperature, T_g, by

$$T_m = 1.12\, T_g - 50 \tag{7}$$

The atmospheric attenuation, in db, is expressed as

$$\alpha_T\,(db) = 10 \log_{10} T_m - 10 \log_{10} (T_m - T_s) \tag{8}$$

Figure 19 shows α_T (db) as a function of T_s for T_g = 0°, 10°, 20°, and 30°C.

Correlation diagrams of measured 15.3 GHz and 16 GHz sky temperature for the five storm events previously described in Section 2 are presented in Figures 20 through 24.

The prediction curves on each plot are computed with the average ambient temperature recorded during the storm period. Both attenuation and sky temperature values are based on 30 second averages. The frequency of occurrence of each point is not noted on the diagram, however, most points above 5 db correspond to a single sample, while those below 2 db consist of two or more samples.

In all cases the major portion of points occurs at or slightly above the prediction curve. On the two days with the highest attenuation (Figures 22 and 24), the correlation was very good throughout and appears better at the higher levels of attenuation.

Figures 22 and 23 show the variations in correlation within a storm itself. In both samples, which occured on the same day, the end portion of the run shows better correlation than the leading portion. This effect is most noticeable in Figure 23, where the measured values before 1711 GMT fall far short of the prediction curve.

The good correlation between directly measured and radiometric predicted attenuation is further demonstrated for long terms cumulative distributions, where small variations will tend to average out.

Figure 25 shows cumulative distributions of directly measured and predicted attenuation for all periods when both satellite and radiometric data was available and the rainfall rate exceeded 1 mm/hr, (a total of 15.65 hrs.).

The two curves are well within 1% of each other for attenuations of 8 db and higher, where the data is normally of interest for outage time predictions.

Sky temperature comparisons with the 35 GHz radiometer and the 31.65 GHz uplink are under investigation but were not available in time for this report.

5. Uplink and Downlink Comparisons

Comparisons of 15.3 GHz and 31.65 GHz attenuation characteristics simultaneously measured through the same precipitation indicates a wide range of attenuation ratios which vary with each storm, and within the storm itself.

Figures 26 through 29 show the uplink attenuation versus downlink attenuation for four storm events. In the first two examples the attenuation ratio remained fairly constant throughout each storm, at 2:5 to 1 for the first event, and 3.33 to 1 for the second. The last two examples show a wide dispersion of attenuation ratio during the storm. All runs were made during relatively continuous

rains with high variations of rain rate occurring for the first two where the ratio was relatively stable.

Variations in drop size distribution will cause a change in the attenuation ratio, and the prediction of attenuation at one frequency based on measurements at another is made difficult by the distribution variations during a storm. An estimate of the drop size distribution may be available, however, for those storms where the ratio remains fairly stable throughout.

Cumulative distributions of uplink and downlink attenuation for days 167, 202, and 231 are shown in Figures 30 through 32. Note that days 162 and 231, which had similar 15.3 GHz attenuation distributions, exhibited 31.65 GHz distributions which were quite different.

6. Attenuation Statistics

Cumulative distributions of attenuation for the 15.3 GHz downlink and 31.65 GHz uplink during periods when the rainfall rate exceeded 1 mm/hr are shown on Figures 33 and 34. The rainfall rate was determined from the near rain gauge at the Rosman station. The rainfall rate exceeded 1 mm/hr for 139.58 hours during the period 1 Oct. 1969 to 1 Oct. 1970. The cumulative distribution of attenuation at 15.3 GHz is based on data collected for 14% of the time that the rainfall exceeded 1 mm/hr over the yearly period, or a total of 19.55 hours. The cumulative distribution at 31.65 GHz is based on data collected for 2% of the time that the rainfall exceeded 1 mm/hr over the year, or a total of 2.62 hours.

Both frequencies typically show attenuations of less than 1 db during periods when the rainfall is less than 1 mm/hr, or during snow or heavy fog.

Since high correlation has been demonstrated between measured attenuation and attenuation predicted from sky temperature, the attenuation statistics from both sources can be combined to produce distributions for the entire rainfall period. Cumulative distributions of downlink and uplink attenuations for the periods when either satellite data or radiometric data was available and the rainfall rate exceeded 1 mm/hr are shown by the solid curves on Figures 35 and 36.

The downlink distribution is based on 19.55 hrs. of 15.3 GHz satellite data and 50.13 hrs of 16 GHz radiometric data, for a total of 69.86 hours. The uplink distribution is based on 2.62 hours of 31.65 GHz satellite data and 38.25 hours of 35 GHz radiometric data, for a total of 40.87 hours. The total periods of data correspond to 50% of the 139.58 hrs. of rainfall for the downlink and 29% of the uplink.

The dashed curves show the distributions which result if the data is extended to the full year rainfall period (139.58 hrs.), with the assumption that the distribution for the rainfall during the period with no measurements was the same as for the period when data was available. The validity of this assumption will be determined by an evaluation of the measured rainfall distributions for the periods of interest, however, this data was not available at the time of preparation of this report.

It should be noted here that the total rainfall measured for the period reported here (Oct. 1, 1969 through Sept. 30, 1970) was 20% below the average rainfall measured for the past 40 years at the ground station.

7. Summary

The 15.3 GHz downlink has been in operation at Rosman since October 1969. A total of 1050 hours of downlink carrier data has been recorded. The measurements typically show attenuations of 1 to 3 db in light rains or dense fog; 3 to 7 db in continuous rains (5 to 50 mm/hr), and a number of fades exceeding 12 db in heavy thunderstorms.

The maximum attenuation of 15 db was exceeded on four separate occasions for a total time of 16 minutes. Single rain gauge readings up to 76.2 mm/hr were recorded, with ground average rates in excess of 70 mm/hr and height averaged rates near 50 mm/hr. during these periods.

Limited sideband data obtained before transmitter power degradations showed no decorrelation effects in amplitude or relative sideband phase.

The 31.65 GHz uplink has been in operation for 147 hours since December 1969.

Sideband measurements at ±50, ±10, and ±1 MHz have shown relative amplitude variations within ±2 db over most periods but with no increase during precipitation events.

Correlation of measured attenuation with ground measured rainfall rate was low for a single gauge but improved significantly with height averaging of ten rain gauges with both uplink and downlink data.

In most instances the measured attenuation was slightly higher than that predicted from the averaged rainfall rates.

If these trends continue with future data, it appears that the utilization of ground measured rainfall rate data may be of some use in predicting earth-satellite path propagation when only long-term or gross effects are desired, such as in outage time predictions for a specific location.

The utilization of rainfall data to evaluate short term attenuation statistics, such as is required for diversity studies, appears quite limited.

It is apparent that more than one gauge is required, however, and that height averaging techniques must be employed to reduce the errors introduced by the increasing distance between the earth-satellite path and the measuring device on the ground.

Correlation of measured attenuation with sky temperature recorded on a small aperture radiometer was very good for most storms. Valid predictions of attenuation from 16 GHz sky temperature measurements were observed for up to 15 db of measured attenuation.

The uplink to downlink attenuation ratio varied with each precipitation event and often varied during a single storm period. The ratio has ranged from 2:1 to 4:1 during heavy precipitation periods.

Correlation of measured attenuation with 15.6 GHz backscatter from a small aperture weather radar has been low, with the response varying with each storm. Repeatable trends are not apparent in the results, as evidenced by the time plots of the storms (Figures 7 through 11). A number of factors will contribute to the lack of point-by-point radars backscatter correlation with signal attenuation. The most significant are: (a) the attenuation experienced at this wavelength limits the penetration capability of the radar signal, (b) the increased beamwidth of the small aperture radar system will enclose a larger storm volume than the satellite antenna beam, and (c) the radar signal is more sensitive to drop size variations, especially at the higher rain intensities.

Radar measurements at longer wavelengths with smaller beamwidths would be expected to exhibit better correlation with attenuation measurements, and this has been demonstrated with ATS-5 data at another station location, as reported in the second paper of this Special Session.

Present plans call for ATS-5 operations through June of 1971. A complete evaluation of the propagation statistics in the two frequency bands under investigation must await the reduction and analysis of the complete weather profile data of all participating stations. From the data reduced to date, however, it appears that both frequency bands exhibit an excellent potential for eventual utilization in reliable high data rate earth-space communications systems.

REFERENCES

1. The ATS-E Millimeter Wave Propagation Experiment, Binkley, Ippolito, King, and Ratliff, April 1968, NASA/GSFC Report X-733-68-196.

2. ATS-V Millimeter Wave Experiment Data Report, October-December 1969, Louis J. Ippolito, March 20, 1970, NASA/GSFC Report X-733-70-123.

3. Millimeter Wave Propagation Measurements from the Applications Technology Satellite (ATS-V), Louis J. Ippolito, IEEE Trans. on Antennas and Propagation, July 1970.

4. Amplitude Variations of 15 GHz Radio Waves Transmitted Through Clear Air and Through Rain, A. W. Straiton, C. R. Bailey, and W. Vogel, Radio Science, Volume 5, Number 3, pages 551-557, March 1970.

5. Comparison of 15 GHz Propagation Data from the ATS-V Satellite with Ground Based Radio and Meteorological Data, A. W. Straiton and B. M. Fannin, University of Texas, Austin, Texas, for presentation to the NATO-AGARD Electromagnetic Wave Propagation Panel, September 1970, Dusseldorf, Federal Republic of Germany.

6. First Result from 15.3 GHz Earth-Space Propagation Study, A. A. Penzias, The Bell System Technical Journal, July-August 1970.

7. Propagation Experiment above 10 GHz for Application to Communications Satellite System, A. Biuge, J. Levatich, and E. Robertson, COMSAT Laboratories, Clarksburg, Maryland, presented at the AIAA 3rd Communications Satellite Conference, April 8, 1970, Los Angeles, California.

8. B. C. Blevis, R. M. Dohoo, and K. C. McCormick, "Measurements of Rainfall Attenuation at 8 and 15 GHz," IEEE Trans. Antennas Propagation Vol. AP-15, pp 394-403, May 1967.

9. R. G. Medhurst, "Rainfall Attenuation of Centimeter Waves: Comparison of Theory and Measurement," IEEE Trans. Antennas Propagation, Vol. AP-13, pp 550-564, July 1965.

10. C. W. Tolbert, A. W. Straiton, and C. O. Britt, "Propagation Studies Between 18.0 and 25.5 kmcs." Elec. Engrg, Res. Lab., University of Texas, Austin, Rept. 110, July 1959.

11. K. Funakawa, T. Kido, K. Kitamura, Y. Otsu, T. Katto, and M. Uratsuka, "Propagational Experiments of 13 GHz and 35 GHz over the 80 kM Path," J. Radio Res. Lab. Jap., Vol. 14, pp 249-265, November 1967.

12. K. L. S. Gunn and T. W. R. East, "The Microwave Properties of Precipitation Particles," J. Royal Meteorol. Sec., Vol. 80, pp 522-555, 1954.

13. K. N. Wulfsberg, "Apparent Sky Temperatures at Millimeter Wave Frequencies," Phys. Sci. Res. Papers, AFCRL, July 1964.

Table 1
ATS-V Millimeter Wave Experiment Participating Stations

STATION		LATITUDE (NORTH)	LONGITUDE (WEST)	NOMINAL ELEVATION ANGLE	ANTENNA SIZE	RECEIVER TYPE
AIR FORCE CAMBRIDGE RESEARCH LABS, BEDFORD, MASS.		42°23'	71°15'	30°	28 FT.	MCW
DEPT. OF TRANSPORTATION, CAMBRIDGE, MASS.		42°36'	71°29'	30°	10 FT. (2)	SB
COMMUNICATIONS RESEARCH CENTRE, OTTAWA, CANADA	PRIME SITE	45°21'	75°54'	30°	30 FT.	SB
	SECOND SITE				8 FT.	MCW
ROME AIR DEV. CENTER, ROME, N.Y.		43°08'	75°37'	32°	15 FT.	SB
BELL TELEPHONE LABORATORIES, HOLMDEL, N.J.		40°23'	74°11'	34°	20 FT.	CW
U.S.A.S.C.A., LAKEHURST, N.J.		40°00'	74°25'	34°	30 FT.	MSB
COMMUNICATIONS SATELLITE CORP., CLARKSBURG, MD.		39°12'	77°16'	36°	15 FT.	SB
GODDARD SPACE FLIGHT CENTER, GREENBELT, MD.	RECEIVE SITE	39°42'	76°48'	36°	15 FT.	MCW
	TRANSMIT SITE*				10 FT.	-
NAVAL RESEARCH LABORATORIES, WALDORF, MD.				36°	60 FT.	MCW
OHIO STATE UNIVERSITY, COLUMBUS, OHIO	FIXED SITE	40°00'	83°02'	39°	30 FT.	MSB▲
	MOBILE SITE				15 FT.	MSB▲
GODDARD TRANSPORTABLE STATION, ROSMAN, N.C.*		35°12'	82°53'	42°	15 FT.	MSB▲
ESSA WAVE PROP. LAB., BOULDER, COLO.		40°00'	105°16'	44°	10 FT.	MCW
WESTINGHOUSE GEORESEARCH, BOULDER, COLO.		40°00'	105°09'	44°	12 FT.	MCW
MARTIN MARIETTA CORP., ORLANDO, FLA.		28°26'	81°26'	48°	12 FT.	MSB
NAVAL ELECTRONICS LABORATORY CENTER, SAN DIEGO, CAL.		32°40'	116°26'	50°	60 FT.	MSB▲
UNIVERSITY OF TEXAS, AUSTIN, TEX.		30°23'	97°43'	54°	10 FT. (2)	MSB▲

* - TRANSMIT STATION
▲-NASA/GSFC PARTICIPATING STATION
MSB -MARTIN SIDEBAND RECEIVER
MCW-MARTIN CW ONLY RECEIVER
SB -SIDEBAND RECEIVER
CW - CW ONLY RECEIVER

Table 2
Operating Characteristics for ATS-V Radiometers

Characteristic	16 GHz Radiometer	35 GHz Radiometer
Antenna	TRG Lens Ant.	TRG Lens Ant.
Diameter	12 inch	12 inch
Gain	32 dB	39 dB
Matching (VSWR)	<1.01	<1.01
Antenna efficiency	~0.8	~0.8
Beam width	4.0°	2.0°
RF Amp.	T.D.A. 15 dB (NF7dB)	Not used.
IF Amp.		
Bandwidth	80 MHz	2.0 GHz
Noise Figure	6 dB	12 dB
Local Oscillators	Klystron (Varian)	Klystron (Varian)
Modulator	Mechanical	Ferrite Switching
Mod. Freq.	94 100 Hz	94 100 Hz
Recorder		
{Amp.	Lock-in Amp	Lock-in Amp
{Out	0 - 5V	0 - 5V
Sensitivity $\left(= K \frac{T_{sys}}{\sqrt{B t}}\right)$ (t = 1 sec · k = 2	0.22°K	0.45°K
Ambient temp. of radiometer (RF, IF)	40°C ± 1°C	40°C ± 1°C
Hot load	318°K (45°C)	318°K (45°C)
Cold load	Liquid Nitrogen (77°K), dry ice (198°K) or ice cubes (273°K)	

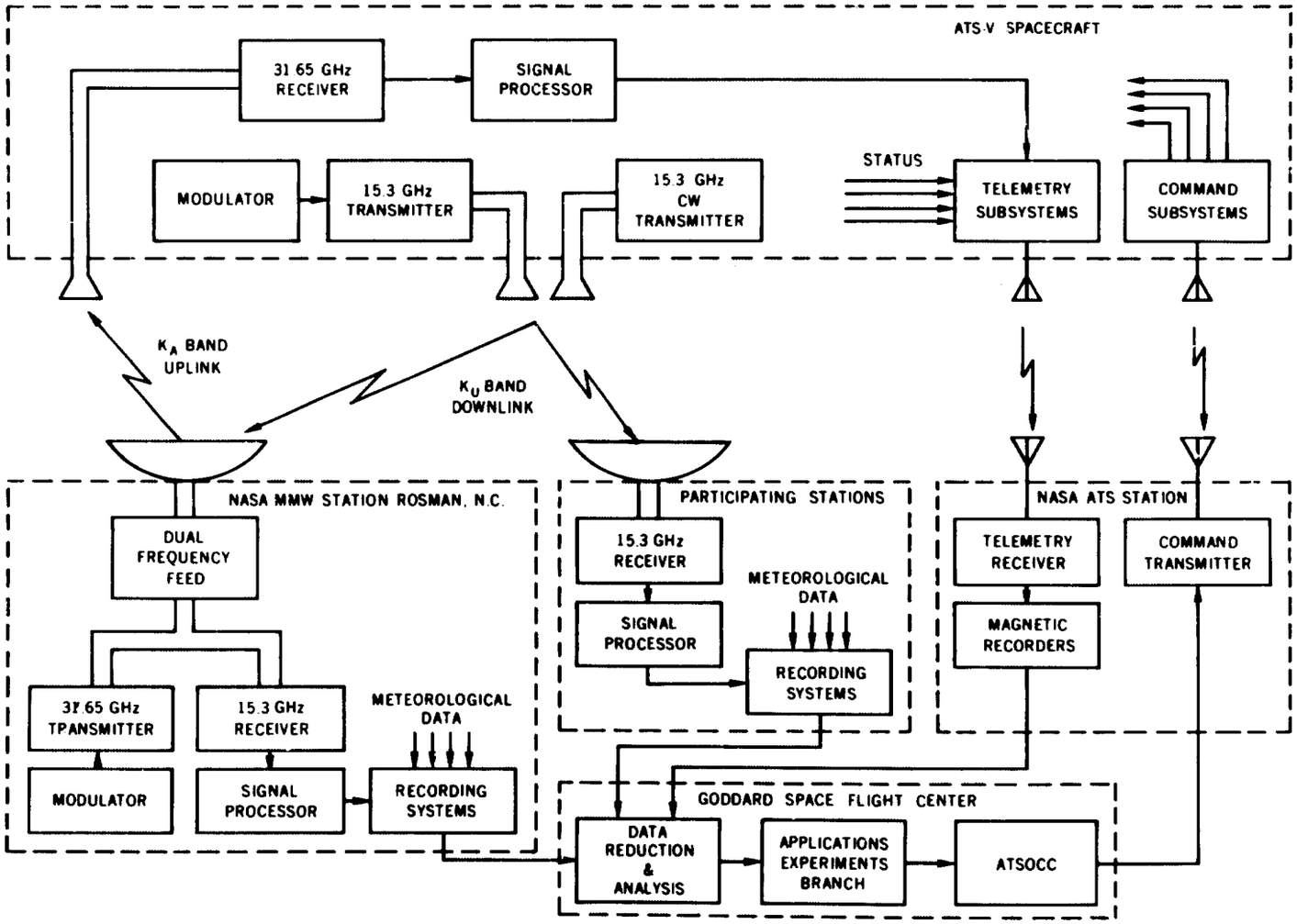

Figure 1. The ATS-V Millimeter Wave Propagation Experiment

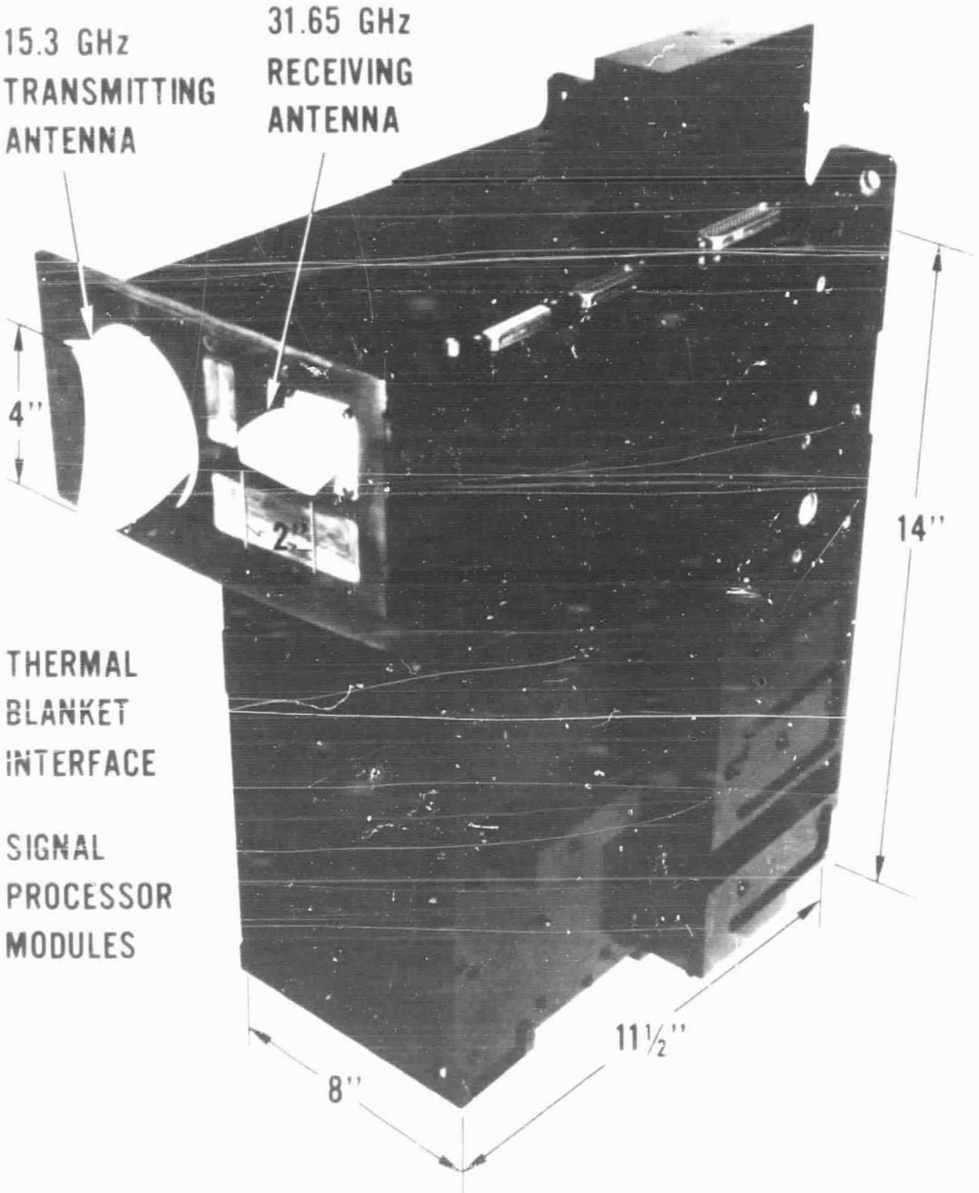

Figure 2. ATS-V Millimeter Wave Experiment Primary Flight Package

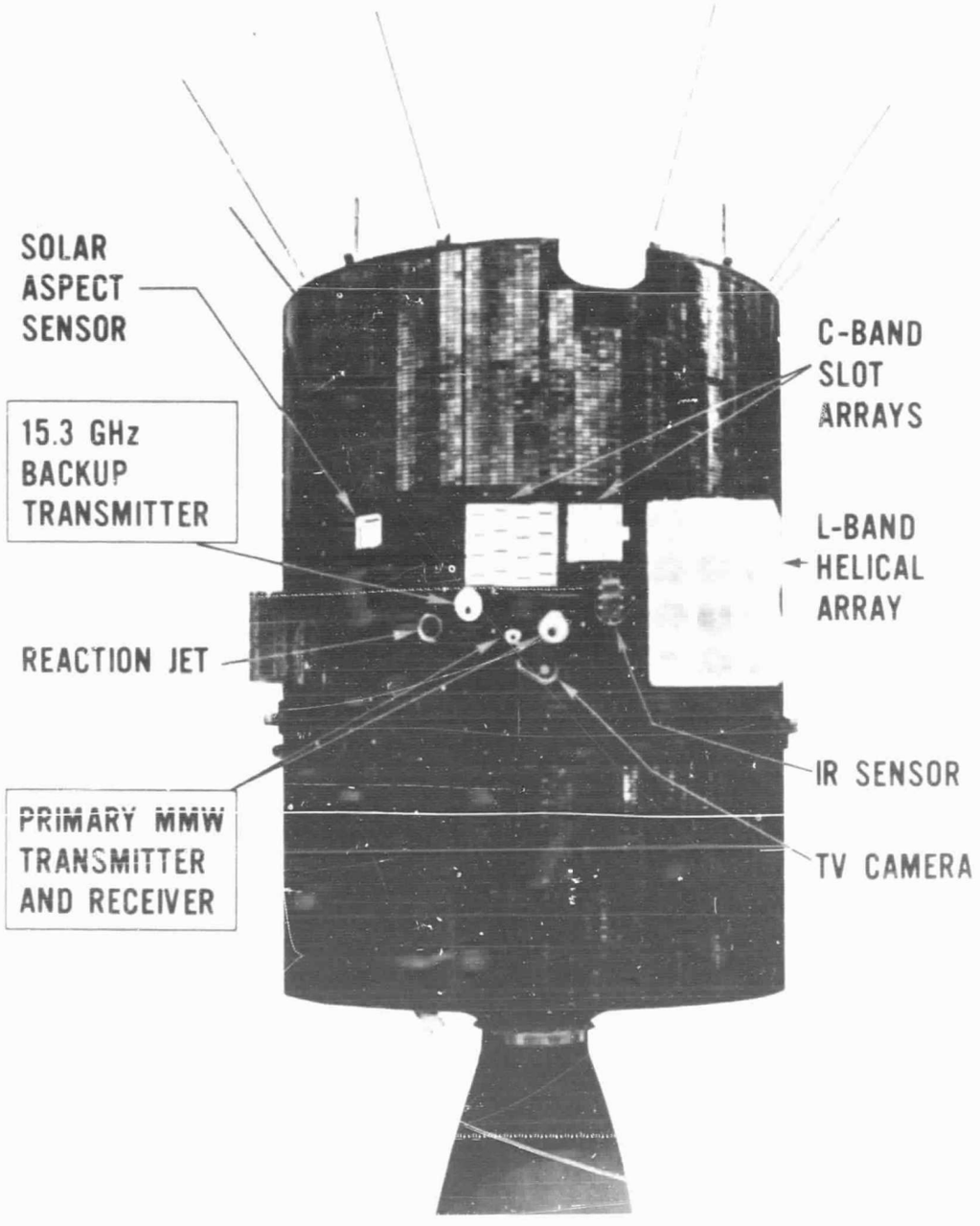

Figure 3. ATS-V Spacecraft

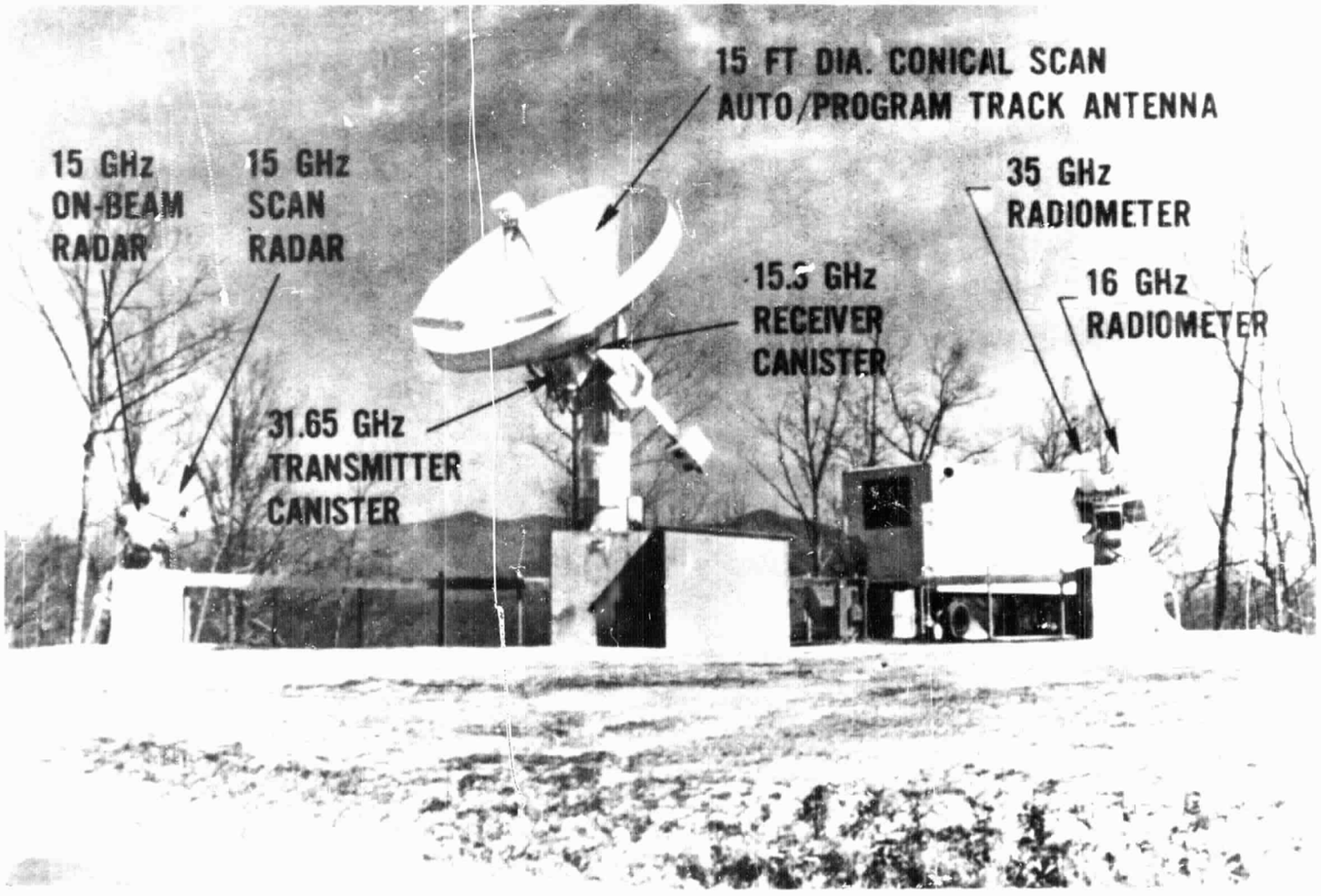

Figure 4. NASA Rosman, North Carolina Station

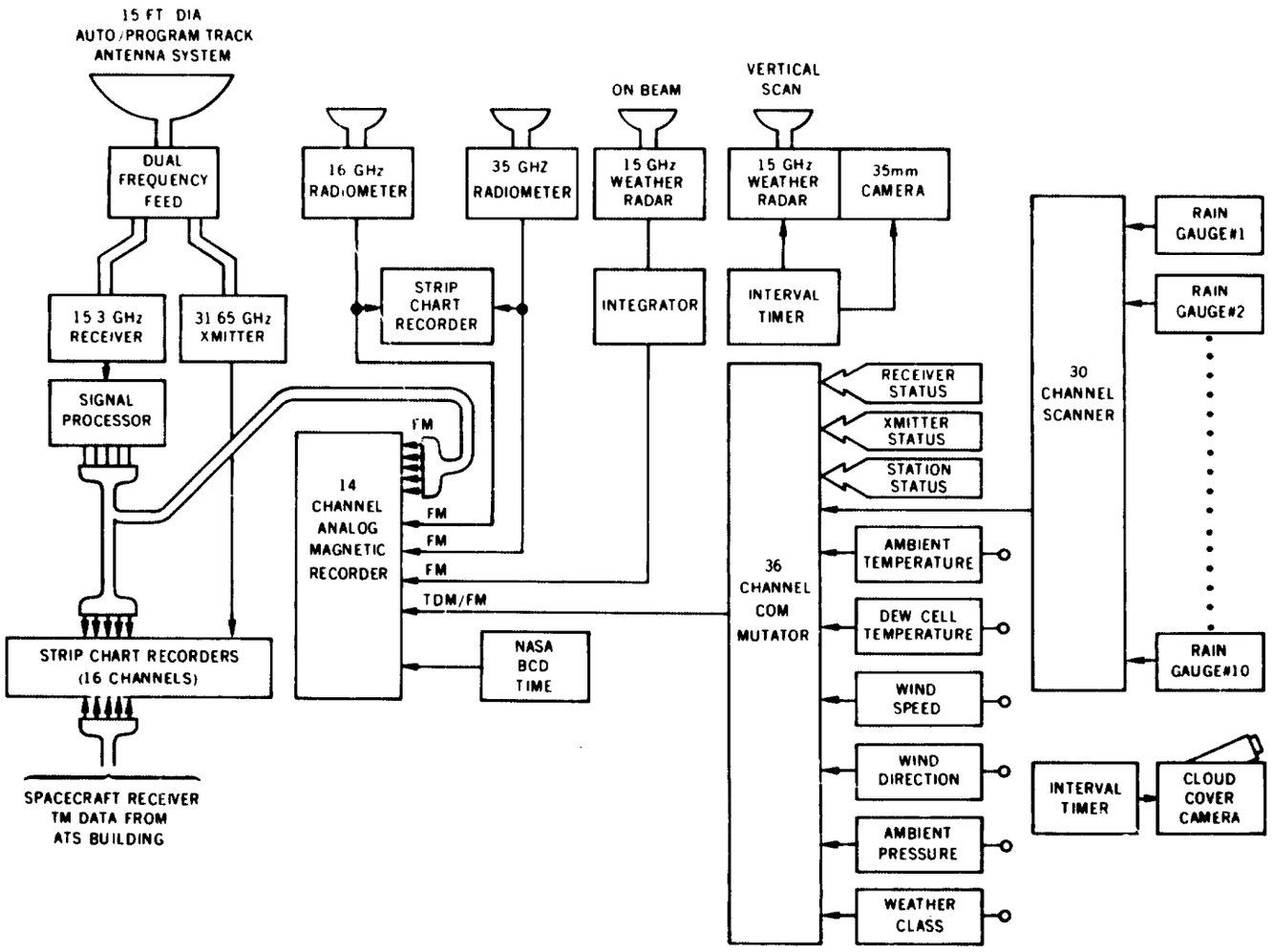

Figure 5. The NASA Rosman, North Carolina, Millimeter Wave Station

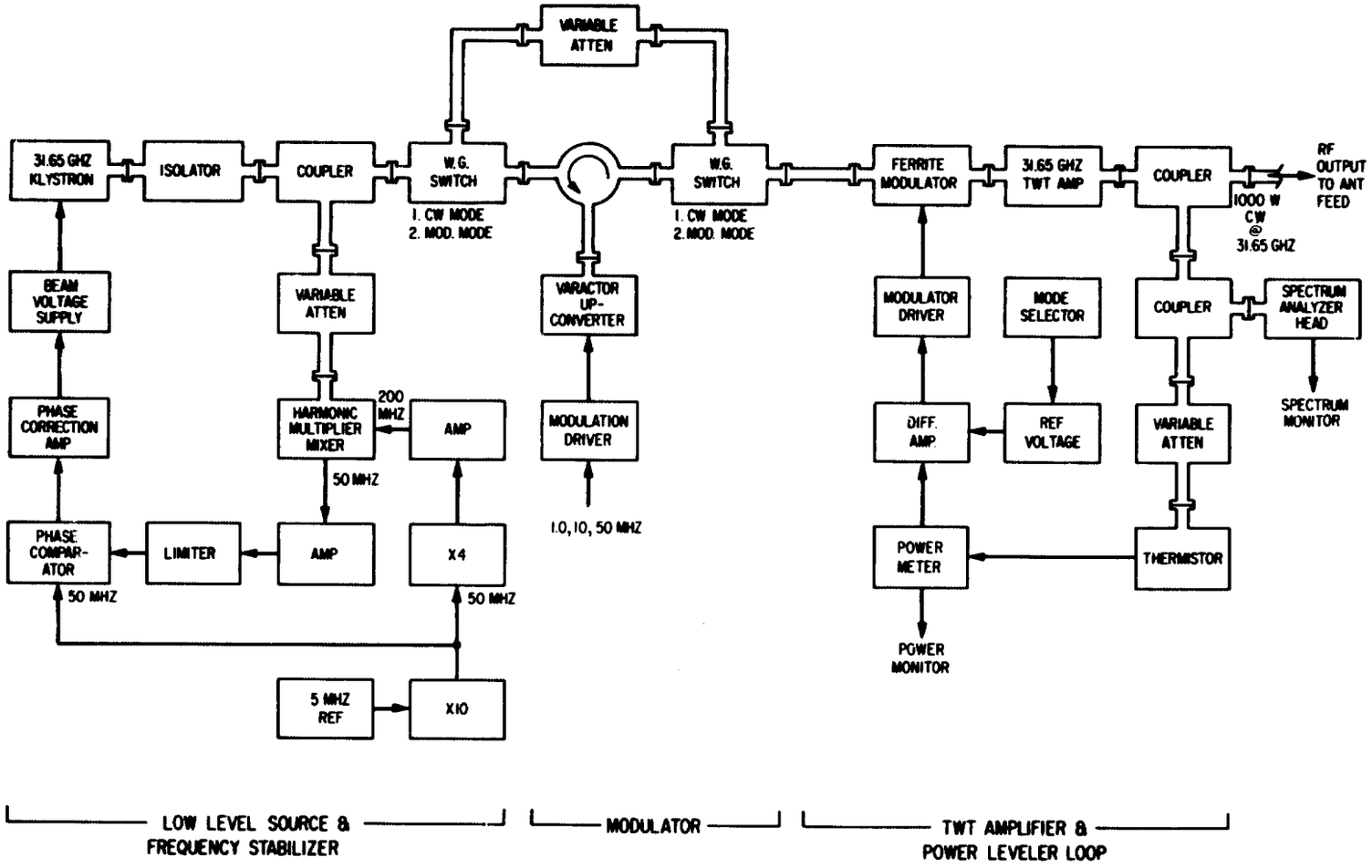
VARIABLE ATTEN
31.65 GHZ KLYSTRON
ISOLATOR
COUPLER
W.G. SWITCH
1. CW MODE
2. MOD. MODE
W.G. SWITCH
1. CW MODE
2. MOD. MODE
FERRITE MODULATOR
31.65 GHZ TWT AMP
COUPLER
RF OUTPUT TO ANT FEED
1000 W CW @ 31.65 GHZ
BEAM VOLTAGE SUPPLY
VARIABLE ATTEN
VARACTOR UP-CONVERTER
MODULATOR DRIVER
MODE SELECTOR
COUPLER
SPECTRUM ANALYZER HEAD
PHASE CORRECTION AMP
HARMONIC MULTIPLIER MIXER
200 MHZ
AMP
MODULATION DRIVER
DIFF. AMP
REF VOLTAGE
VARIABLE ATTEN
SPECTRUM MONITOR
50 MHZ
1.0, 10, 50 MHZ
PHASE COMPAR-ATOR
LIMITER
AMP
X4
POWER METER
THERMISTOR
50 MHZ
50 MHZ
POWER MONITOR
5 MHZ REF
X10
LOW LEVEL SOURCE & FREQUENCY STABILIZER
MODULATOR
TWT AMPLIFIER & POWER LEVELER LOOP

Figure 6

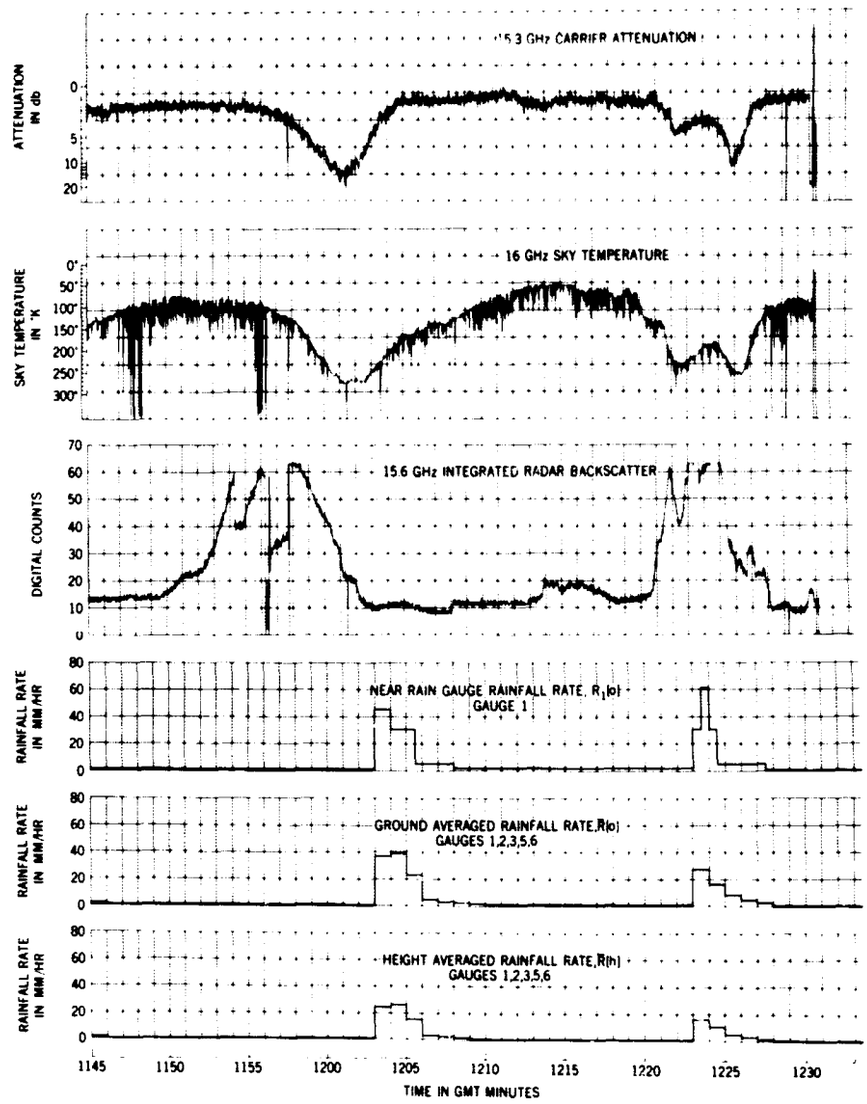

Figure 7. Propagation Measurements During Rainstorm, Rosman, N.C. Day 92, April 2, 1970, 1145 to 1233 GMT

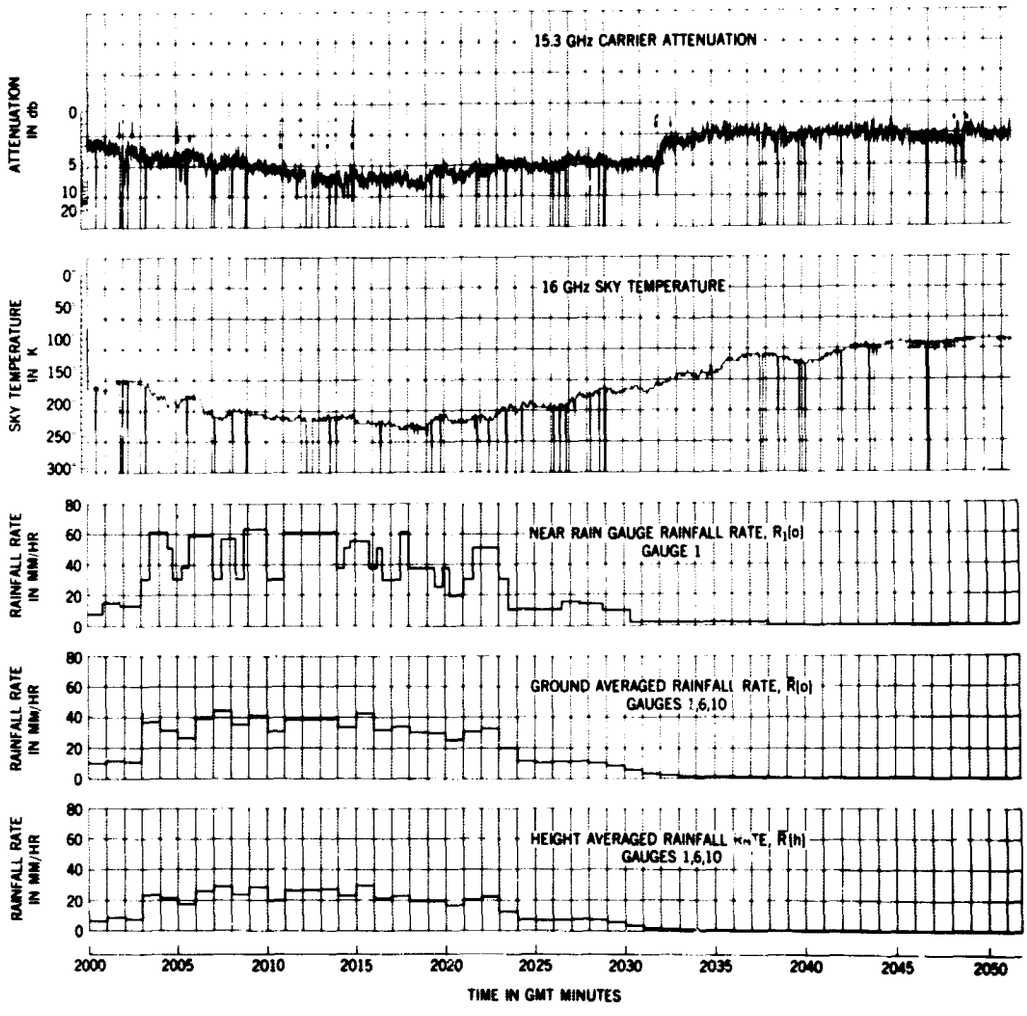

Figure 8. Propagation Measurements During Hailstorm, Rosman, N.C. Day 142, May 22, 1970, 2000 to 2100 GMT

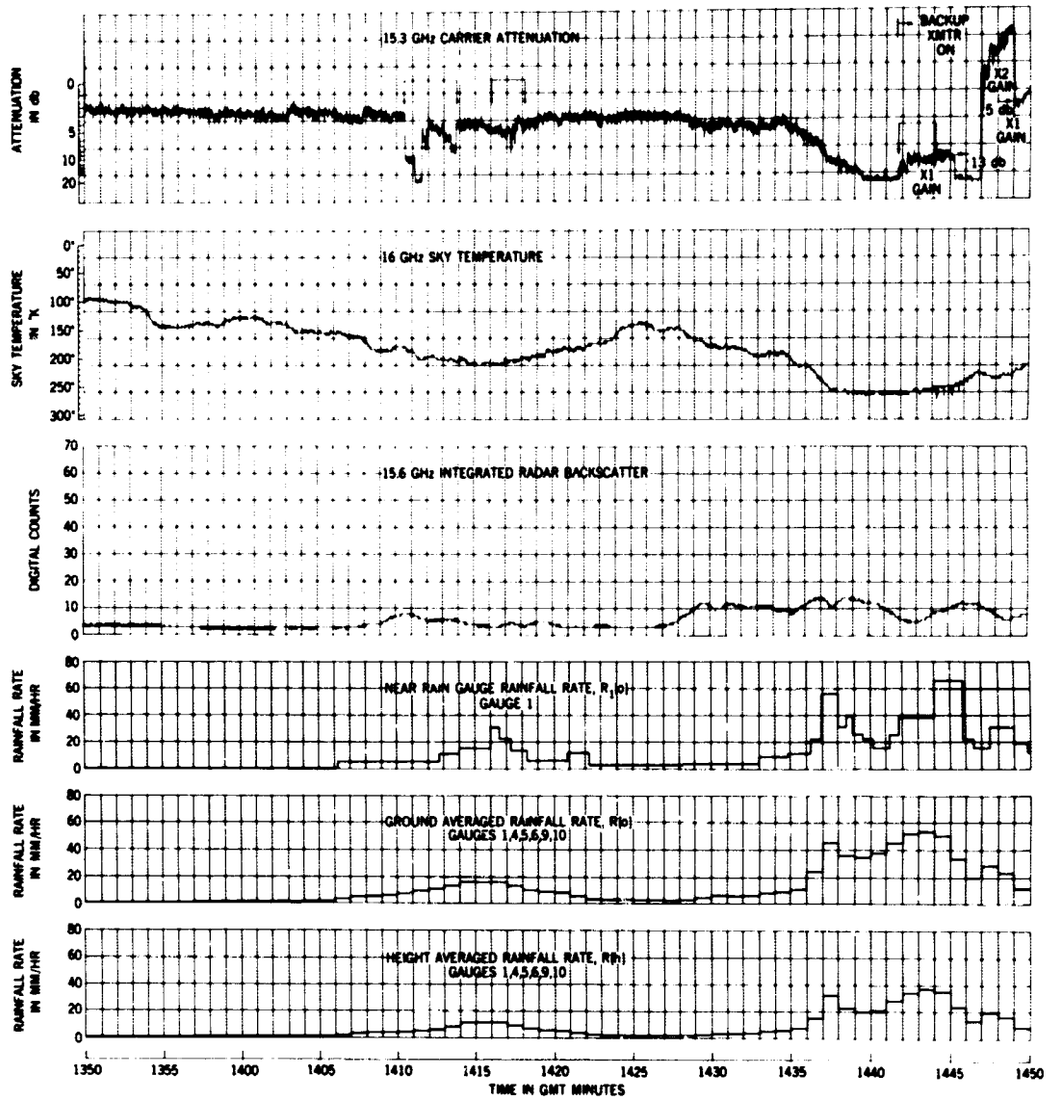

Figure 9. Propagation Measurements During Rainstorm, Rosman, N.C.
Day 155, June 4, 1970, 1350 to 1450 GMT

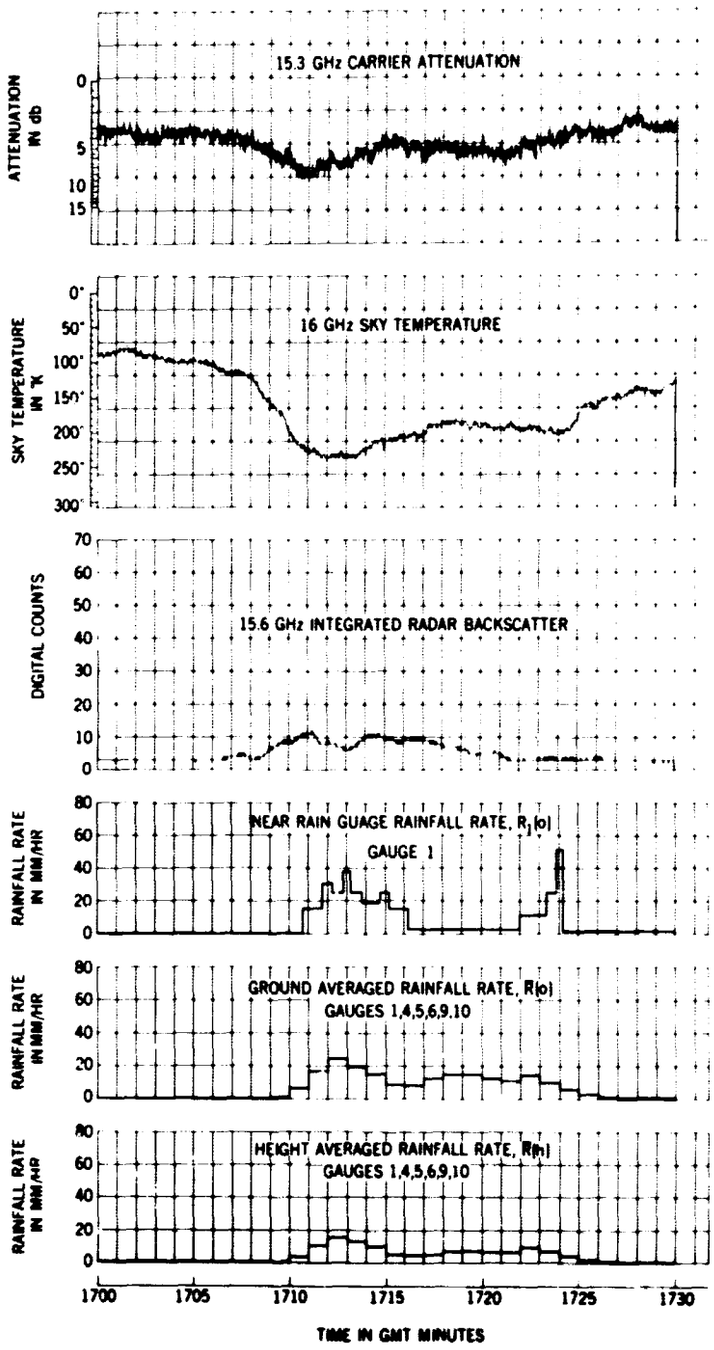

Figure 10. Propagation Measurements During Rainstorm, Rosman, N.C.
Day 155, June 4, 1970, 1700 to 1730 GMT

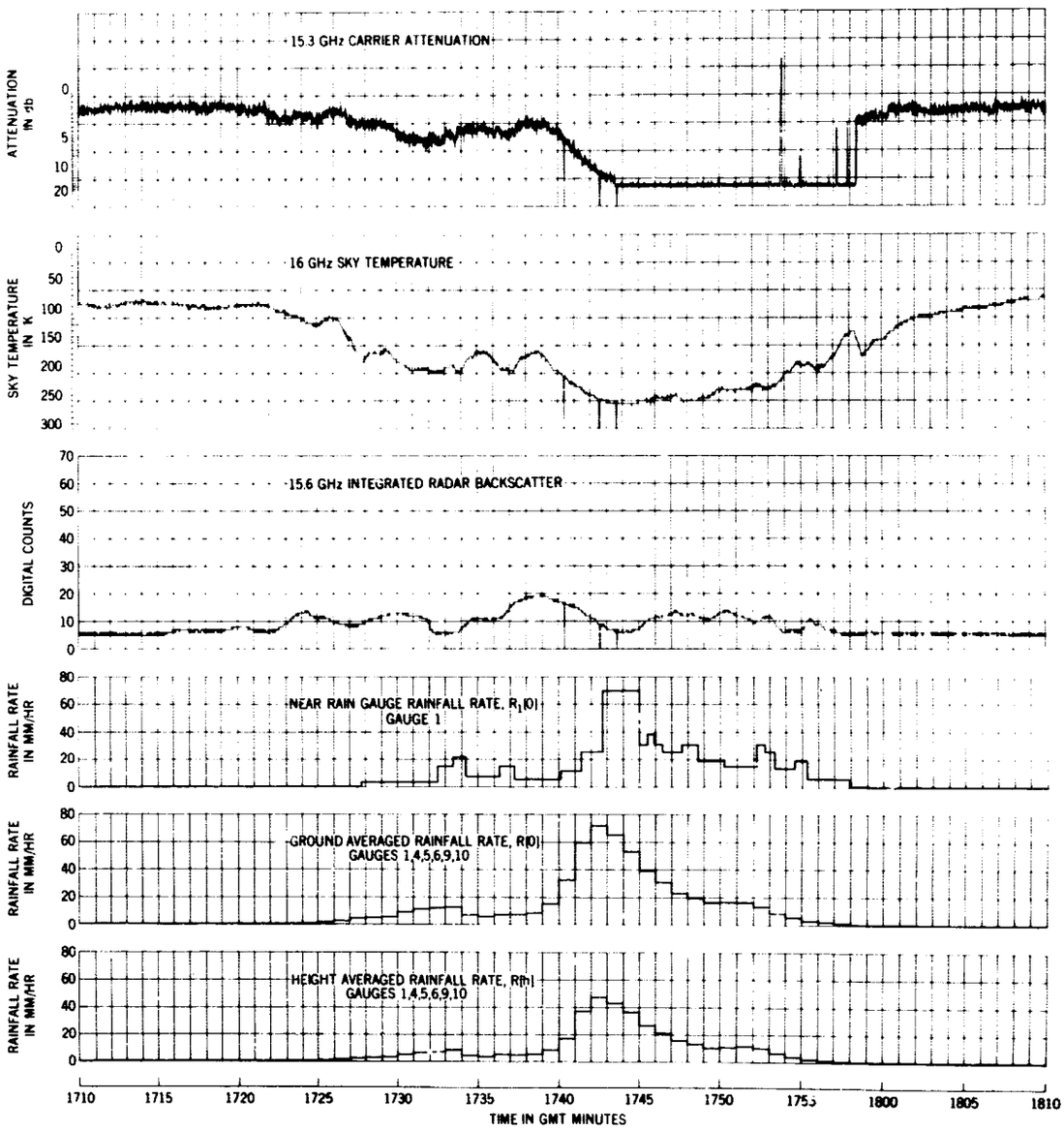

Figure 11. Propagation Measurements During Rainstorm, Rosman, N.C.
Day 156, June 5, 1970, 1710 to 1810 GMT

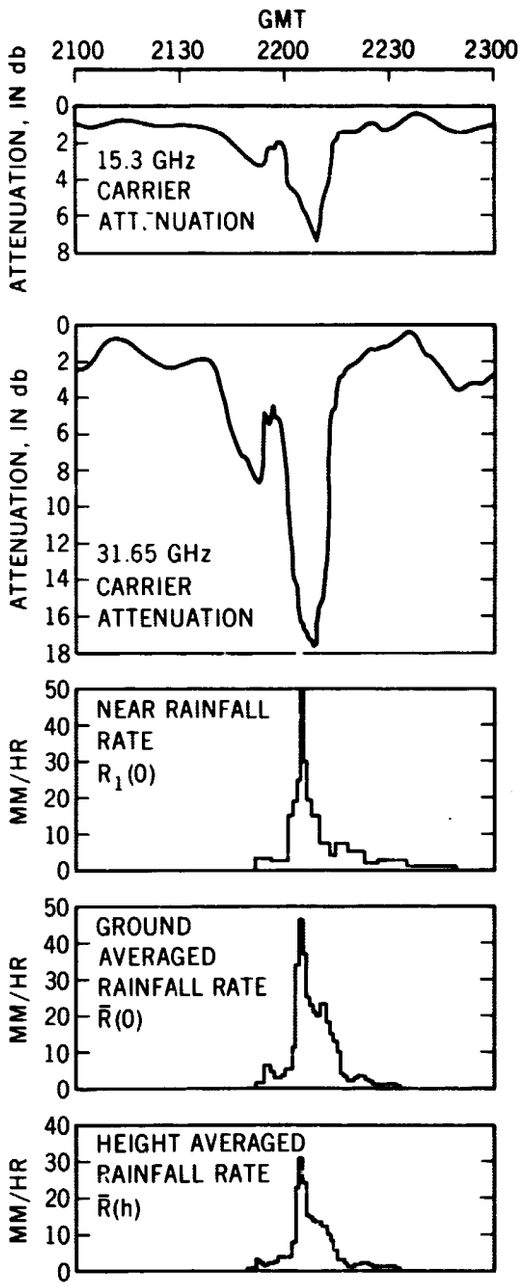

Figure 12. Uplink-Downlink Attenuation During Rainstorm, Day 167, June 16, 1970 2100 to 2300 GMT WC-7 (Continuous Rain)

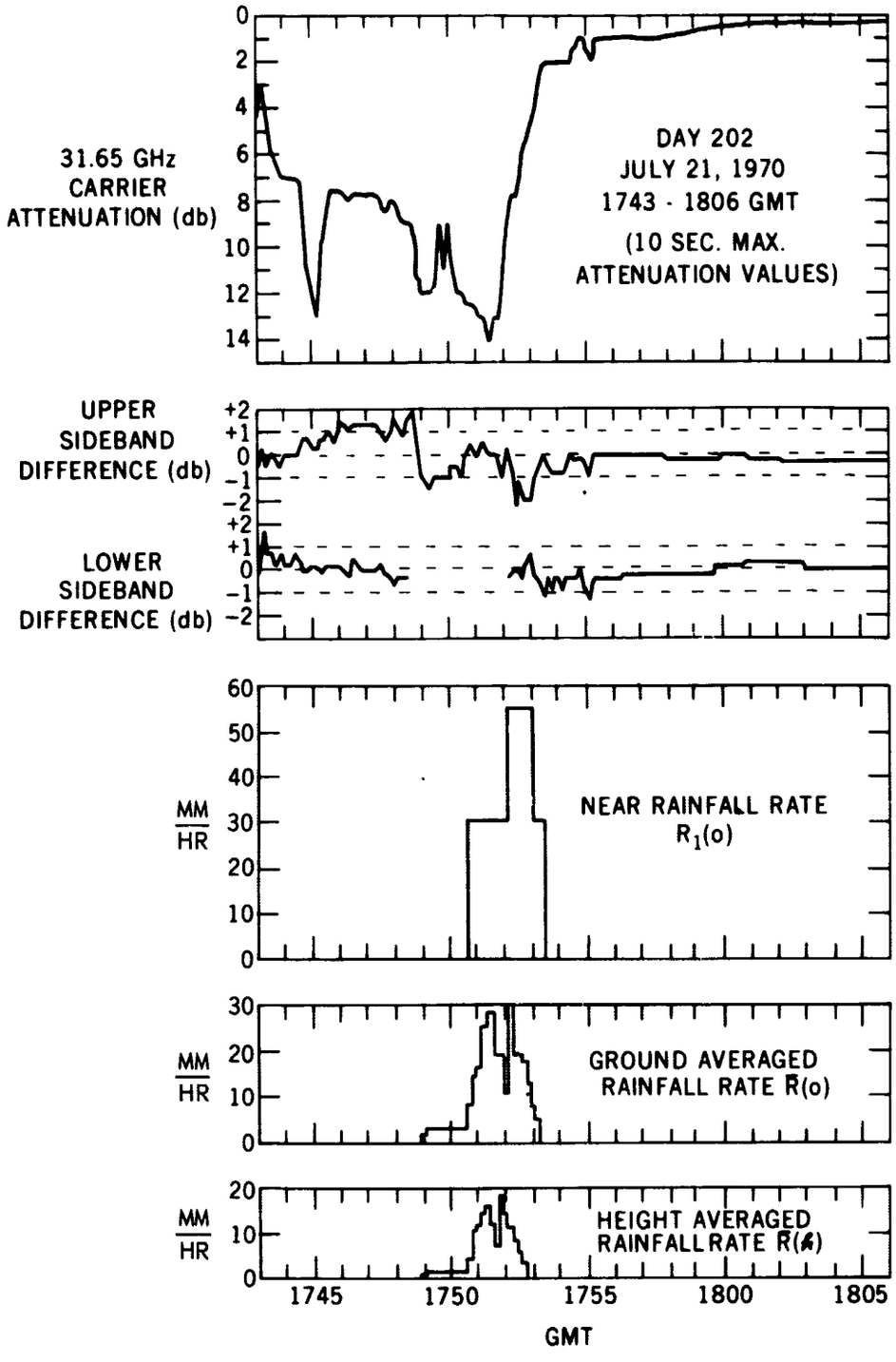

Figure 13. Uplink 50 MHz Sideband Variations During Rainstorm

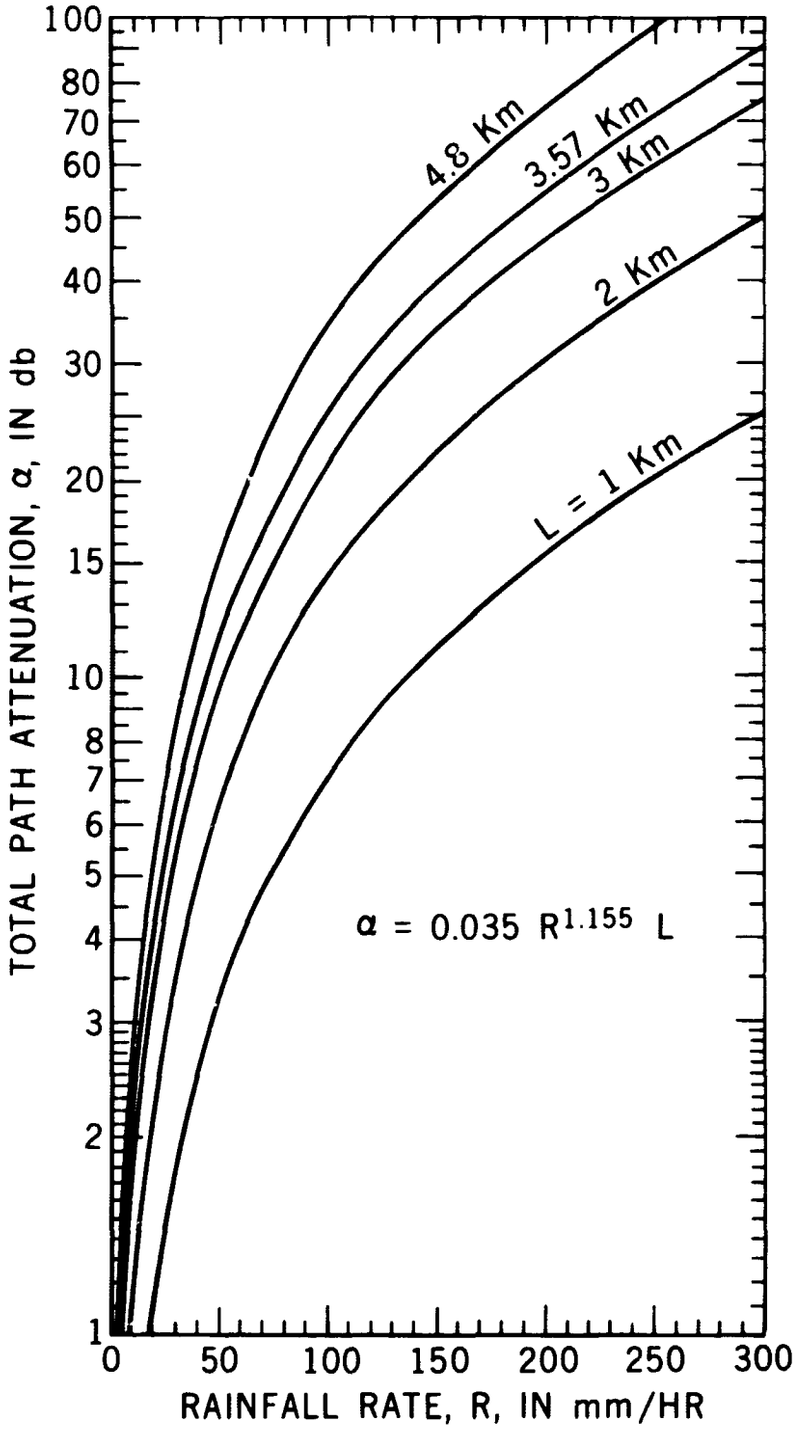

Figure 14. 15.3 GHz Total Path Attenuation Predicted From Rainfall Rate

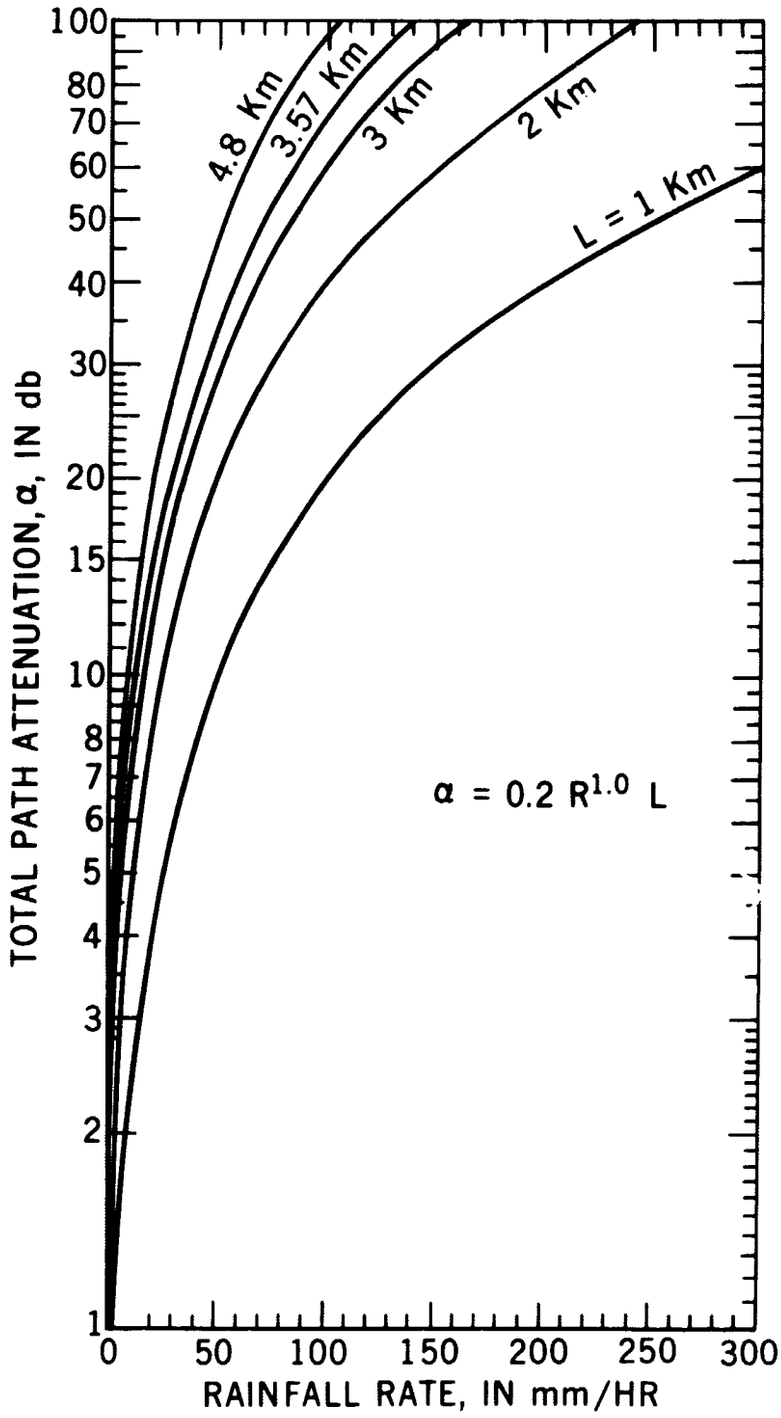

Figure 15. 31.65 GHz Total Path Attenuation Predicted From Rainfall Rate

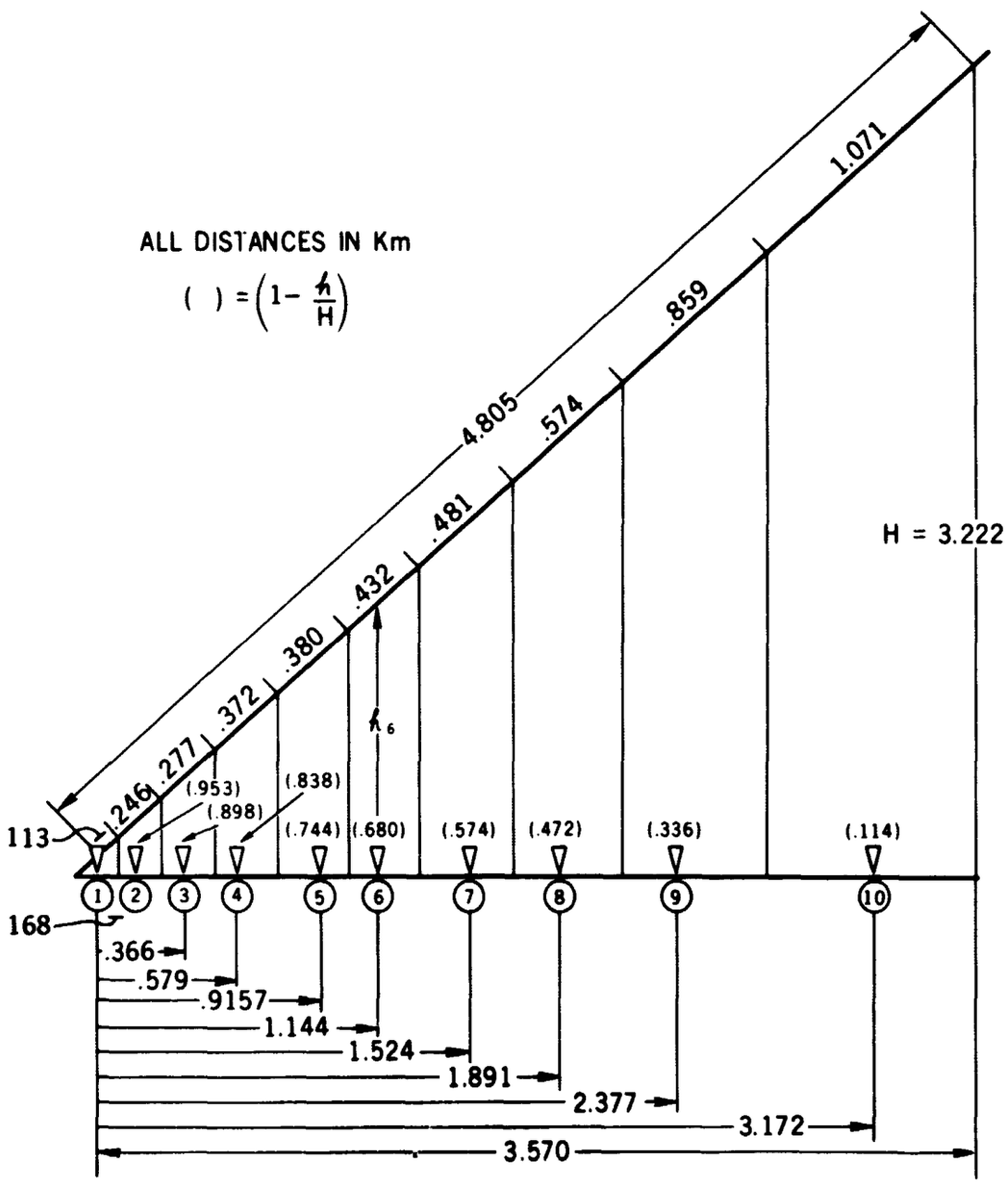

Figure 16. Rain Gauge Network At Rosman, North Carolina
Millimeter Wave Terminal

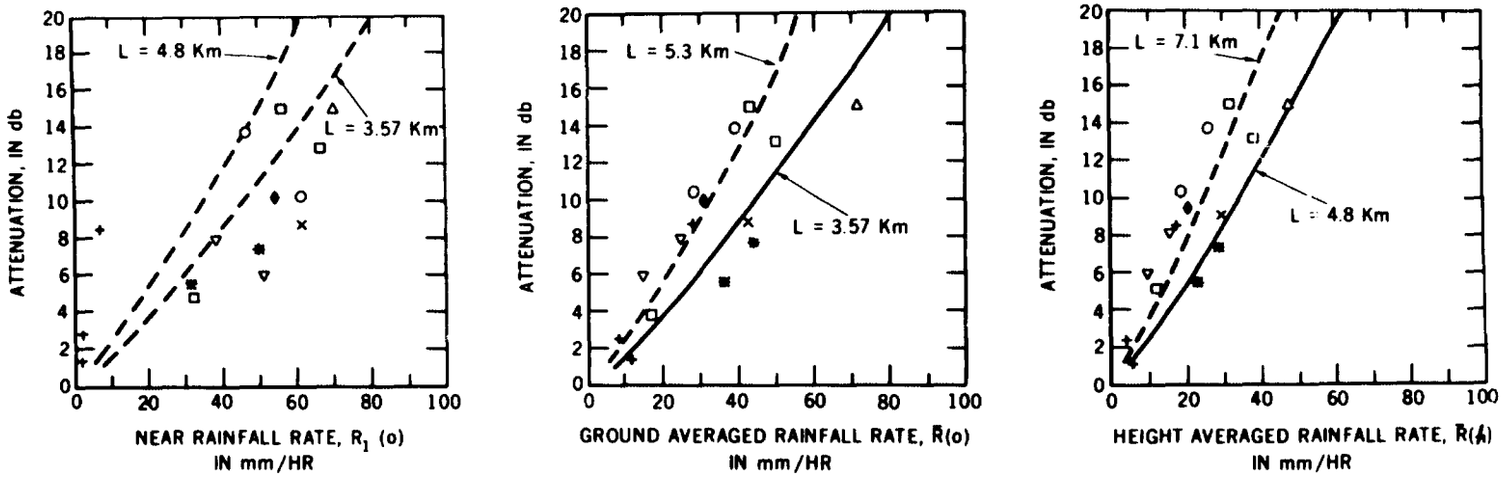

o DAY 92, CONTINUOUS RAIN
× DAY 142, THUNDERSTORM, HAIL
□ DAY 155, CONTINUOUS RAIN
▽ DAY 155, CONTINUOUS RAIN
△ DAY156, CONTINUOUS RAIN
■ DAY 167, CONTINUOUS RAIN
♦ DAY 202, CONTINUOUS RAIN
+ DAY 231, CONTINUOUS RAIN

PREDICTED ATTENUATION = $0.035\ R^{1.115}\ L$

Figure 17. Peak 15.3 GHz Carrier Attenuation vs Peak Rainfall Rate

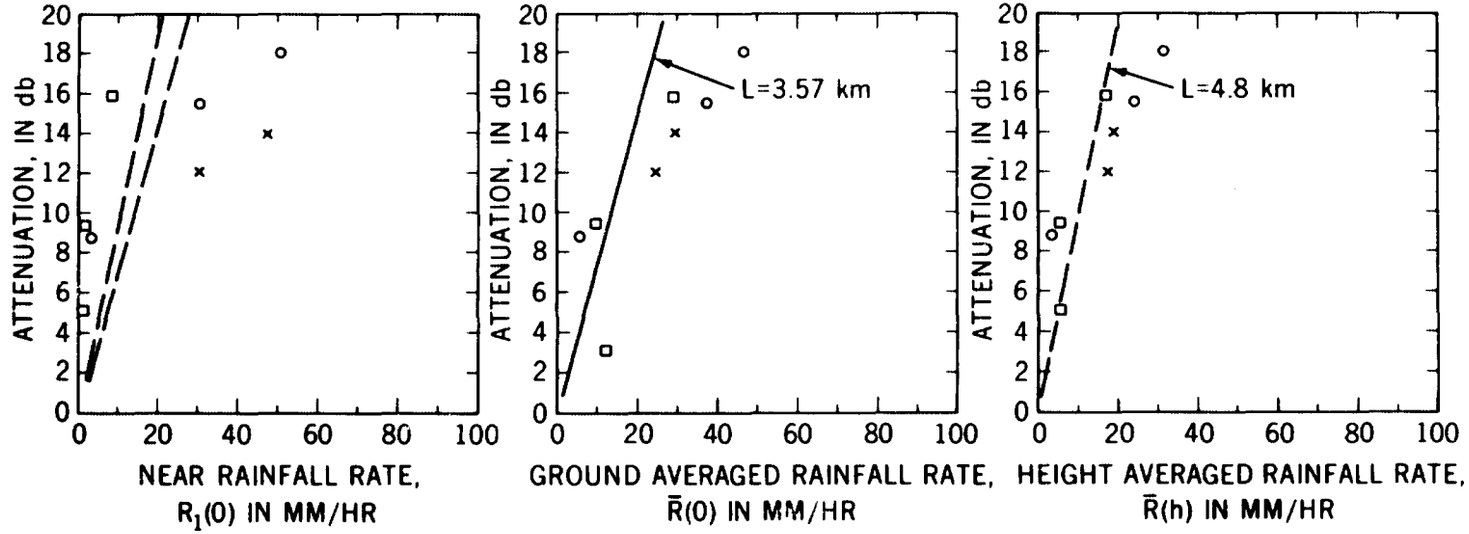

Figure 18. Peak 31.65 GHz Carrier Attenuation vs. Peak Rainfall Rate

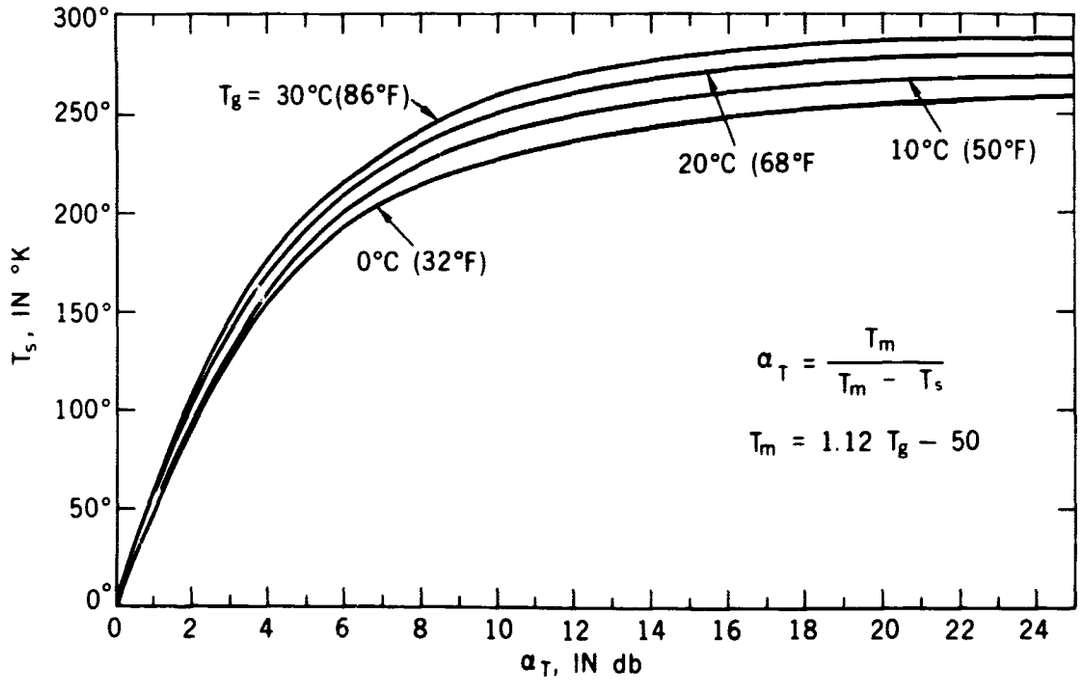

Figure 19. Atmospheric Attenuation Predicted From Sky Temperature

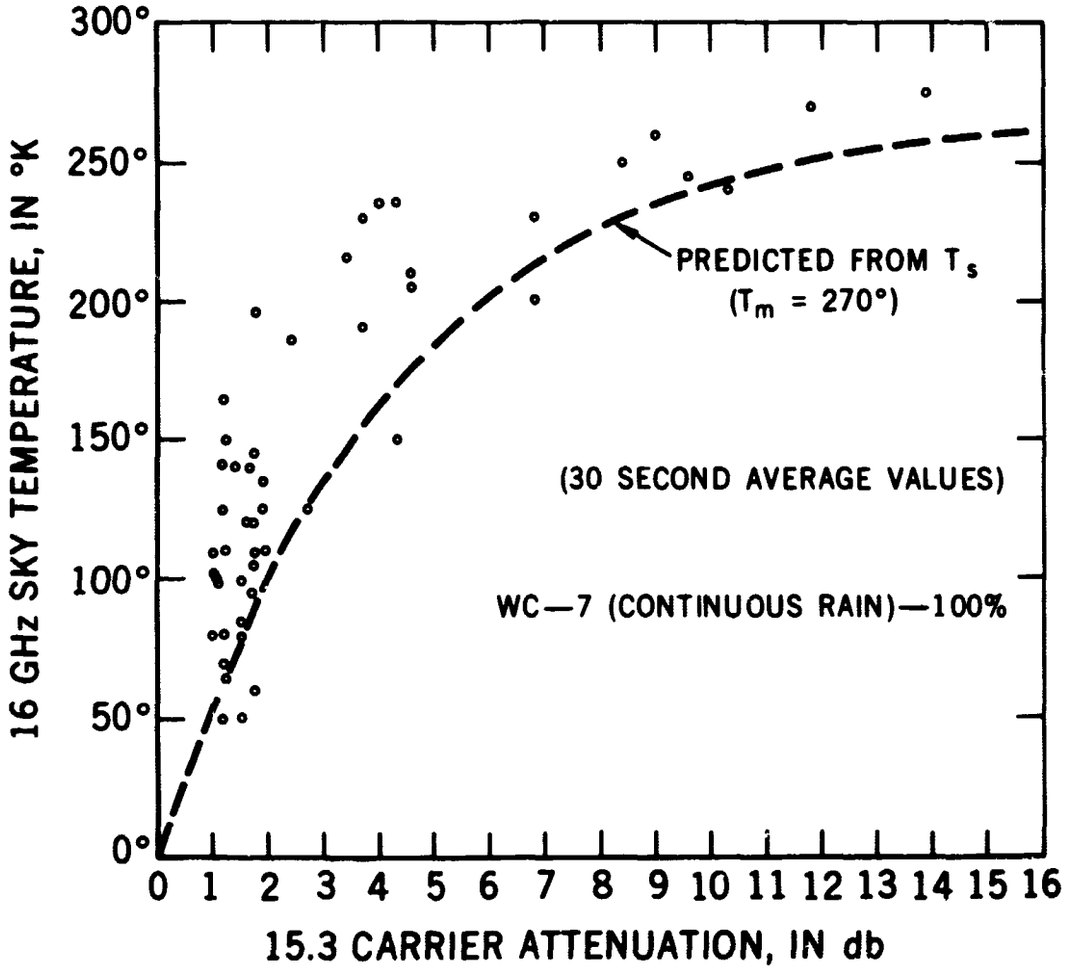

Figure 20. Attenuation-Sky Temperature Correlation Plot
Day 92, April 2, 1970, 1145 to 1230 GMT

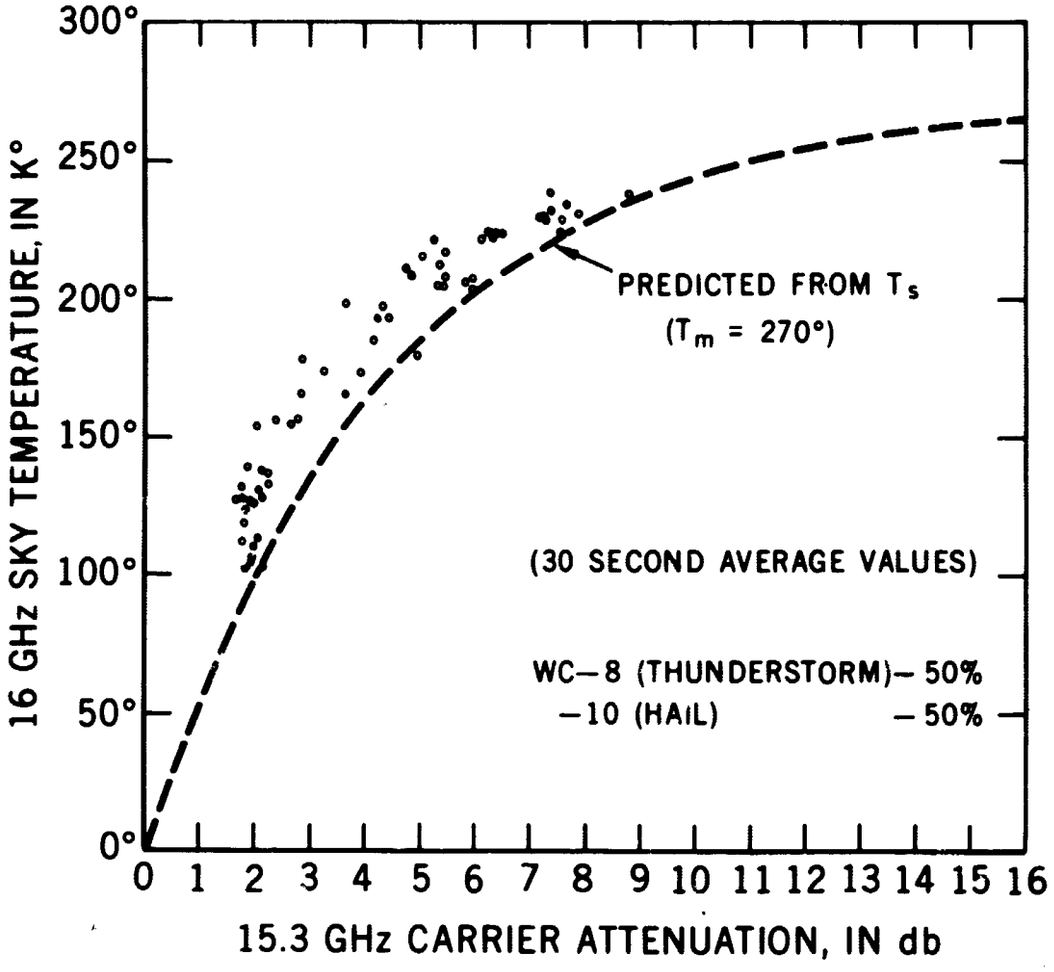

Figure 21. Attenuation-Sky Temperature Correlation Plot
Day 142, May 22, 1970, 2000-2052 GMT

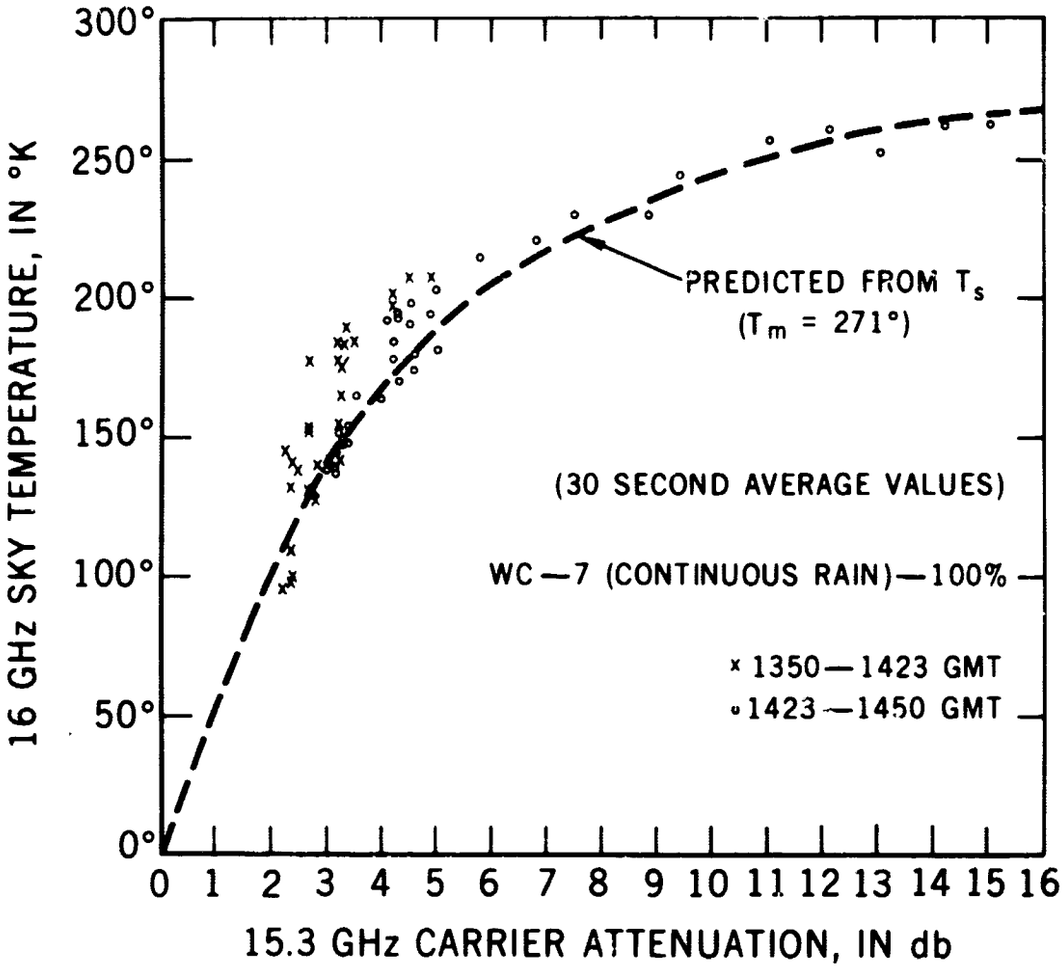

Figure 22. Attenuation-Sky Temperature Correlation Plot
Day 155, June 4, 1970, 1350 to 1450 GMT

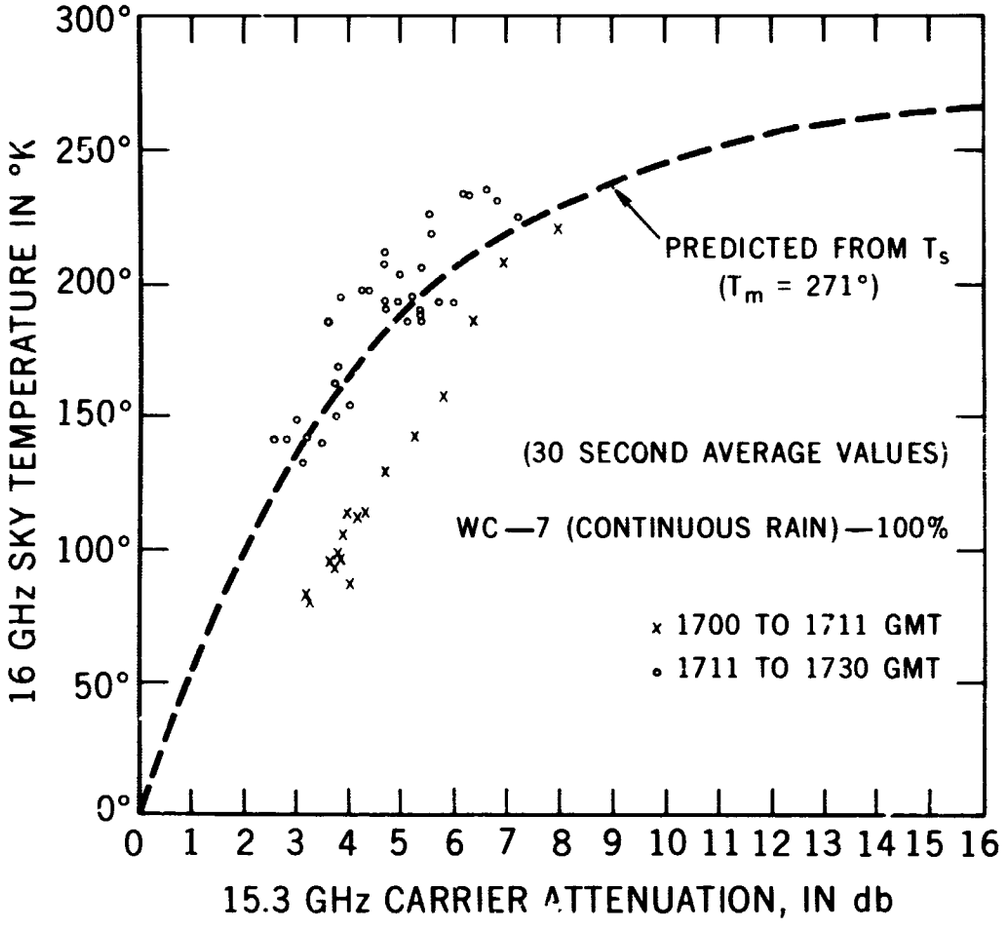

Figure 23. Attenuation-Sky Temperature Correlation Plot
Day 155, June 4, 1970, 1700-1730 GMT

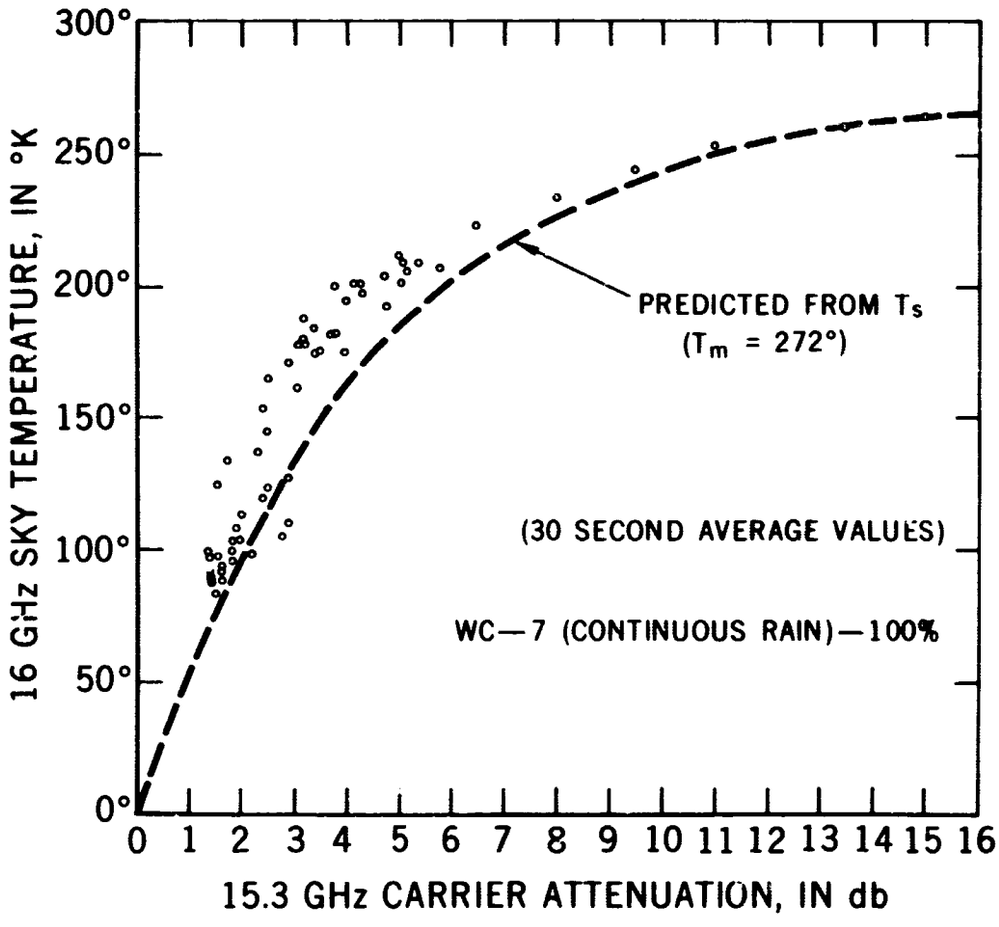

Figure 24. Attenuation-Sky Temperature Correlation Plot
Day 156, June 5, 1970, 1710-1810 GMT

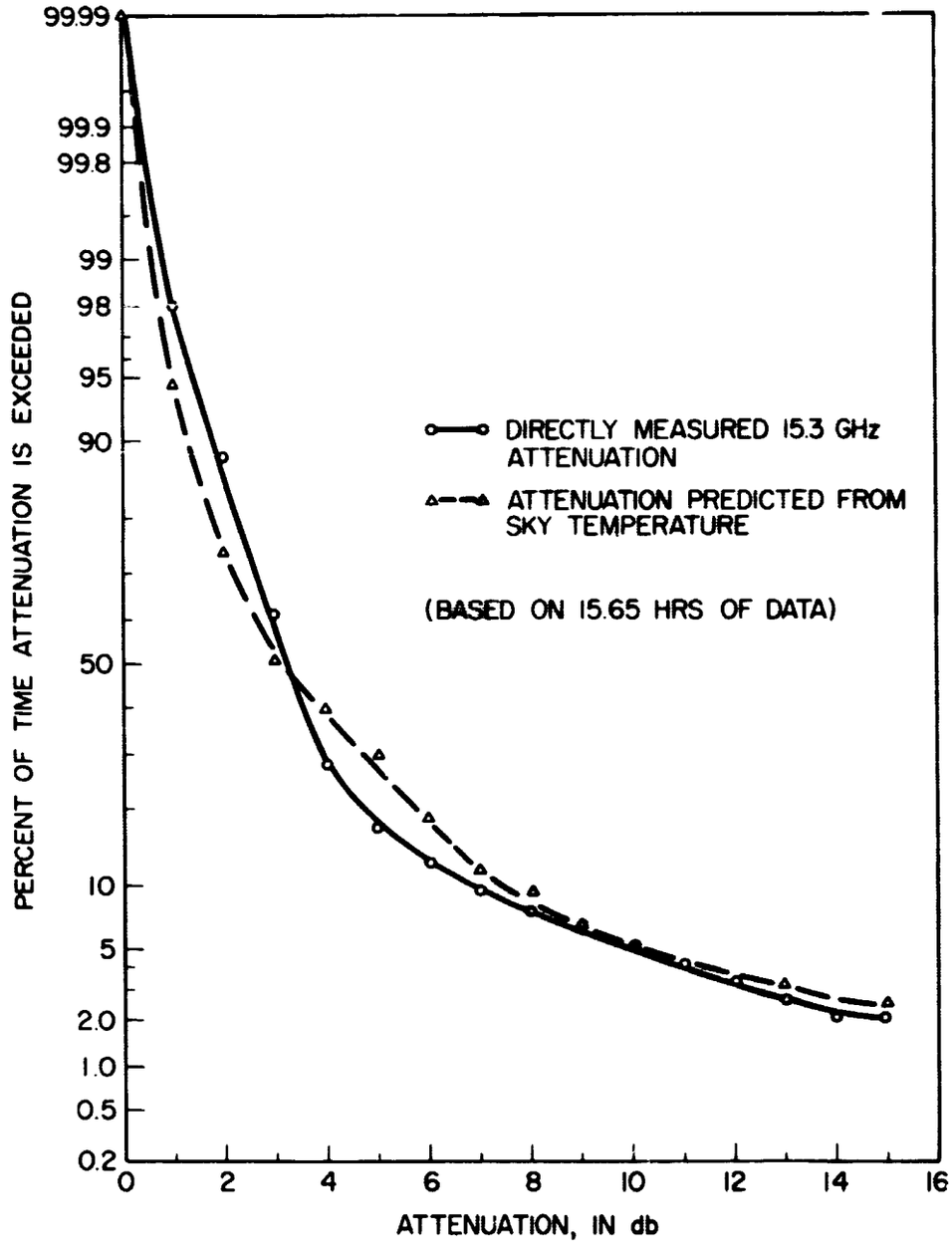

Figure 25. Comparison of Directly Measured 15.36 GHz Attenuation With Attenuation Predicted From Measured 16 GHz Sky Temperature During Rainfall > 1 $\frac{MM}{HR}$

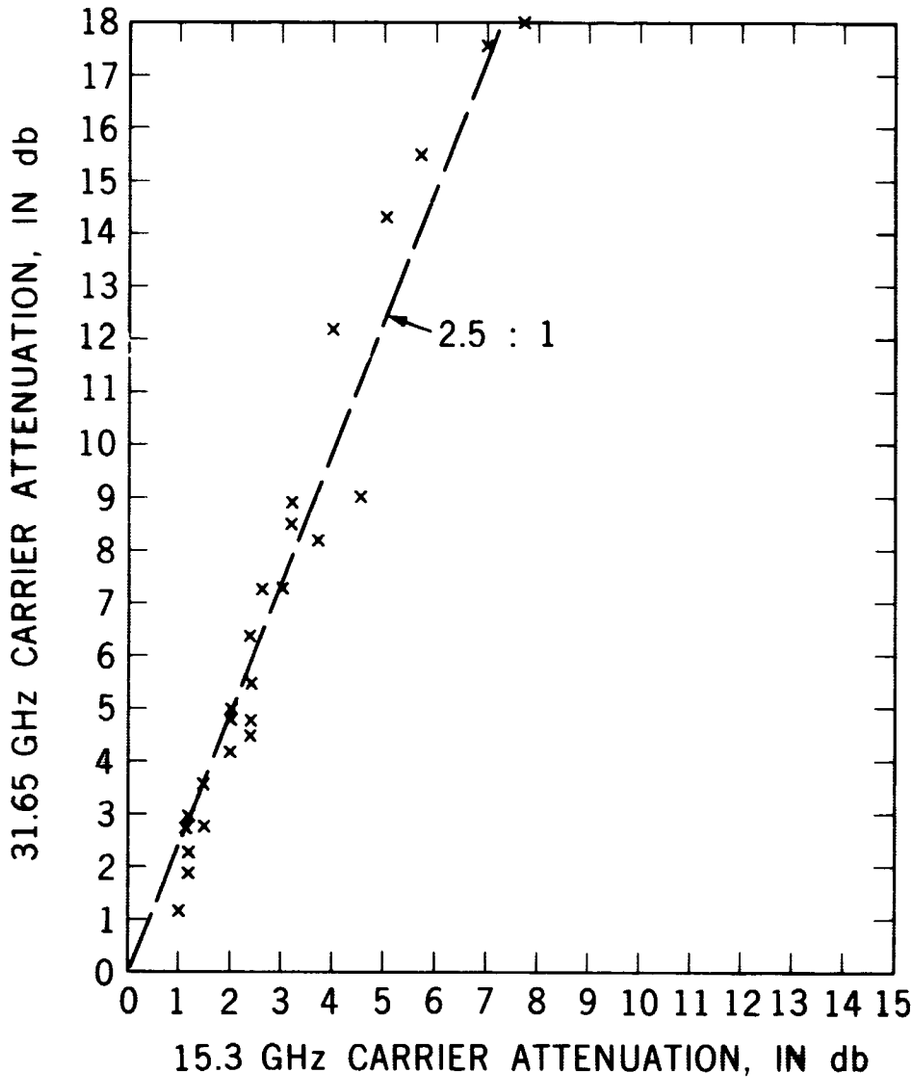

Figure 26. Uplink-Downlink Attenuation Comparison, Day 167, June 16, 1970, 2000 to 2300 GMT WC-7 (Continuous Rain)

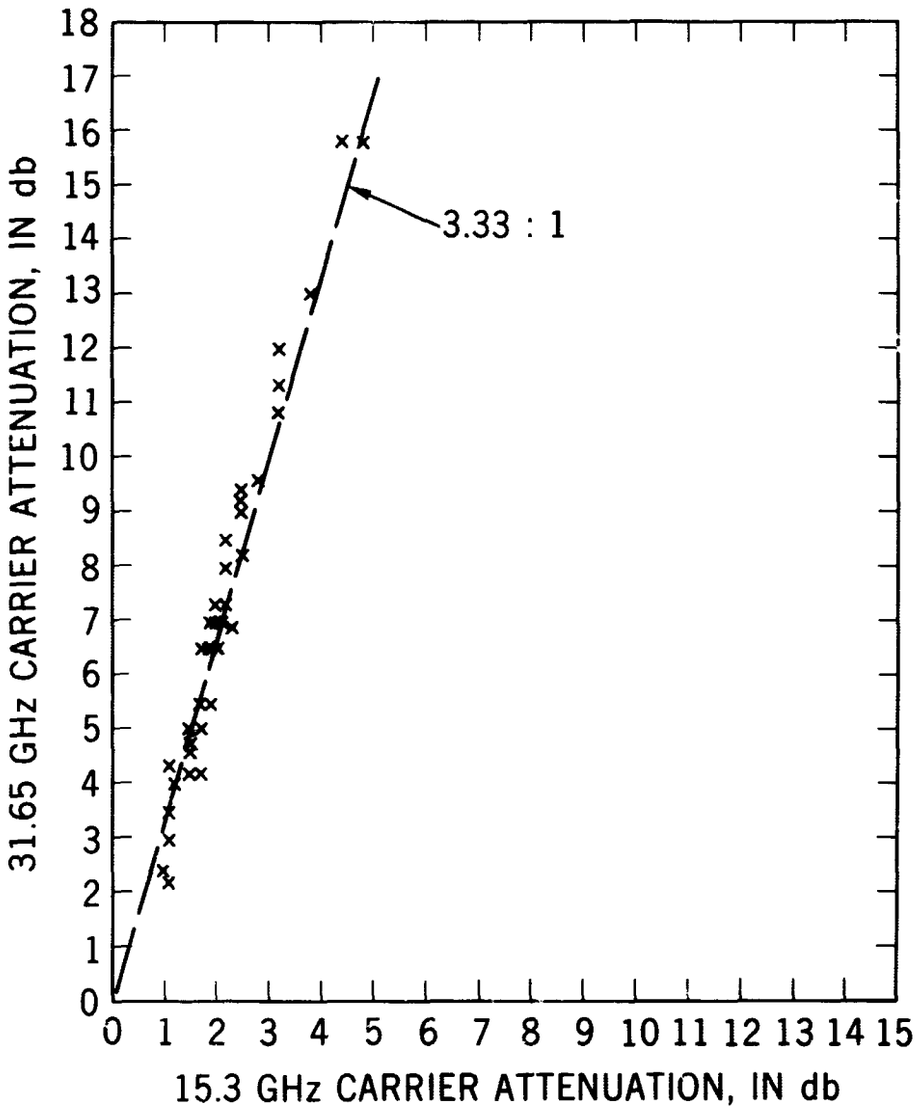

Figure 27. Uplink-Downlink Carrier Attenuations, Day 231, Aug. 19, 1970
1750-1905 GMT WC-7 (Continuous Rain)

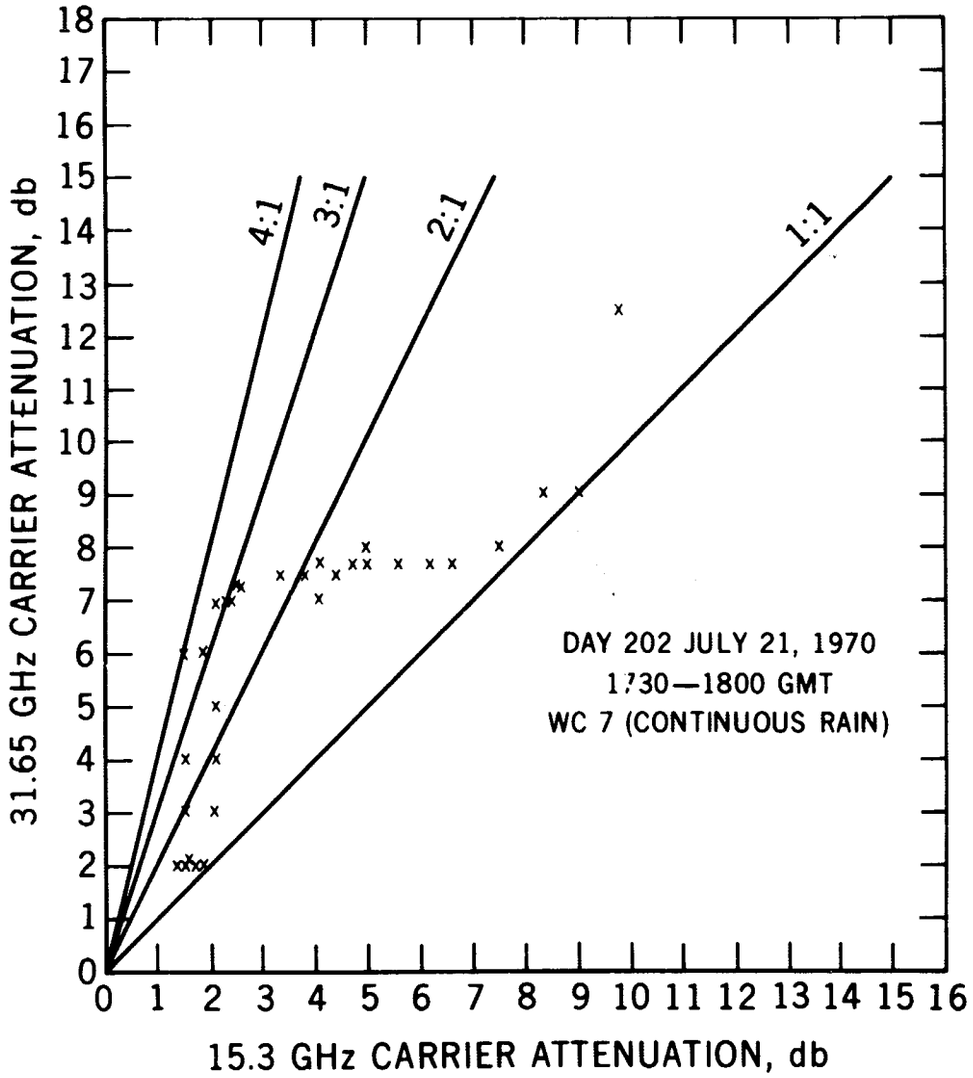

Figure 28. Uplink-Downlink Carrier Attenuations

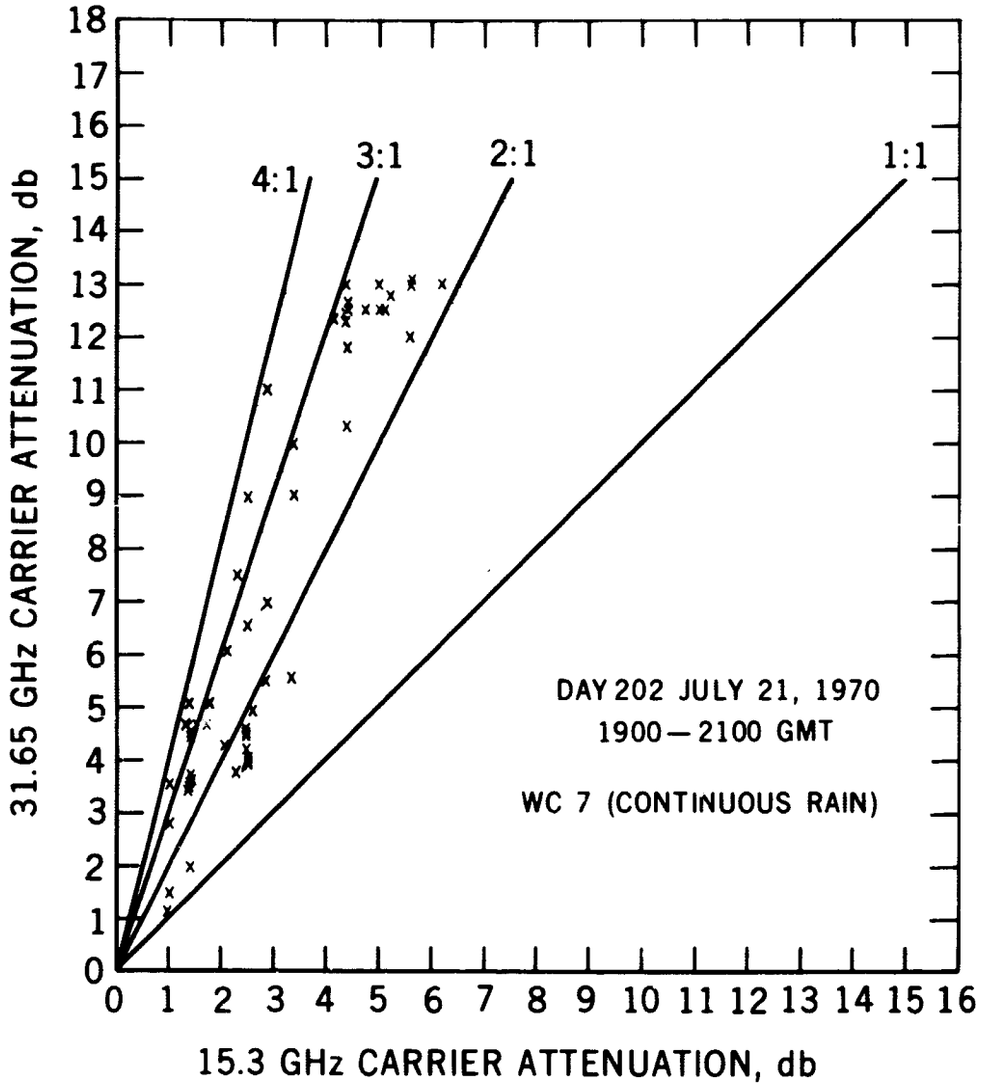

Figure 29. Uplink-Downlink Carrier Attenuations

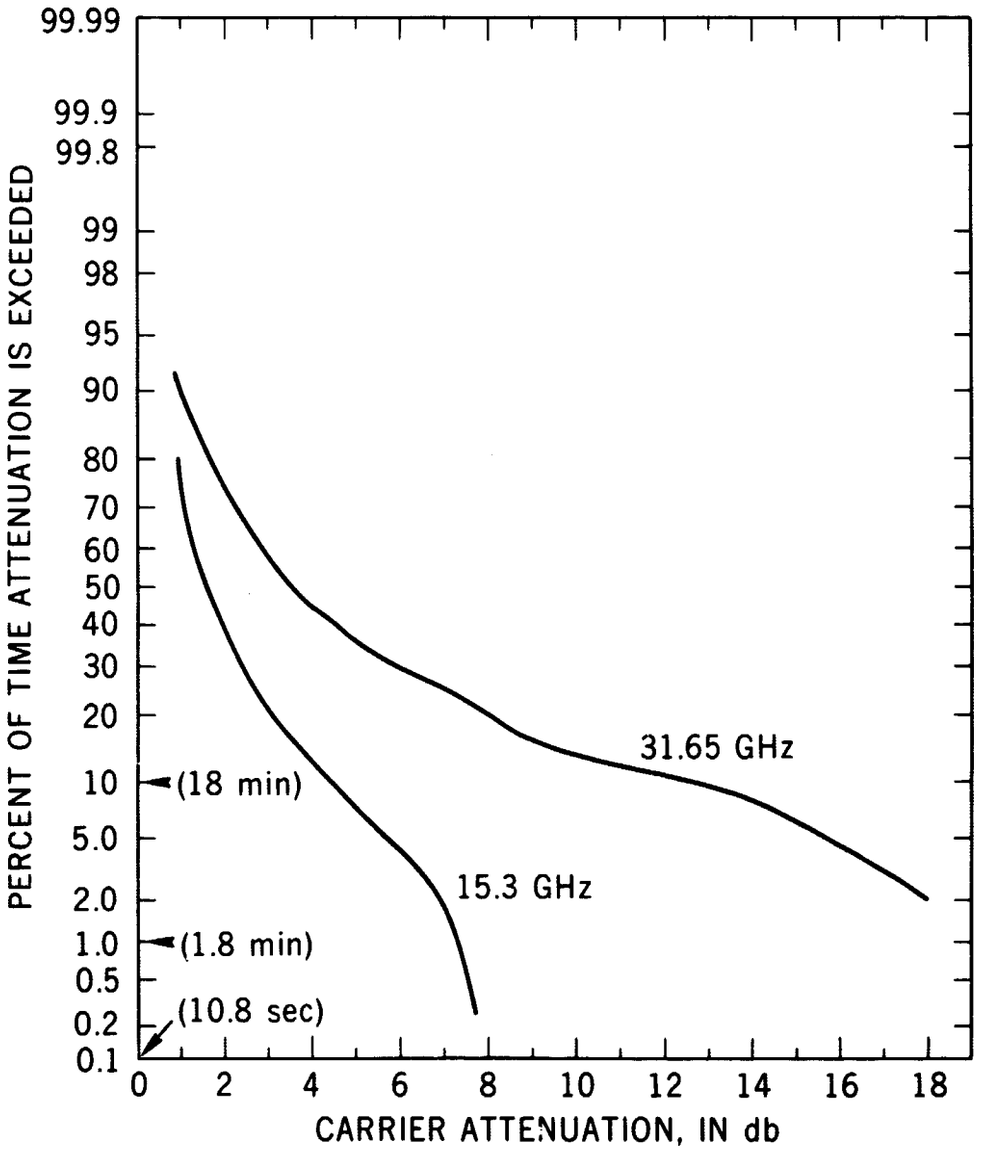

Figure 30. Cumulative Distributions Uplink and Downlink During Rainstorm Day 167, June 16, 1970, 2100 to 2300 GMT

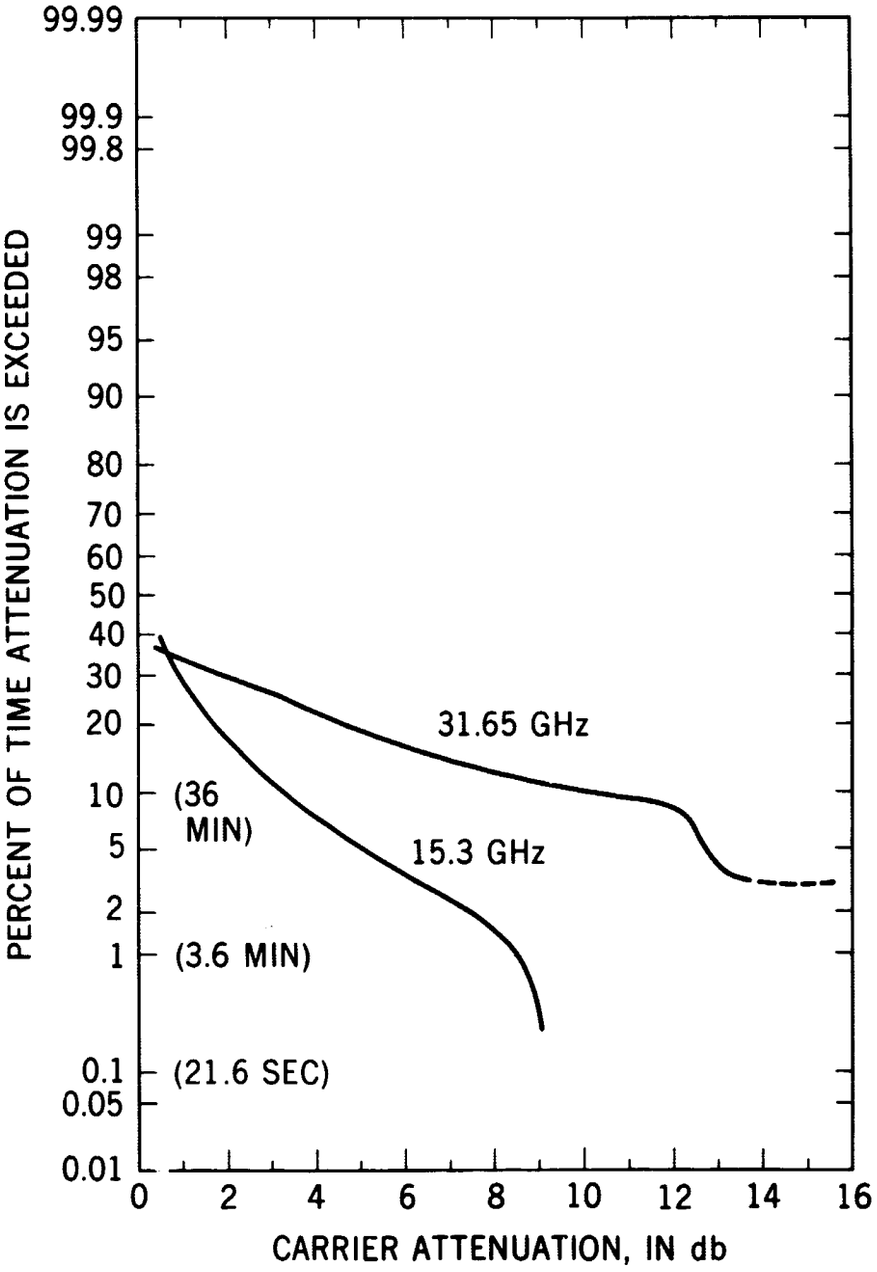

Figure 31. Cumulative Distributions Uplink-Downlink During Rainstorm
Day 202, July 21, 1970, 1730-2330 GMT

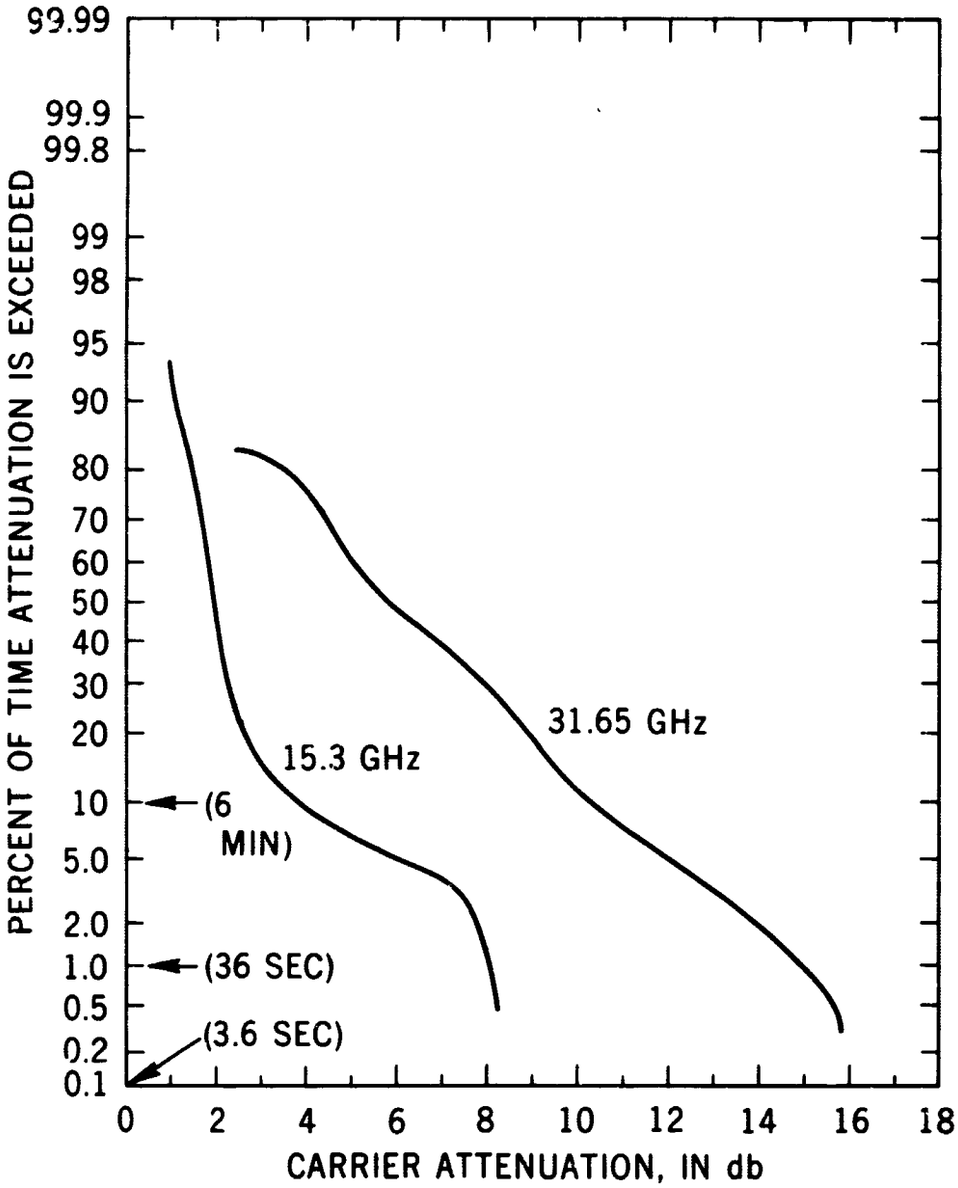

Figure 32. Cumulative Distributions Uplink-Downlink During Rainstorm Day 231, August 19, 1970, 1750 to 1850 GMT

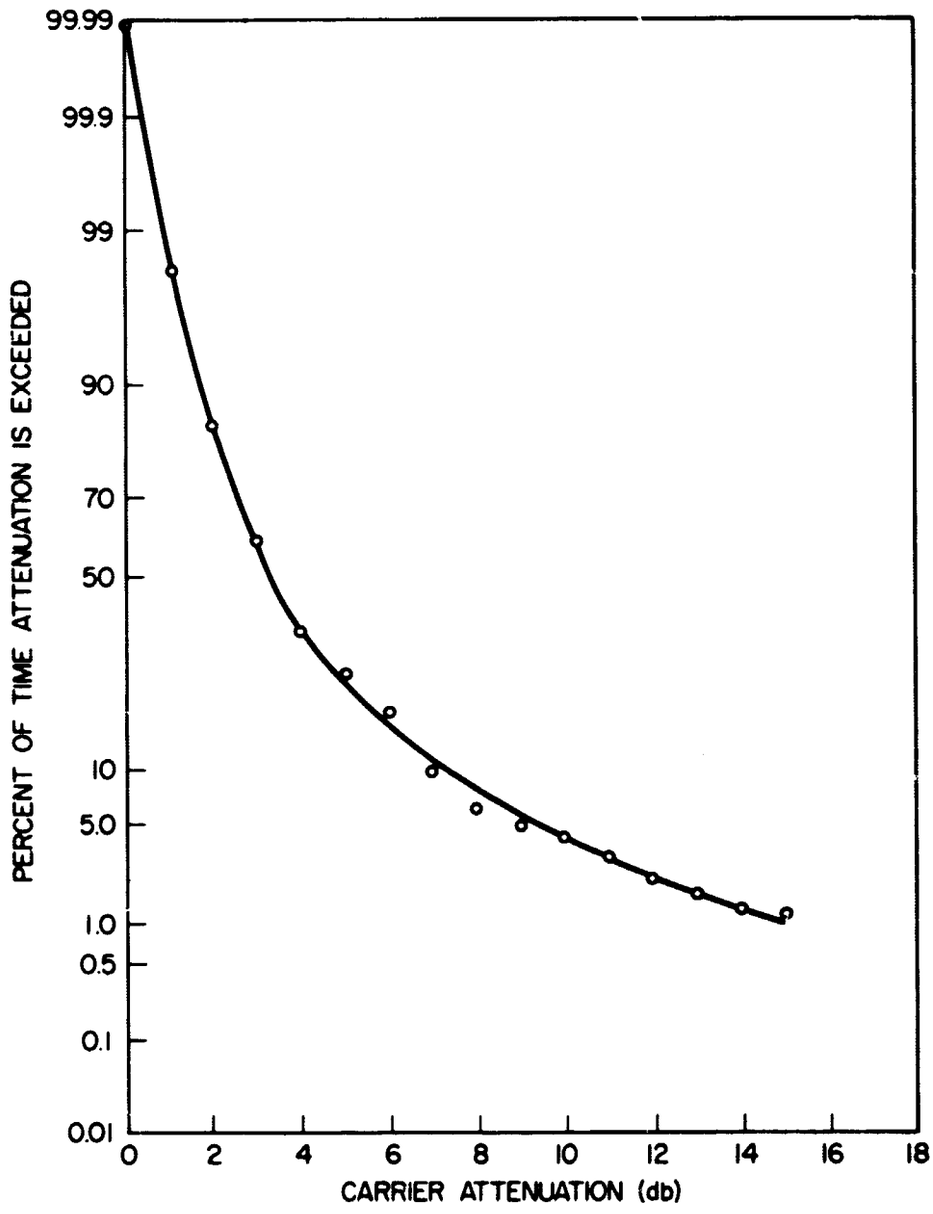

Figure 33. Cumulative Distribution of 15.3-GHz Carrier Attenuation at Rosman, North Carolina During Rainfall Greater Than 1 mm/hr (Based on 19.55 Hours of Downlink Data Recorded 10/1/69 to 9/30/70).

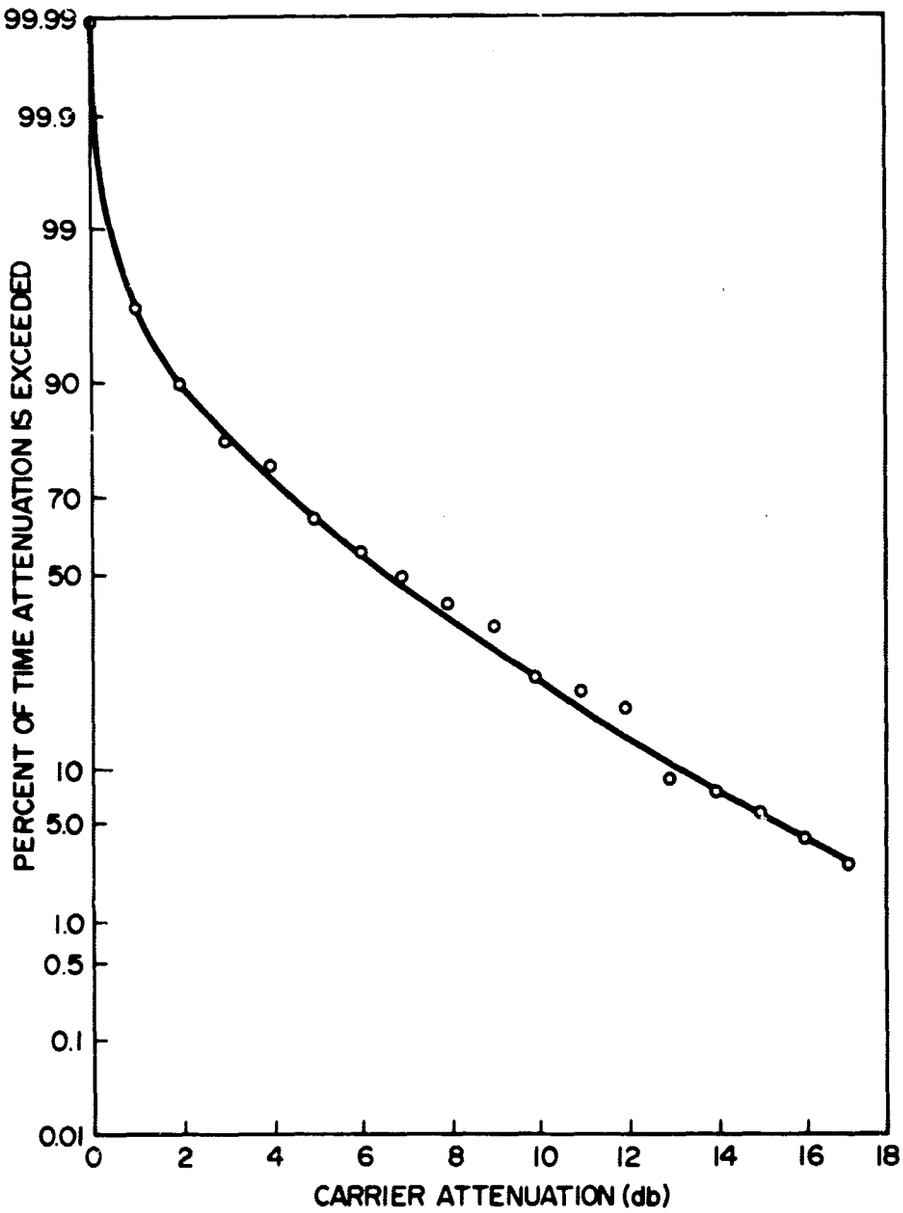

Figure 34. Cumulative Distribution of 31.65-GHz Carrier Attenuation at Rosman, North Carolina During Rainfall Greater Than 1 mm/hr (Based on 2.62 Hours of Uplink Data Recorded 10/1/69 to 9/30/70).

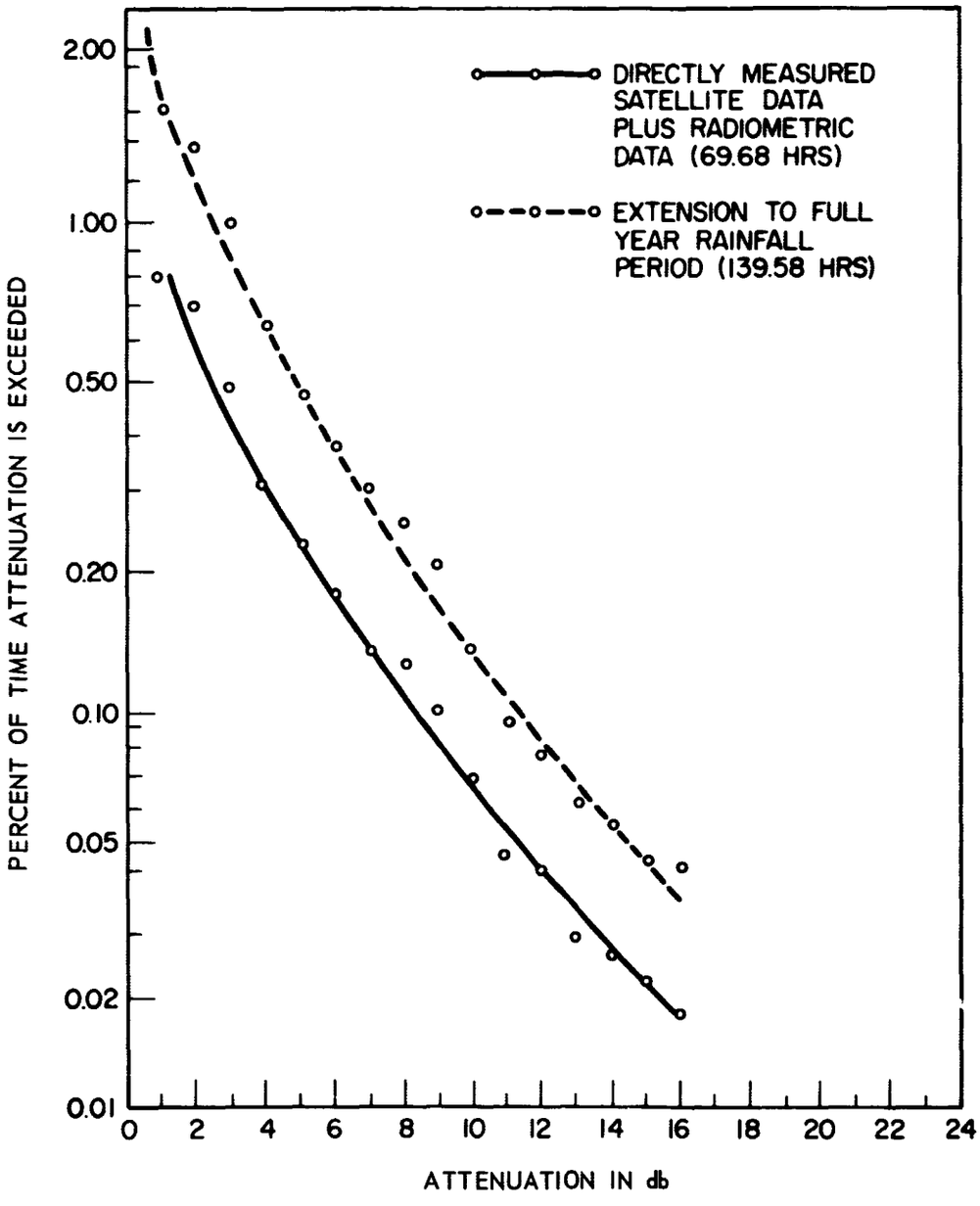

Figure 35. Cumulative Distribution of 15.3 GHz Carrier Attenuation for 1 Year Period (10/1/69 to 9/30/70) At Rosman, North Carolina, Based on Directly Measured Satellite Data And Radiometric Data.

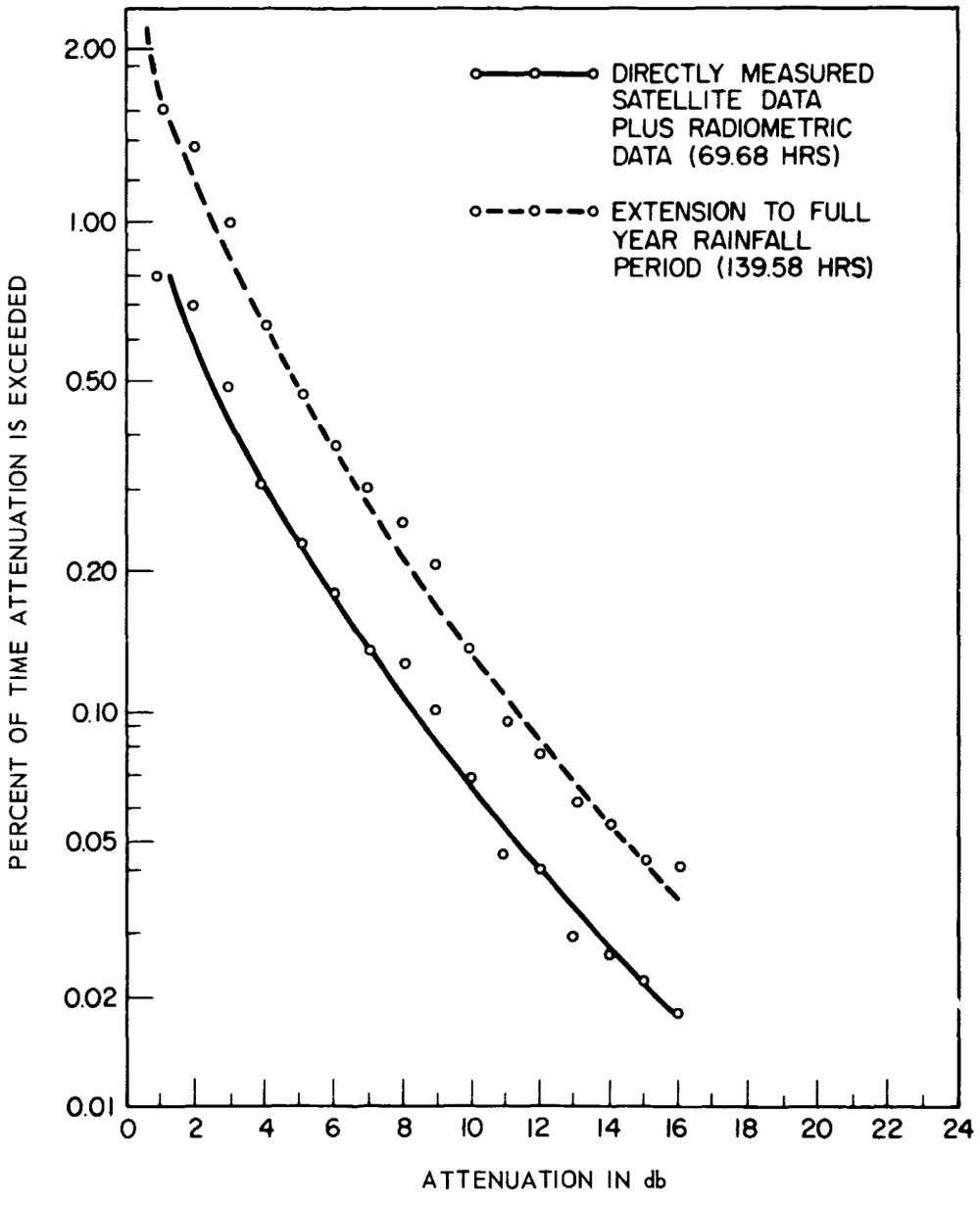

Figure 35. Cumulative Distribution of 15.3 GHz Carrier Attenuation for 1 Year Period (10/1/69 to 9/30/70) At Rosman, North Carolina, Based on Directly Measured Satellite Data And Radiometric Data.

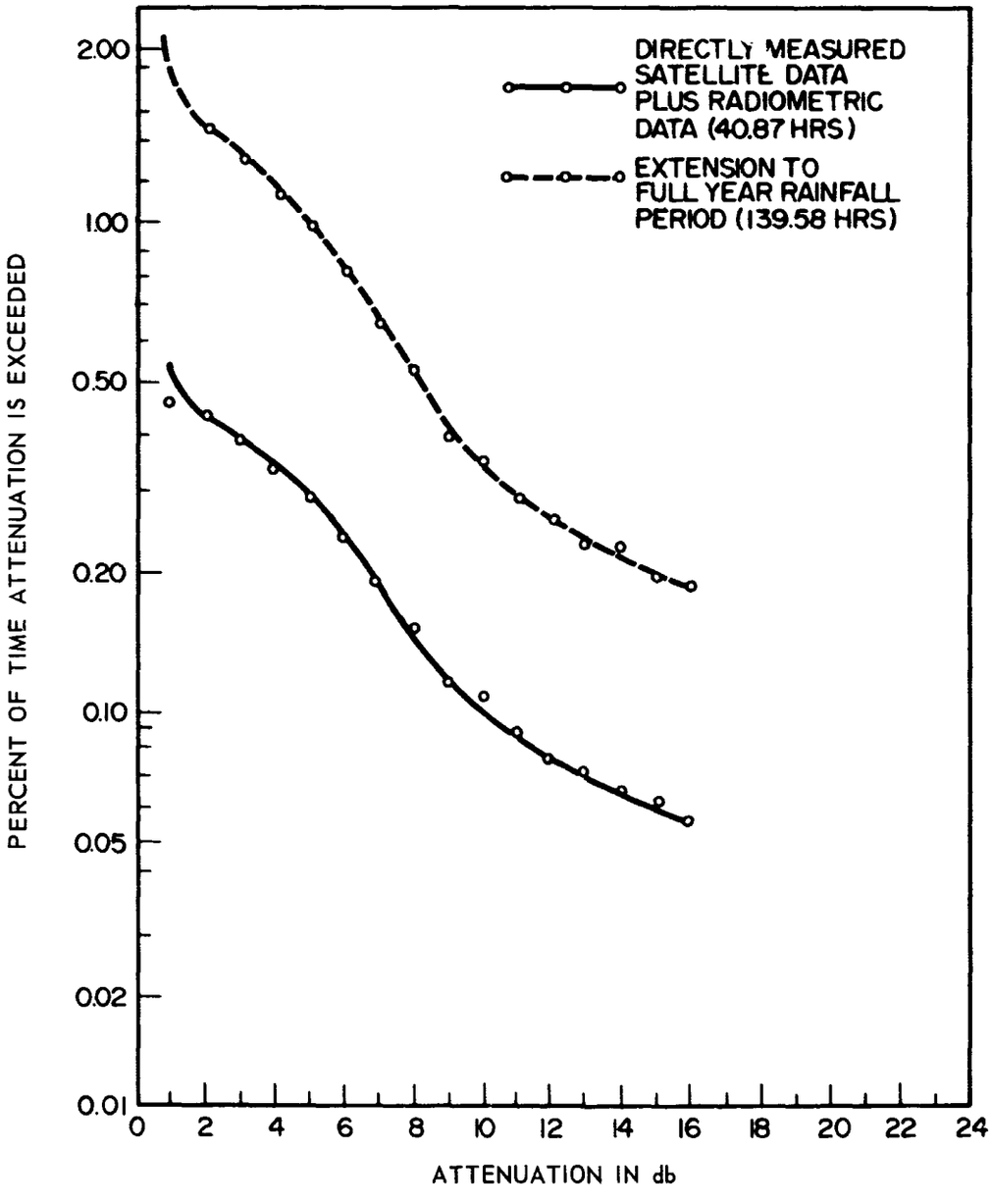

Figure 36. Cumulative Distribution of 31.65 GHz Carrier Attenuation for 1 Year Period (10/1/69 to 9/30/70) At Rosman, North Carolina, Based on Directly Measured Satellite Data And Radiometric Data.

ATTENUATION, EMISSION AND BACKSCATTER BY PRECIPITATION

John I. Strickland
Communications Research Centre
Department of Communications
Ottawa, Canada

1. INTRODUCTION

The experimental determination of precipitation attenuation along slant paths has been hindered by the lack of suitable sources of radiation at the desired frequencies. Experiments conducted at the Communications Research Centre (CRC), Ottawa, Canada in 1967[1] and 1968[2] used an aircraft equipped with microwave beacons at 4, 8 and 15 GHz to measure slant path attenuation. Simultaneous measurements of backscatter along the propagation path were obtained with a weather radar, and measured path attenuations were compared with those calculated from the radar data.

Since September 1969, the ATS-5 satellite has provided an appropriate source of coherent radiation at 15.3 GHz. The Communications Research Centre is participating as an independent experimenter in the NASA ATS-5 Millimetre Wave Experiment as part of a continuing study at CRC of microwave propagation. In the present experiments, as in the earlier experiments using beacons carried by an aircraft, a weather radar is used to determine the spatial distribution of intensities of backscattered radiation, at 2.9 GHz, from precipitation along the propagation path. The attenuations measured using ATS-5 are compared with those calculated from the radar data. In addition, path attenuations can be predicted from measurements of sky temperature in the direction of the satellite. The comparison of attenuations measured directly at 15.3 GHz with those predicted from sky temperature and radar backscatter measurements will be discussed in this paper.

2. THEORY

The radar equation for a pulse volume uniformly filled with raindrops can be written[2] as

$$Z = C_R \, \ell^2 \, \bar{P}_r$$

These measurements have been carried out at the Communications Research Centre as a part of the research program of the Department of Communications, Canada.

where Z is the radar reflectivity factor of the rain, $\bar{P}_r$ is the average received power, ℓ is the distance from the radar to the pulse volume, and C_R is a constant including not only the characteristics of the radar but also the dielectric constant of the raindrops. It is assumed that the raindrop diameters are much less than the wavelength, and that the signal is unattenuated by rain, an assumption that is justified for a frequency of 2.9 GHz. Because of the fluctuating nature of the power backscattered from an ensemble of randomly distributed scatterers, such as rain, several independent samples of P_r are required to estimate the average received power $\bar{P}_r$.[3] Alternatively, an estimate of $\bar{P}_r$ can be obtained from the maximum received power in a set of n measured values of P_r by applying a correction which depends on n.[4] Since the radar signal is not significantly attenuated by the rain, the radar reflectivity factor can be related to the rainfall rate R by an equation of the form $Z = aR^b$, where a and b are constants, independent of frequency. Similarly, for frequencies which are attenuated, the specific attenuation A (dB/unit length) varies with rainfall rate as $A = kR^{\gamma}$, where k and γ depend on frequency. By combining these equations, the path attenuation A′ is given by

$$A' = C \sum_i Z_i^{\beta} \Delta r_i \qquad \text{(in db)}$$

where c and β depend on frequency, and the summation is over all intervals of path length Δr_i from which significant echoes are received. The values of c and β used were derived from the standard Z-R and A-R relations and are given by 7.15×10^{-4} and 0.725 respectively.

For most meteorological conditions, calculated path attenuations show generally good correlation with those measured directly. However, path attenuations calculated from radar data can be excessive if the radar beam includes hydrometeors of enhanced reflectivity, such as hail, snow, or melting snow.

Path attenuations may also be calculated from measurements of the sky temperature provided it can be assumed that attenuation arises primarily from absorption. For large loss factors, the measured sky temperature T_S approaches T_R, the temperature of the absorbing medium, and thus the predicted attenuation A′ is strongly influenced by the assumed value of T_R and inaccuracies in the measured value of T_S. In this work, a rain temperature of 275°K is assumed.

3. EXPERIMENTAL ARRANGEMENT

The ATS-5 satellite is in a near geo-stationary orbit and is visible from Ottawa at an average elevation angle of 30°. Due to launch difficulties, it is

spinning at approximately 76 rpm. Since the satellite employs an earth-coverage antenna, the received signal at 15.3 GHz consists of a 40 millisecond pulse every 785 milliseconds. Although the original output power of the main transmitter was 250 milliwatts, this power has dropped twice resulting in a stable transmitted power of approximately 30 milliwatts. The back-up transmitter on ATS-5 provides 250 milliwatts output. Its usefulness in the measurement of attenuation is restricted, however, since it can be energized only for short periods of time.

A block diagram of the experimental system is shown in Figure 1. The receiving antenna consists of a 30 foot precision paraboloidal reflector and a modified near-field Cassegrainian feed system.[5] No radome is used, and the design of the feed system ensures that the waveguide window remains dry at all times. The required antenna position is determined every second by the computer using linear interpolation between calculated values of azimuth and elevation tabulated at hourly intervals. Offsets in azimuth and elevation can be entered into the computer at any time to adjust the actual position of the antenna and ensure reception of the maximum possible signal.

The received signal is down-converted to 60 MHz using Schottky-barrier mixer diodes and a gain stabilized preamplifier of 20 MHz bandwidth. A portion of the 60 MHz signal is sent to a phase-lock receiver, which acquires phase-lock on each signal pulse from the satellite. The output of the receiver, which is very nearly proportional to the logarithm of the received signal power, is stored by a peak-riding detector with an automatic reset synchronized to the rotation period of the satellite (Figure 2). The output of the peak-riding detector is sampled by an A/D converter every 50 milliseconds, and the maximum voltage in a one second interval is retained. The overall resolution of the receiver and peak-riding detector is better than 0.2 dB. The receiver retains phase-lock on signals as low as -133 dBm, resulting in a dynamic range of about 18 dB when receiving the main transmitter of the ATS-5 satellite.

The remaining portion of the 60 MHz signal is amplified by a gain-stabilized 60 MHz amplifier of 10 MHz bandwidth and detected by a square-law detector to form a total power radiometer. The output, integrated with a 2 second time constant, is sampled by the computer. The theoretical sensitivity of the radiometer is 0.2°K. With gain stabilization and a controlled temperature environment for all amplifiers, the uncertainty in the measured temperature due to gain instability is less than ±2.5°K. A total power radiometer introduces no radio frequency losses due to radio frequency switching components, and since the signal to the phase lock receiver is unaltered, no degradation of the phase lock loop acquisition or hold thresholds occurs. Since the radiometer uses the main receiving antenna, its beamwidth is 0.15 degrees, and alignment with the propagation path is ensured.

Backscatter from precipitation is measured by a weather radar operating at 2.86 GHz, a frequency at which attenuation by rain is insignificant. A 10 foot diameter antenna provides a conical beam of 2.3 degrees width. The radar is operated with a peak output power of approximately 150 kW, a pulse width of 0.67 μs, or 0.1 km in space, and a pulse repetition time of 682.7 μs resulting in a maximum range of 102.4 km. The overall dynamic range, including the logarithmic IF amplifier, is greater than 70 dB.

The two principal modes of operation of the radar antenna are computer and slave. In computer mode, the antenna follows a programmed scan determined by the computer. The antenna in incremented in azimuth by 2 degrees every second, requiring 3 minutes to complete one azimuthal sweep. Within each second, the antenna is virtually stationary for 0.7 seconds during which time A-scan data is acquired. A complete scan cycle consists of 3 such azimuthal scans at elevation angles of 5, 10 and 20 degrees. A survey of precipitation within a slant range of 100 km of the radar is obtained for three elevation angles every 10 minutes.

During periods for which it is expected that the signal from the satellite will be attenuated by precipitation, the radar antenna is pointed in the same direction as the 30 foot receiving antenna to record backscatter from precipitation along the satellite-earth propagation path.

Radar backscattered power as a function of range is sampled with a device which is an extensive modification of one described previously.[6] The basic time interval, or range gate of the device, has been reduced to 0.67 μs, which corresponds to a range quantization interval of 0.1 km. A transmitter pulse occurs over 1024 range gates. Following each transmitter pulse 16 samples of the radar video output, each separated in time by 64 range gates, are obtained. Thus 64 transmitter pulses, or 42.7 milliseconds, are required to obtain one complete digital A-scan. For convenience, successive A-scans are acquired every 50 milliseconds. During the acquisition of each A-scan within a 0.7 second period, the return within each range gate is retained only if it exceeds that recorded previously. An estimate of the backscattered power and hence radar reflectivity factor is obtained for each range interval from the maximum of 14 samples of backscattered power. One complete digital A-scan consists of 1024 such estimates of backscattered power. An additional 0.3 seconds is required for data manipulation and recording on digital magnetic tape. Thus, radar data specifying the power backscattered from precipitation as a function of range at a given azimuth and elevation can be acquired every second.

4. RADAR REFLECTIVITY FACTOR

The radar constant, C_R, is calculated from the measured parameters of the radar system, assuming an antenna efficiency of 40%.

Values of reflectivity factor for precipitation are then calculated. Attenuations, predicted from these values of reflectivity factor, are smaller than those directly measured using the ATS-5 satellite. They can be brought into agreement, as are done here, by an increase in the radar constant of 5 dB. This discrepancy agrees with that found by McCormick [2] although the receiving system has now been completely changed, and further investigation is being carried out.

When the radar antenna is pointed at the satellite, values of the reflectivity factor of precipitation within the radar volume centred on the propagation path from the satellite are obtained as a function of slant range and time. By rounding these values of reflectivity factor to the nearest 10 dBZ (db above $Z = 1\ mm^6/m^3$), contour maps are constructed which show the passage of cells of precipitation through the radar volume and hence across the propagation path from the satellite.

5. RESULTS

The millimetre wave transmitters on the ATS-5 satellite were first energized on September 27, 1969. On that date, and at frequent intervals since then, the received signal strength of the beacons has been measured at CRC during both clear weather and periods of precipitation. During periods of light to moderate rain, attenuations up to 5 dB have been observed. On a few occasions, heavier precipitation has caused attenuations exceeding 10 dB. Two such events will be discussed.

The received signal strength and attenuations predicted from radiometric and radar measurements for the period 2000-2030 GMT on 29 June 1970 are shown in Figure 3. Attenuation of the 15.3 GHz signal exceeded 10 dB on two occasions for a total time of approximately 3.8 minutes. Attenuations predicted from the radiometric data agree very closely with those measured directly, except for the peak of attenuation at 2010. In this case, the measured attenuation exceeds 14 dB, whereas the maximum attenuation predicted by the radiometer is only 8 dB. Since the radiometer beamwidth at a distance of 10 km is only 25 m, the rain cell almost certainly filled the radiometer beam at this time. It is possible that, for this cell, scattering by rain caused a significant portion of the attenuation observed at 15.3 GHz.

Attenuation of the satellite signal exceeded the dynamic range of the receiver from 2015 to 2018 GMT. The attenuation predicted from the radiometer data exceeds 20 dB during this period. However, as stated previously, accuracy of the prediction decreases as the attenuation increases, and predicted values which exceed approximately 10 dB are expected to be greatly in error.

Attenuations predicted from the radar data agree fairly closely with those measured directly. The predicted attenuation exceeds 14 dB for more than 3 minutes, in good agreement with the measured attenuation. In addition, the radar predicted attenuation shows a small maximum of approximately 6 dB at 2012. This is probably due to precipitation which is illuminated by the radar antenna but which does not significantly intercept the direct propagation path from the satellite or the radiometer beamwidth.

The radar map for this period shows three areas whose reflectivity factor is 50 dBZ. Two small areas of 60 dBZ correspond to the first peak of attenuation. The second peak of attenuation exceeding 14 dB is due to the large area of 50 dBZ, including two areas of 60 dBZ, which lasted from 2015 to 2018 GMT. The third area of 50 dBZ extending from 2011 to 2014 is responsible for the additional radar predicted attenuation of 6 dB.

The received signal strength and attenuations predicted from radiometer and radar measurements for the period 2210-2310 GMT on 20 July 1970 are shown in Figure 4. From 2248 to 2301, attenuation of the satellite signal exceeded the dynamic range of the receiving system. At 2301, the attenuation decreased sufficiently that phase lock was achieved. At 2302, the main transmitter was turned off and the back-up transmitter turned on at the request of another participant. Since the transmitted frequency had changed by more than 30 kHZ, phase lock was not achieved until 2306. However, the attenuation even was essentially complete, and no additional attenuation data were obtained.

The attenuations predicted from the radiometer data agree very closely with those measured directly for the interval from 2210 to 2248. However, at 2248, the predicted attenuation does not increase as rapidly as that measured directly. For less than 30 seconds before the main transmitter was turned off at 2302, the predicted and directly measured attenuations could once again be compared and show very good agreement.

Attenuations calculated from the radar data agree fairly well with the measured attenuations, although not, in general, as well as those predicted by the radiometer. However, the increase in attenuation at 2248 calculated from the radar data agrees very closely with that measured directly. In addition, the radar data predict a peak attenuation of nearly 32 dB, which would be unobservable with either the radiometer or the ATS-5 satellite.

The radar map for this period shows an area having a reflectivity factor of 60 dBZ from 2248 to 2256. For this time interval, the radiometer predicted attenuations are smaller than those measured directly, whereas the radar predicted attenuations show close agreement. Reflectivities of 50 dBZ extend from 2245 to 2305. From 2256 to 2310, the radar data underestimate the radiometer predicted and directly measured attenuations.

6. CONCLUSIONS

Path attenuations at 15.3 GHz have been calculated for slant paths of 30 degrees elevation from simultaneous measurements of sky temperature at 15.3 GHz and radar backscatter measurements at 2.86 GHz. These predicted attenuations have been compared with path attenuations measured directly using the ATS-5 satellite beacons at 15.3 GHz. Generally good agreement between measured and predicted attenuations has been found.

7. ACKNOWLEDGMENTS

The use of beacon transmitters at 15.3 GHz on the ATS-5 satellite launched by the United States National Aeronautics and Space Administration and the kind cooperation of the Applications Technology Satellite Control Center is gratefully acknowledged.

REFERENCES

1. Strickland, J. I. and K. S. McCormick, "Slant Path Microwave Attenuation due to Precipitation," IEE Conference on Tropospheric Wave Progation, Conference Publication No. 48, pp. 143-150, London, 1968.

2. McCormick, K. S., "Simultaneous Measurements of Precipitation Attenuation and Radar Reflectivity at Centimetre Wavelengths," Preprints of the 14th Radar Meteorology Conference, Am. Meteor. Soc., Boston, pp. 19-24, 1970.

3. Marshall, J. S. and W. Hitschfeld, "Interpretation of the Fluctuating Echo from Randomly Distributed Scatterers" – Part 1, Can. J. Physics, Volume 31, pp. 962-994, 1953.

4. Smith, P. L., Jr., "Interpretation of the Fluctuating Echo from Randomly Distributed Scatterers" – Part 3, Stormy Weather Group Report MW-39, McGill University, Montreal, December 1964.

5. Cogdell, J. R., et al, "High Resolution Millimeter Reflector Antennas, IEEE Trans. on Antennas and Propagation," AP-18, pp. 515-529.

6. Pawzuik, W. J., K. S. McCormick and N. K. Hansen, "A Digital System for Recording Radar A-Scans," Proc. Thirteenth Radar Meteorology Conference, Am. Meteor. Soc., Boston, pp. 336-338, 1968.

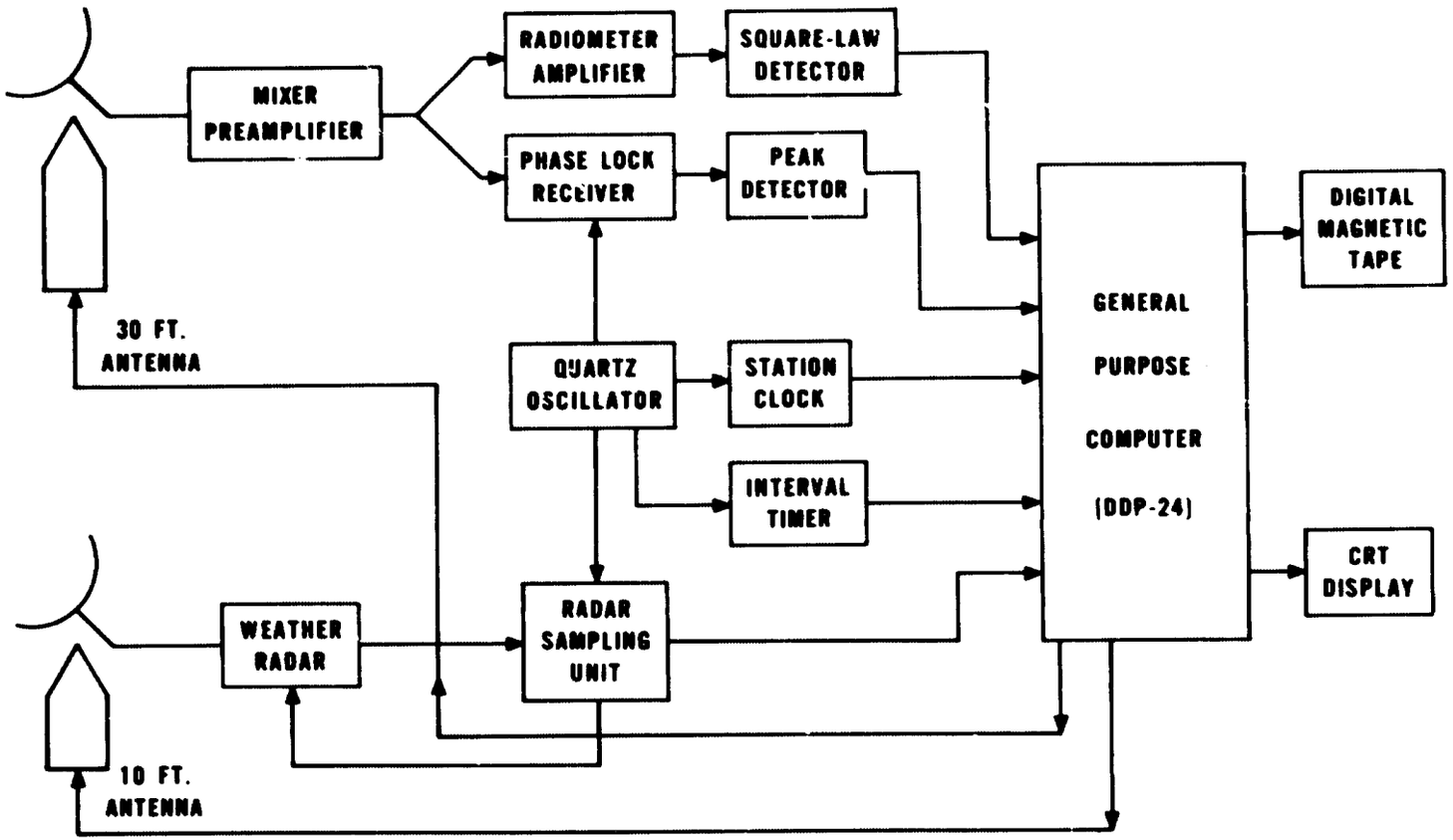

Figure 1. Block diagram of the experimental system

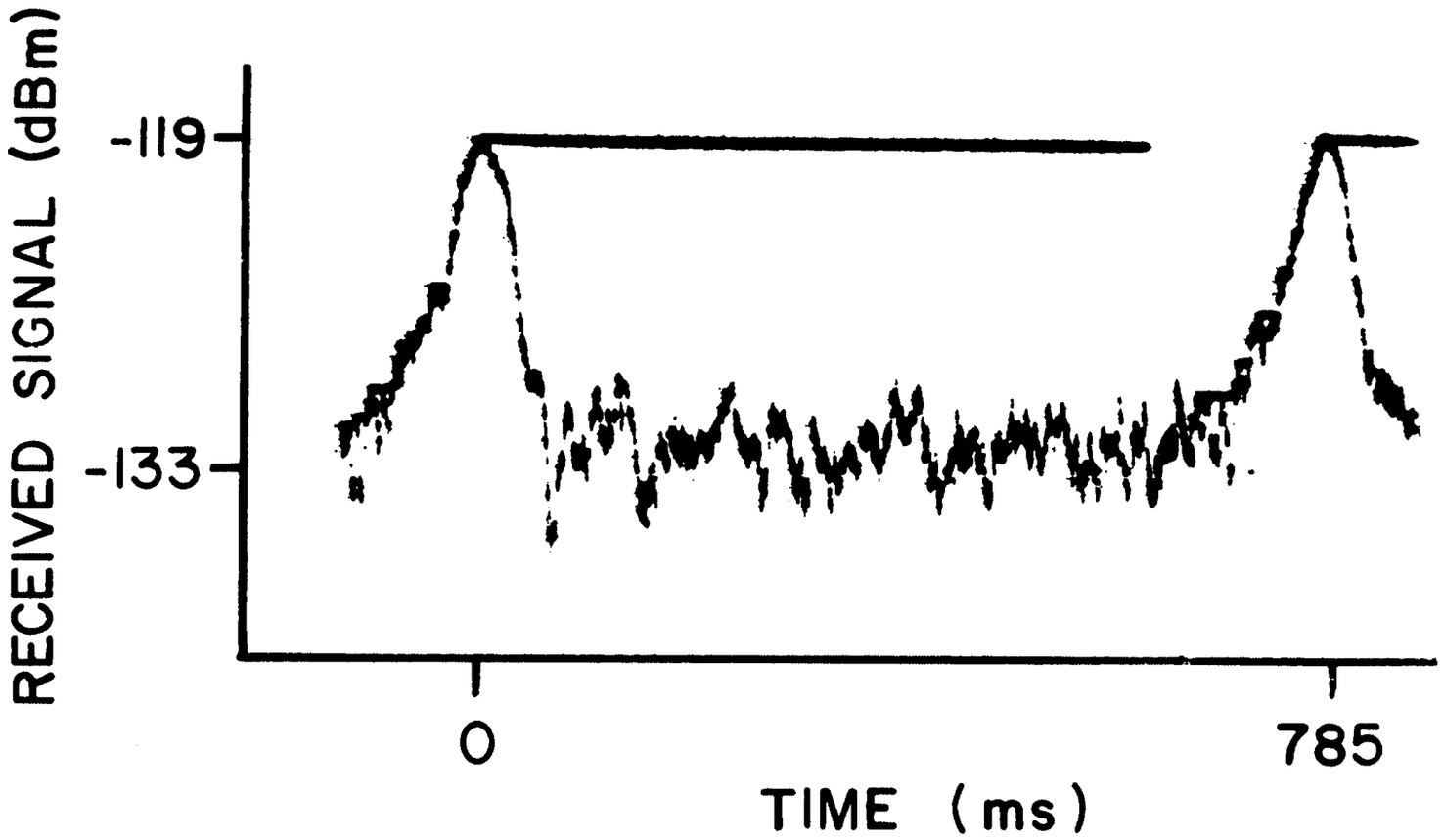

Figure 2. Phase lock receiver output showing the received signal pulse from the ATS-5 satellite. The output of the peak-riding detector is superimposed for comparison.

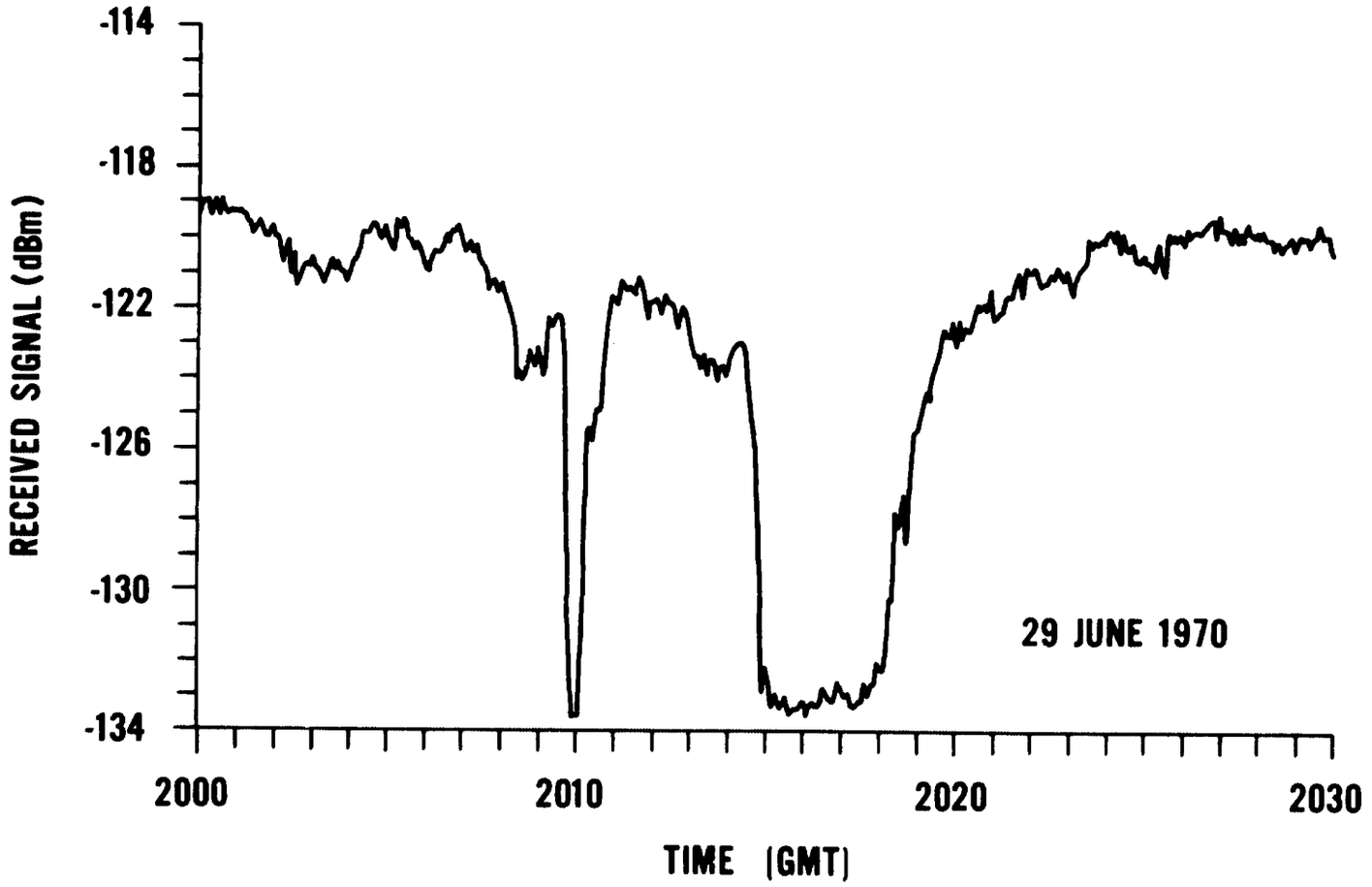

Figure 3(a). Received signal strength – 29 June 1970

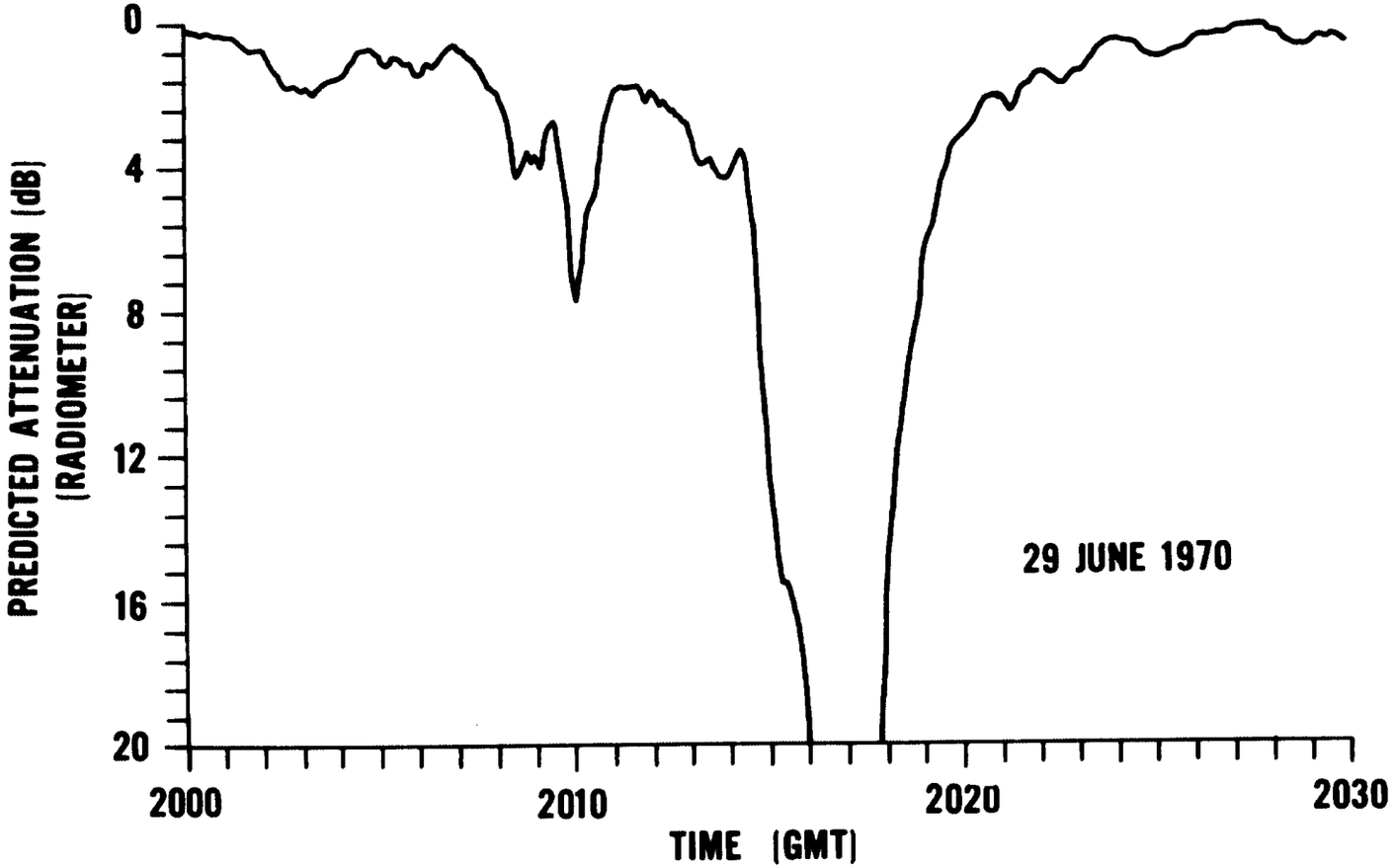

Figure 3(b). Attenuations calculated from sky temperature measurements
29 June 1970

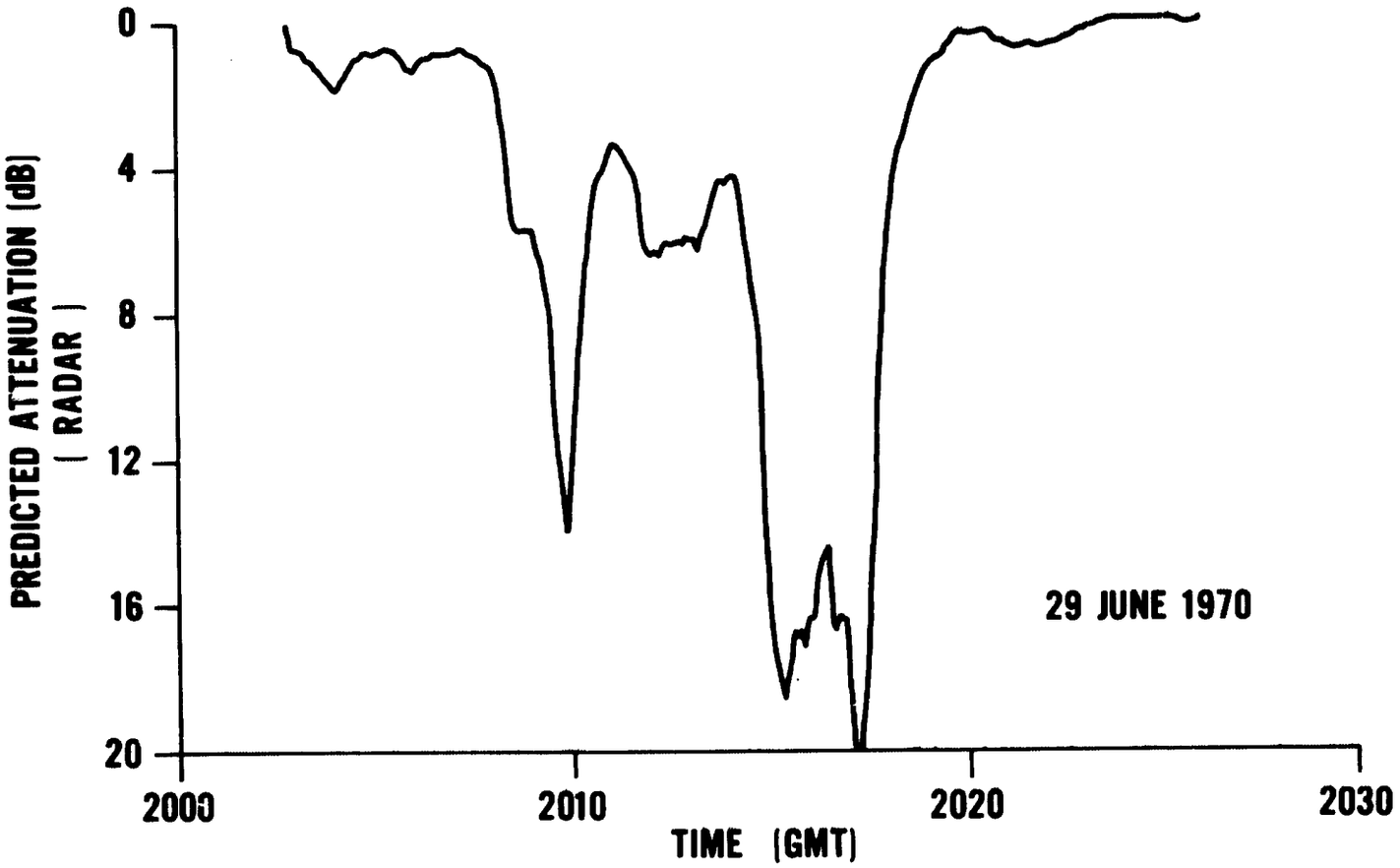

Figure 3 (c). Attenuations calculated from radar backscatted power measurements – 29 June 1970

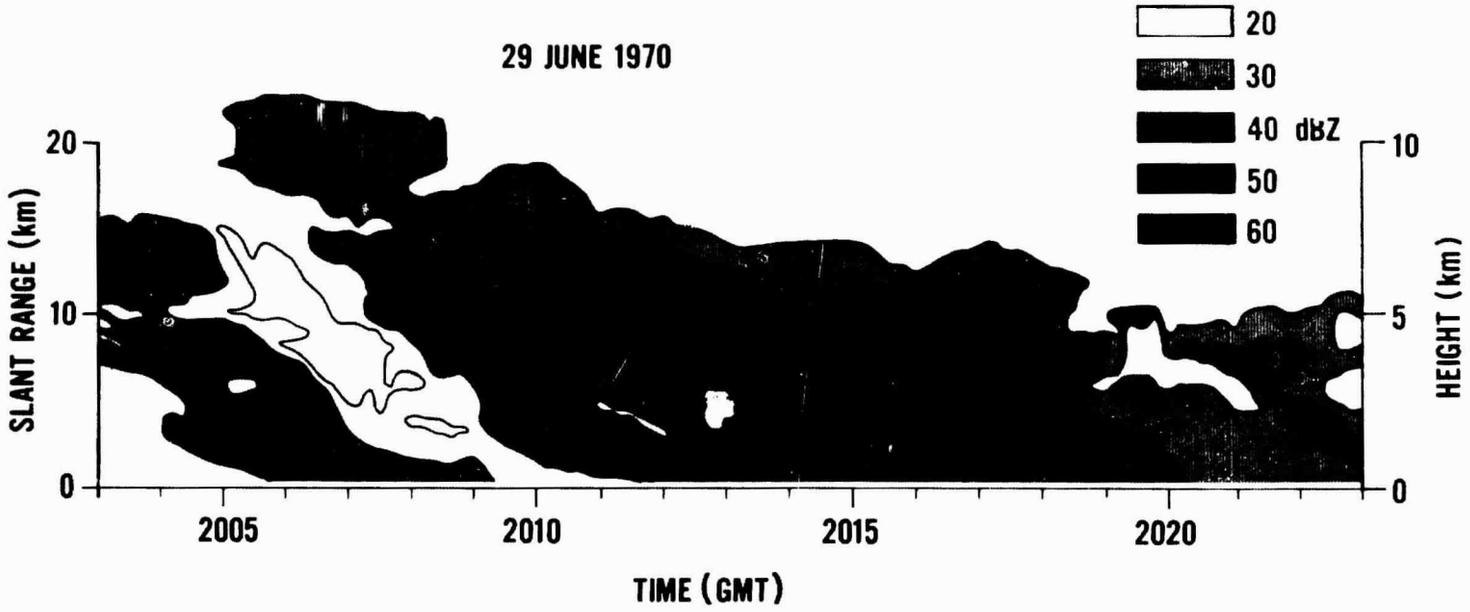

Figure 3 (d). Radar reflectivity map - 29 June 1970. An area of 50 dBZ includes all reflectivites from 45 dBZ to 55 dBZ, etc.

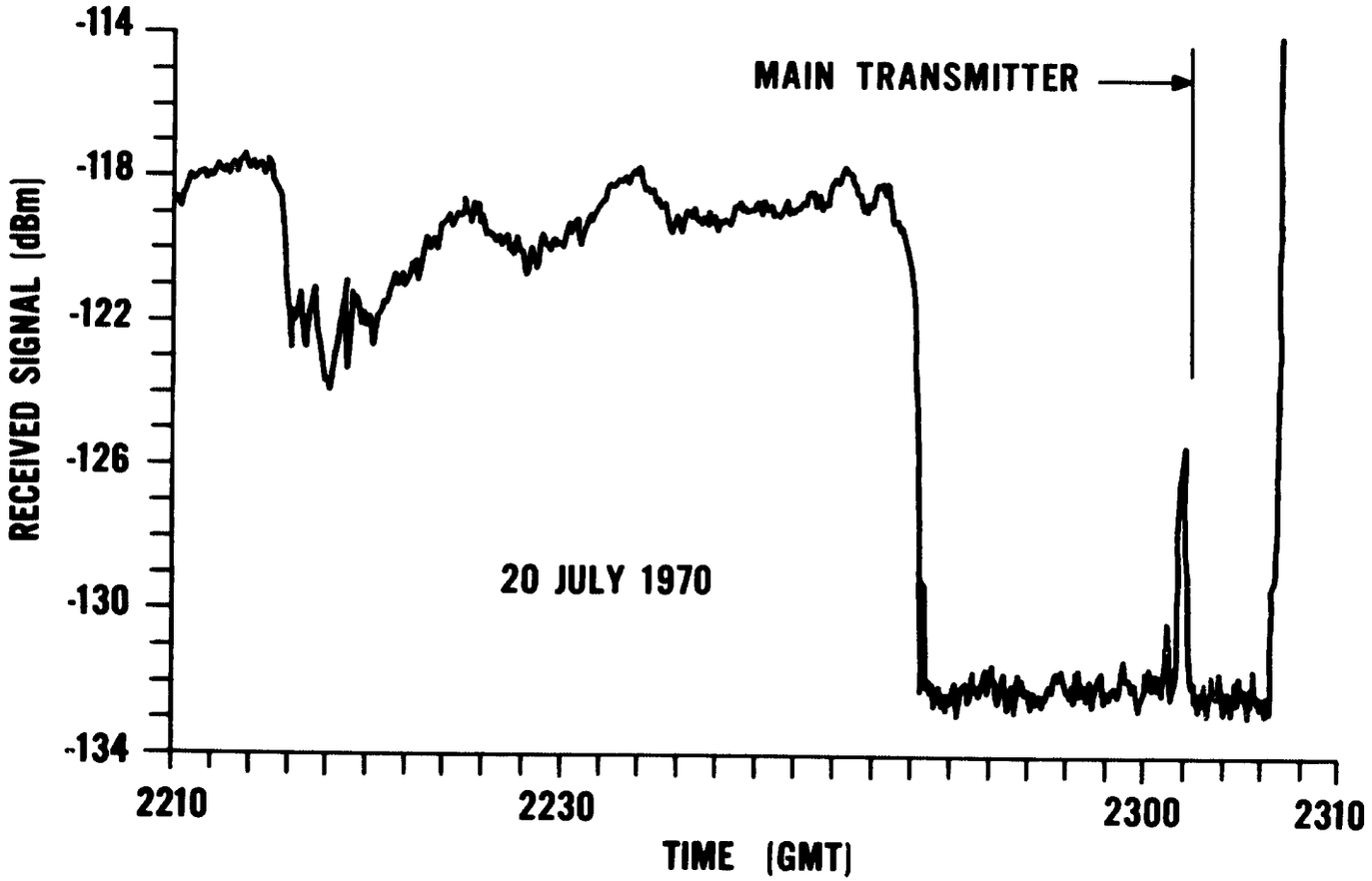

Figure 4(a). Received signal strength – 20 July 1970

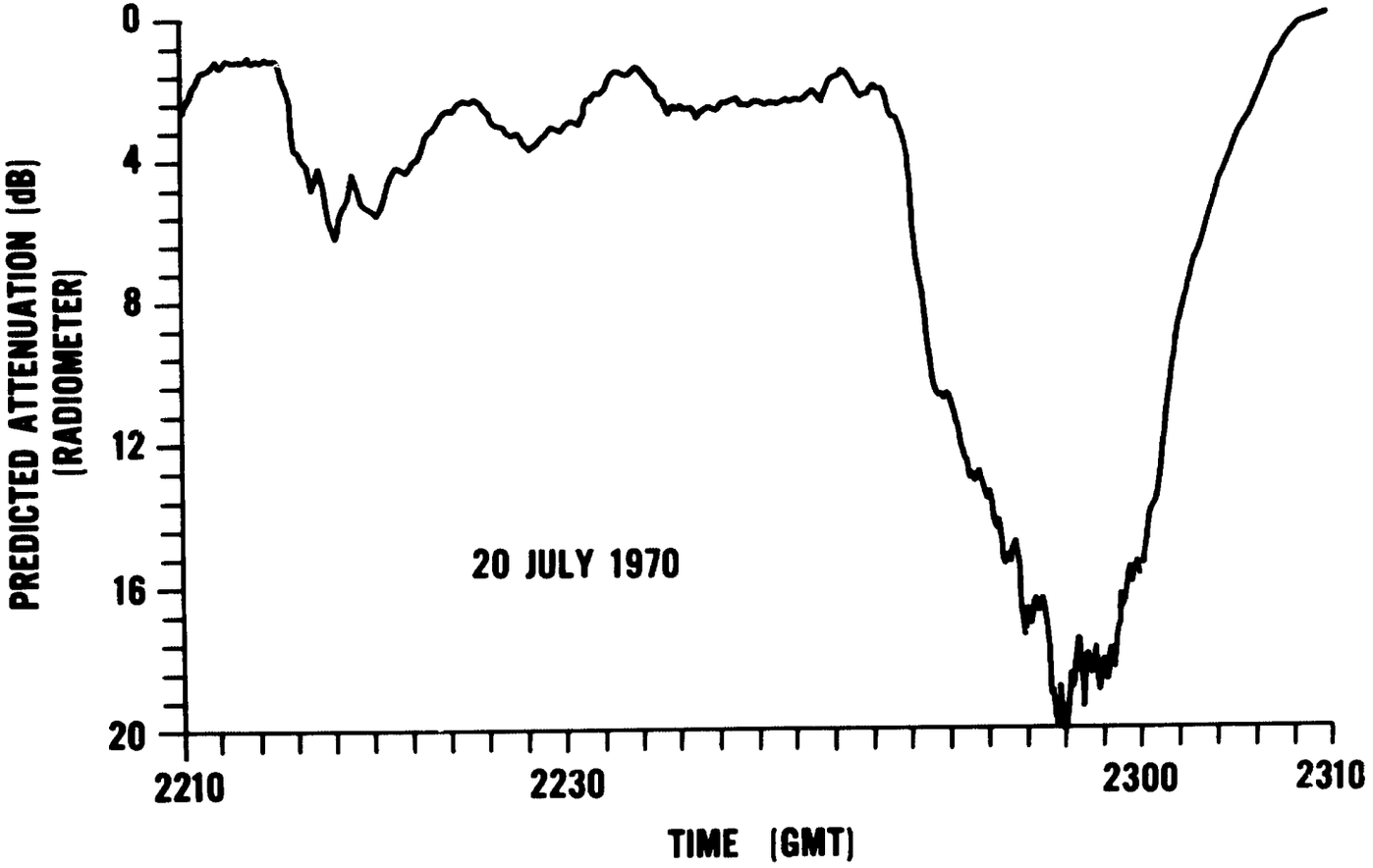

Figure 4(b). Attenuations calculated from sky temperature measurements
20 July 1970

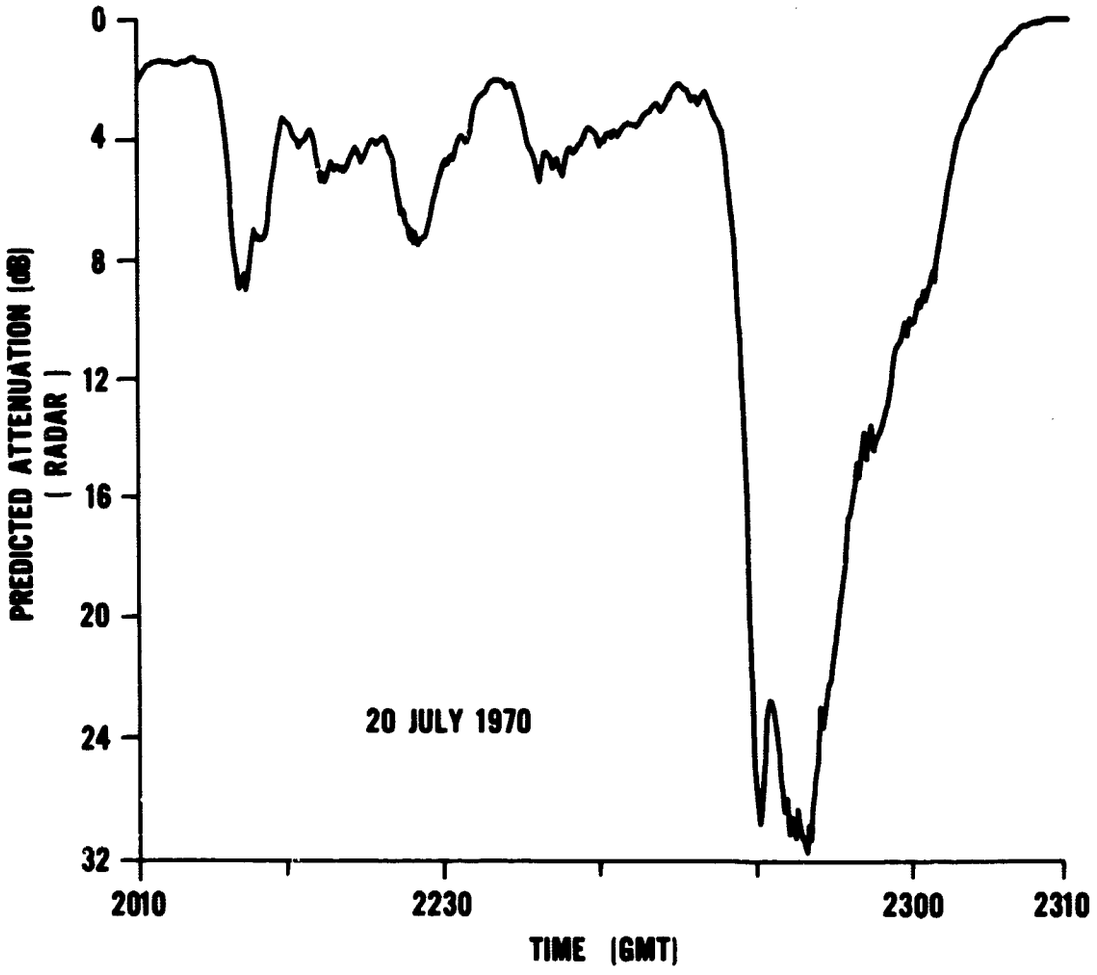

Figure 4 (c). Attenuation calculated from radar backscattered power measurements - 20 July 1970

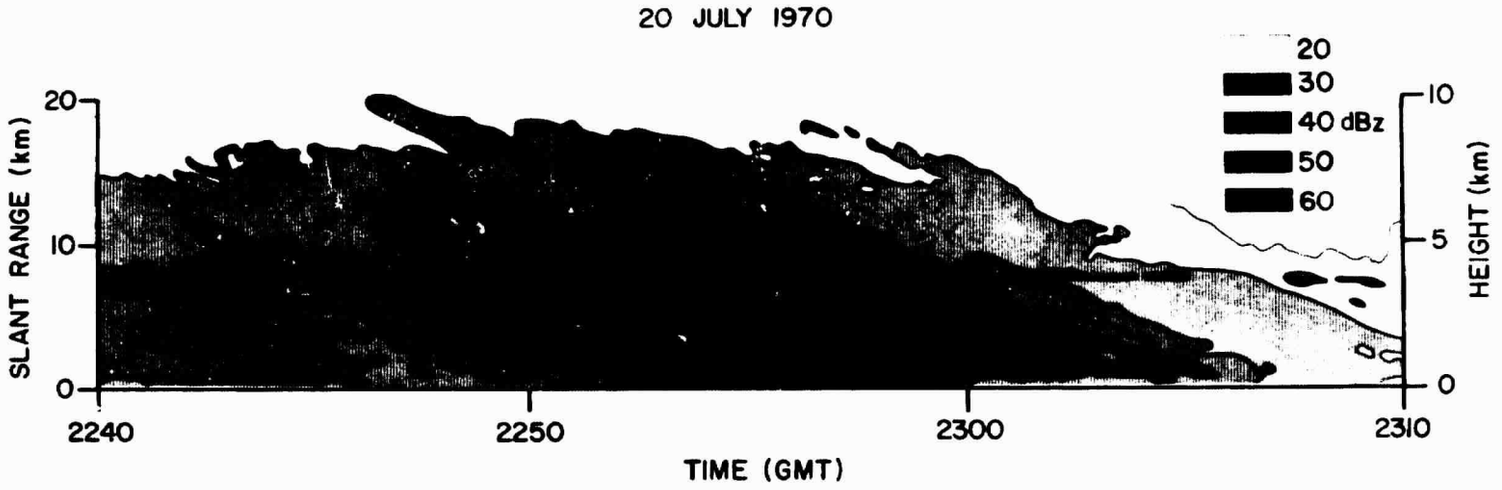

Figure 4 (d). Radar refelctivity map - 20 July 1970. An area of 50 dBZ concludes all reflectivities from 45 dBZ to 55 dBZ, etc.

PROPAGATION DATA FROM CRAWFORD HILL

A. A. Penzias
Bell Telephone Laboratories, Incorporated
Crawford Hill Laboratory
Holmdel, New Jersey

A considerable amount of rain attenuation data has been obtained in the 16- and 30-GHz sun tracker and 16-GHz radiometer programs underway at the Crawford Hill Laboratory.[1,2] From the data obtained by radiometer measurements, one may calculate the attenuation expected on an earth-space path by assuming a value for the effective temperature of the rain. Such attenuation calculations are in good agreement with sun tracker measurements.[1] One of the principal aims of the present experiment was to check further the validity of the radiometer results by comparing the attenuation deduced from 16-GHz radiometer data with the attenuation measured directly by transmission from the 15.3-GHz transmitter aboard the Fifth Applications Technology Satellite.

The receiving antenna was the 20-foot horn-reflector at Crawford Hill. Although originally designed for the 2.39-GHz Echo project, it was found to be quite satisfactory at 15 GHz, having a gain of 57.3 dB and a 45% aperture efficiency.

The measurement employed two separate RF systems, the 15.3-GHz receiver and a 16-GHz radiometer supplied by R. W. Wilson. These were mounted at the antenna throat to receive orthogonal polarizations, with their outputs recorded simultaneously on a two-pen chart recorder.

The receiver used a conventional 15.3-GHz waveguide balanced mixer receiver with an IF amplifier 100-kHz wide at 70 MHz. Since signal phase information was not required, no phase locking to the signal was used; the local oscillator was merely stabilized at 15,230 MHz.[3] The output of the IF detector was connected through a capacitor to a peak detector. This peak detector was sensitive only when the transmitted signal was "on," hence approximately maintaining the signal to noise ratio expected without spinning of the satellite. The time constant of the circuit was designed to be ~4 sec in order to reduce the noise fluctuation level by "averaging" over about four pulses. The minimum peak pulse power that could be reliably detected by this system was -132 dBm.

Data were taken at our site for rainstorms occurring during the time the satellite was transmitting in the three-month period following the initial ATS-5

transmitter turn-on in October 1969 as well as in the late Spring and early summer of 1970. The maximum attenuation for which reliable data was obtained was 12 dB. Because of the simplicity of the receiver, the station normally operated unattended.

Figure 1 shows a portion of the chart record obtained on June 5, 1970. The lower curve of Fig. 1 is a logarithmic representation of received peak signal power. The scale is 4 dB per large division; time increases to the left. The thickened line at the right is the noise fluctuation level of the receiver in the absence of a signal. After transmitter turn on, the satellite signal is seen to increase in power, then level off at a steady value, with dips in the record due to rain attenuation. (The sharp spike at the extreme left of the lower curve is a time marker.)

The upper curve is the radiometer record, taken simultaneously on the same chart. Because both pens are designed to travel the full width of the chart, they are displaced by about two millimeters in order to pass each other freely. Thus simulteneous events are displaced on the records by about one tenth of a large division. This effect can be readily seen on the record by noting that all features on the upper record appear slightly to the right of corresponding features on the lower record. No actual time delays were found for any of the features occurring on the two records, within the limits of our measurement accuracy.

Although the excellent correspondence of the detailed structure in the two curves is evident from even a cursory examination of the figures, the fact that these pairs of features also correspond to the same attenuation require some analysis. The radiometer features appear deeper and broader than those in the corresponding satellite signal because of the inherent nonlinearity of the radiometer record. The middle line of the chart corresponds to an effective input temperature equal to the temperature of the reference termination of the radiometer, 295°K. Temperature is plotted on the chart decreasing upward, reaching the value in the absence of rain near the top of the chart. We take this point on the scale to be zero in our calculations since the effect of the background is negligibly small to the accuracy of our measurements, never exceeding 0.05 dB correction. Thus, having set our scale in terms of equivalent radiometer input noise temperature, T_I, we can compute an attenuation by solving the relation,

$$T_I = T_R (1 - e^{-\alpha})$$

where T_R is the effective temperature of the rain and α is the attenuation at the radiometer frequency. Thus

$$\alpha_{15\ GHz} = \frac{-\ell n \left(\frac{T_R - T_I}{T_R} \right)}{0.23} \quad db$$

The corresponding attenuation at 15.3 GHz which is required for comparison with the satellite data can readily be obtained from the relation

$$\alpha_{15.3\ \mathrm{GHz}} = \alpha_{16\ \mathrm{GHz}} \left(\frac{15.3}{16}\right)^2$$

since the attenuation due to rain is approximately proportional to the square of the frequency at the wavelengths in question.

In order for radiometer data to provide useful attenuation data one must have a method for determining T_R. Since T_R is determined both by the physical temperature distribution in the rainstorm as well as the effects of scattering, an analytic approach is difficult. It seems most profitable to determine T_R empirically from attenuation measurements. Indeed, it is fair to say that the main purpose of our experiment is the determination of T_R for use in radiometer studies.

In order to test the ability of the radiometer to provide accurate attenuation statistics, the data shown in the Fig. 1 was analyzed on a time-attenuation basis. The percent of time during the 9 hour period that the satellite signal attenuation exceeded each of the one dB steps, to ten dB, was computed and plotted as horizontal dashes in Fig. 2. A similar computation was made for the radiometer data using two "reasonable" values for T_R, 273°K and 285°K (open and filled circles, Fig. 2). These two values for the temperature are seen to bracket the actual data rather well. The scatter in the points due to the limited size of the sample is evident in the figure. (A dashed curve approximating the smoothed satellite data is included in Fig. 2.) Evidently the use of 273°K for storms such as those shown could provide conservative but useable attenuation statistics. The use of 285°K would provide somewhat optimistic results.

Another approach, used extensively by R. W. Wilson with his sun tracker data, is to treat T_R as the unknown quantity and compute it from a combination of the measured attenuation and corresponding radiometer data. A compilation of temperatures computed from the satellite data for all recorded rainstorms shows a slow monotonic increase in temperature with increasing attenuation, going from 265°K at 5 dB attenuation to near 275°K at 12 dB. (A similar result has been obtained by Wilson.) An eight degree temperature difference at 6 dB attenuation only amounts to ~ .3 dB which is not large enough to affect most system design considerations. Thus since a value of 273°K fits the higher attenuation data quite well, its use would give results consistent with the data we have obtained in the ATS-5 experiment.

Figure 3 shows all our rainstorm signal attenuation data plotted against attenuation computed from radiometer data using 273°K for T_R. The correlation while not perfrect, is seen to be quite satisfactory.

REFERENCES

1. Wilson, R. W., "Sun Tracker Measurements of Attenuation by Rain at 16 and 30 GHz," B.S.T.J., 48, No. 5, (May-June 1969), pp. 1383-1404.

2. Wilson, R. W., "A Three-Radiometer Diversity Experiment," B.S.T.J., 49, No. 6, (July-August 1970), pp. 1239-1242.

3. Penzias, A. A., "The Microwave Radiometer as a Simple Sensitive Propagation Receiver," to be published.

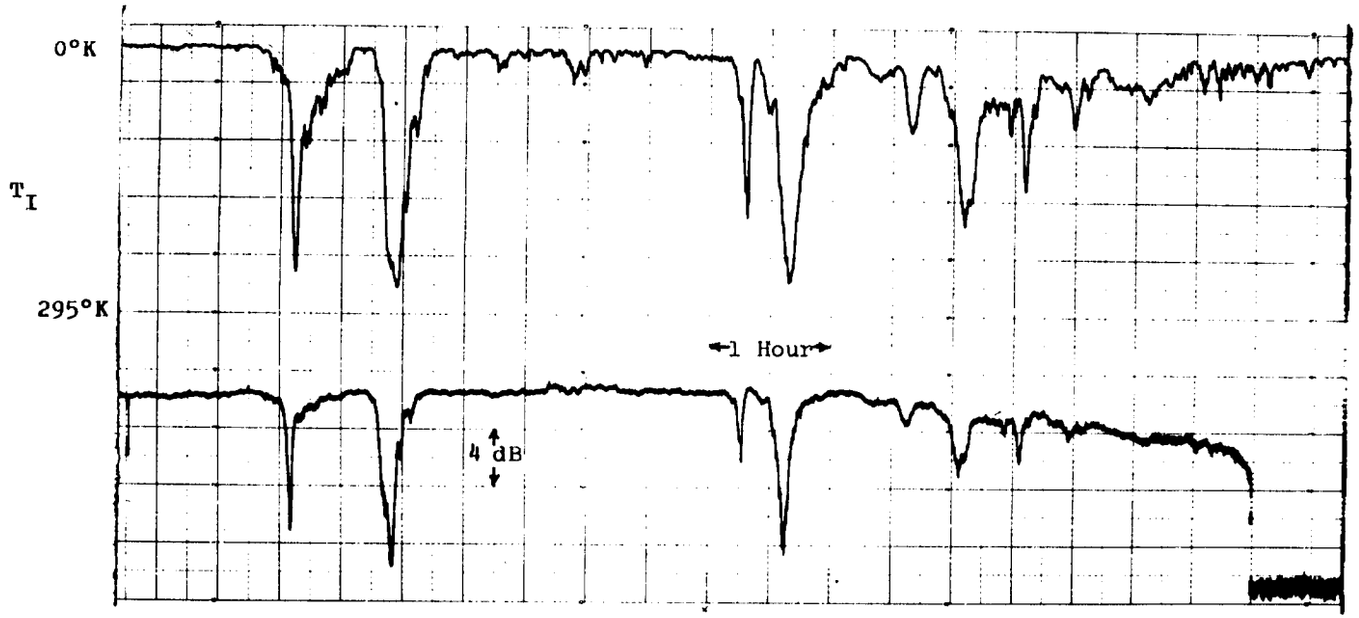

Figure 1.

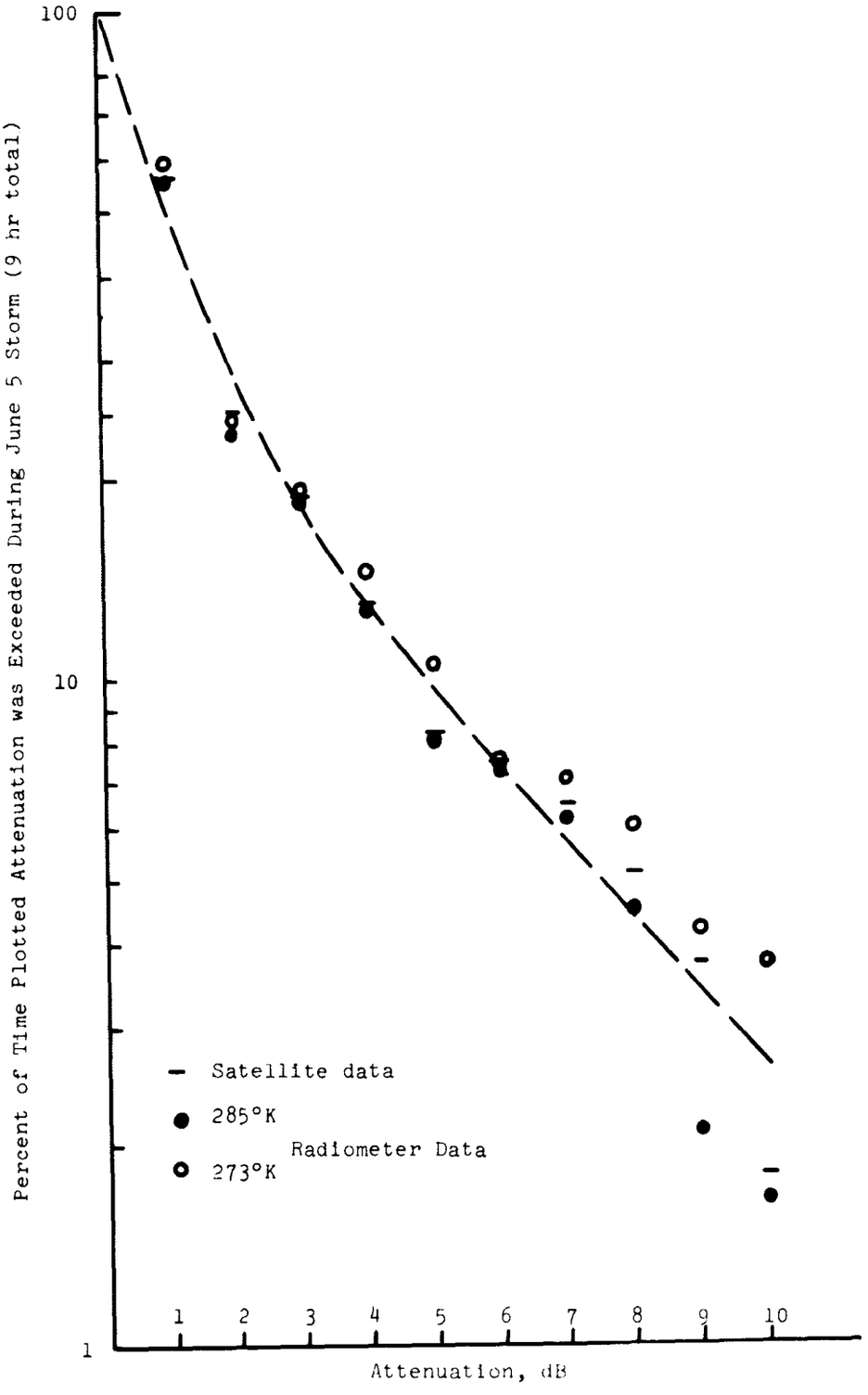
100
10
1
Percent of Time Plotted Attenuation was Exceeded During June 5 Storm (9 hr total)
Satellite data
285°K
Radiometer Data
273°K
1
2
3
4
5
6
7
8
9
10
Attenuation, dB

Figure 2.

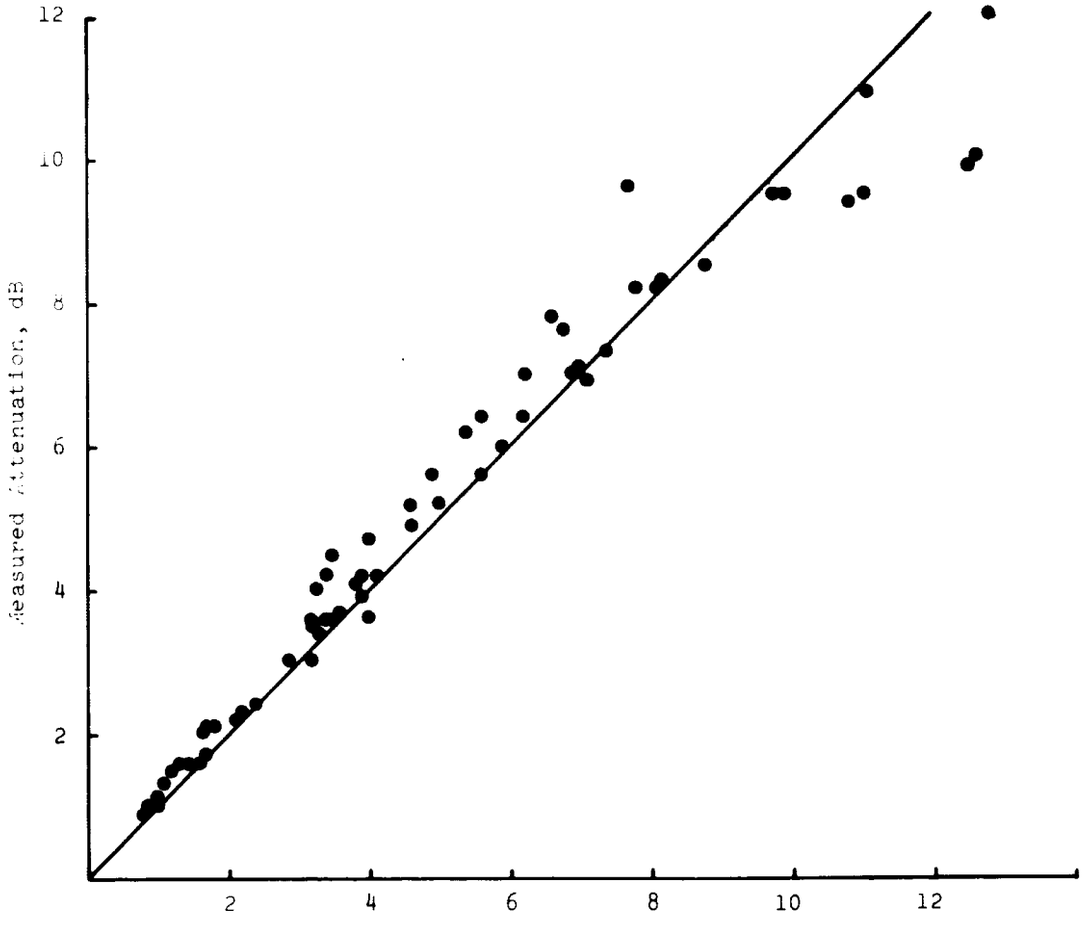
12
10
8
6
4
2
Measured Attenuation, dB
2
4
6
8
10
12
Attenuation, dB, Computed from Radiometer Data T_R = 273°K

Figure 3.

MILLIMETER WAVE PROPAGATION MEASUREMENTS WITH ATS-5 AT COMSAT LABS*

A. Buige, H. D. Craft, Jr., J. Levatich, E. Robertson

COMSAT Labs is participating in a measurement program to collect propagation data at 15 GHz over space/earth paths using transmissions from the NASA ATS-5 satellite. ATS-5 was intended to be capable of radiating a phase-modulated signal, consisting of a carrier at 15.3 GHz and sidebands at ±100 kHz, ±1 MHz, ±10 MHz or ±50 MHz, with respect to the carrier. From these transmissions it was intended to gather data on atmospheric attenuation and coherence bandwidth. However, due to a launch malfunction that resulted in ATS-5 being spin-stabilized rather than gravity gradient-stabilized, and due to a subsequent 9-dB degradation in the satellite transmitter power, it is not possible to obtain the coherence bandwidth measurement. Useful data have been obtained concerning the attenuation due to atmospheric hydrometeors.

Figure 1 shows a block diagram of the overall ATS-5 measurement configuration. The antenna is of the Cassegrain type and is provided with a fully steerable, AZ-EL mount, capable of maintaining a pointing accuracy of .03 degree in a steady wind of 30 miles per hour. The antenna has a parabolic reflector, 16 feet in diameter with an rms surface tolerance of better than 0.025 inch. The hyperbolic subreflector is 1.5 feet in diameter, and has an rms surface tolerance of 0.005 inch. The main reflector is made of fiber glass with a metalized reflecting surface.

The receive system front end, consisting of a tunnel diode amplifier (TDA), a down-converter, and a 1.05-GHz amplifier, is housed in a temperature-controlled enclosure located at the antenna feed. The remainder of the receiving system consists of a 3-channel, phase-locked receiver capable of providing outputs proportional to the received carrier and sideband amplitudes and the relative differential phase of the sidebands with respect to the carrier.

When the ATS-5 is not transmitting, radiometric measurements of the sun noise power or the sky temperature are used for obtaining 15.3 GHz-attenuation. The noise power from the sun collected by the antenna is measured with a total

* This paper is based upon work performed in COMSAT Labs under the sponorship of the International Telecommunications Satellite Consortium (INTELSAT). Any views expressed in this paper are not necessarily those of INTELSAT.

power radiometer. The equivalent antenna noise temperature, T_A, when pointed at the sun is

$$T_A = t\,T_s + (1 - t)\,T_p$$

where T_s is the antenna temperature due to the sun (about 5000°K at 15 GHz for a 16-foot antenna), t is the transmission coefficient of the atmosphere, and T_p is the average physical temperature of the atmospheric hydrometeors. Since T_p is known only approximately, the useful measurement range on t with this setup is limited to about 20 dB. The increase, ΔT, in sky temperature is given by

$$\Delta T = (1 - t)\,T_p$$

When monitoring the sky temperature, ΔT, is measured with a dicke switch radiometer. The useful measurement range on t is limited to about 10 dB with this setup.

Meteoroligical Instrumentation

The meteorological instrumentation consists of two weather radars and a number of rain gauges as indicated in Figure 1. The rain gauges are of the capacitive type, for measuring instantaneous rain rate, and are sited in front of the antenna under the propagation path to the satellite. Data obtained from the rain gauges are used to establish the correlation between earth-satellite path attenuation and surface rain rate.

A 15-GHz weather radar has been arranged to scan vertically along the aximuth direction of the propagation path to the ATS-5 satellite. Pictures of the display are used to give a qualitative measure of the variation of the hydrometeor distribution with altitude.

A 5.4 GHz weather radar is used to scan in azimuth to give a qualitative picture of the surrounding weather conditions. The transmissions from this radar can be fixed to coincide with the direction of propagation to the ATS-5 satellite. In this mode, the radar returns are fed to a digital processor which samples the return at one mile increments over a 20-mile range. Each sample will give an estimate of the reflectivity at the corresponding range.

These data give a quantitative measure of the distribution of hydrometeors along the propagation path. It can be correlated with attenuation measurements to determine the usefulness of weather radars in predicting attenuation.

Data Reduction and Analysis

Data on atmospheric attenuation have been obtained for the period November 1, 1969 to July 31, 1970. Data have been collected in three modes of operation; by monitoring the ATS-5 transmissions, by monitoring the noise power radiated by the sun and by monitoring the sky noise temperature. Generally, when the weather predictions indicated precipitation was likely at Clarksburg, NASA was asked to turn on the 15 GHz ATS-5 transmitter and the satellite was monitored. When not tracking the satellite, whenever possible, the sun was monitored during daylight hours and the sky temperature was measured at night. Table 1 indicates the number of hours of data gathered in these three modes, with the sky temperature and sun noise power measurements combined under the radiometer column. In an attempt to increase the data base as much as possible, beginning in mid-April, the periods during working hours, when the sky was clear but no data were taken, were recorded. These hours are included under the clear sky column and could safely be counted as periods with no attenuation.

Figure 2 provides the attenuation data gathered while monitoring the ATS-5 transmissions. Plotted in the figure are the total number of minutes for which the attenuation exceeded the values given on the abscissa. The dashed portions of the curve are due to the fact that the system dynamic range for attenuation measurements varied from storm to storm. This variation arose from two factors. Due to the orbital inclination of the ATS-5 satellite, the power received from the satellite at Clarksburg has a diurnal variation of about 3.5 dB. Also, for some storms, it was possible to increase the dynamic range by using the satellite beacon transmitter which has about 9 dB more signal power than the main transmitter. Unfortunately, the beacon can only be utilized for about one and a half hours every eight hours. In all cases, the dynamic range exceeded 11 dB. To generate the upper dashed curve labeled "pessimistic estimate," it was assumed that if the dynamic range was less than 18 dB and a fade greater than the dynamic range occurred, that the fade depth was greater than 18 dB. To generate the lower curve labeled "optimistic estimate," it was assumed that if the dynamic range was less than 18 dB and a fade greater than the dynamic range occurred, that the fade depth was no greater than the dynamic range. The true distribution curve would lie somewhere between these limits.

Figures 3 and 4 provide fade duration histograms for fades greater than 4 dB and 9 dB respectively. These figures indicate that most fades last for less than 10 minutes with a few in the 20- to 30-minute range. Figure 5 provides the attenuation data obtained while tracking the sun and monitoring the sky temperature. Figure 6 provides the corresponding fade duration histograms. Most of the sun tracker attenuation data occurred during one storm. The 51-minute, 4-dB fade

and the 43-minute, 9-dB fade represent sun tracker data with the rest of the radiometer histogram obtained from sky temperature measurements.

Due to various equipment malfunctions in the non-redundant meteorological instrumentation, the data gathered to date are not sufficient to provide meaningful comparisons between the attenuation and meteorological measurements.

Table 1

Summary of 15 GHz Attenuation Measurement Operational Hours

Month	ATS-5	Radiometer	Clear Sky	Total Hours	% of Month
Nov. 69	44 hrs 45 min	0 hrs	-	44 hrs 45 min	6.2
Dec. 69	84 hrs 24 min	22 hrs	-	106 hrs 24 min	14.3
Jan. 70	27 hrs 39 min	42 hrs	-	69 hrs 39 min	9.3
Feb. 70	30 hrs 50 min	0 hrs	-	30 hrs 50 min	4.5
Mar. 70	43 hrs 0 min	236 hrs 25 min	-	279 hrs 25 min	37.5
Apr. 70	35 hrs 25 min	331 hrs 35 min	23 hrs 45 min	390 hrs 45 min	54.2
May 70	26 hrs 15 min	94 hrs 40 min	116 hrs 50 min	237 hrs 45 min	32.0
Jun. 70	63 hrs 35 min	399 hrs 47 min	51 hrs 58 min	515 hrs 20 min	69.3
Jul. 70	108 hrs 59 min	543 hrs 27 min	51 hrs 19 min	703 hrs 45 min	94.5

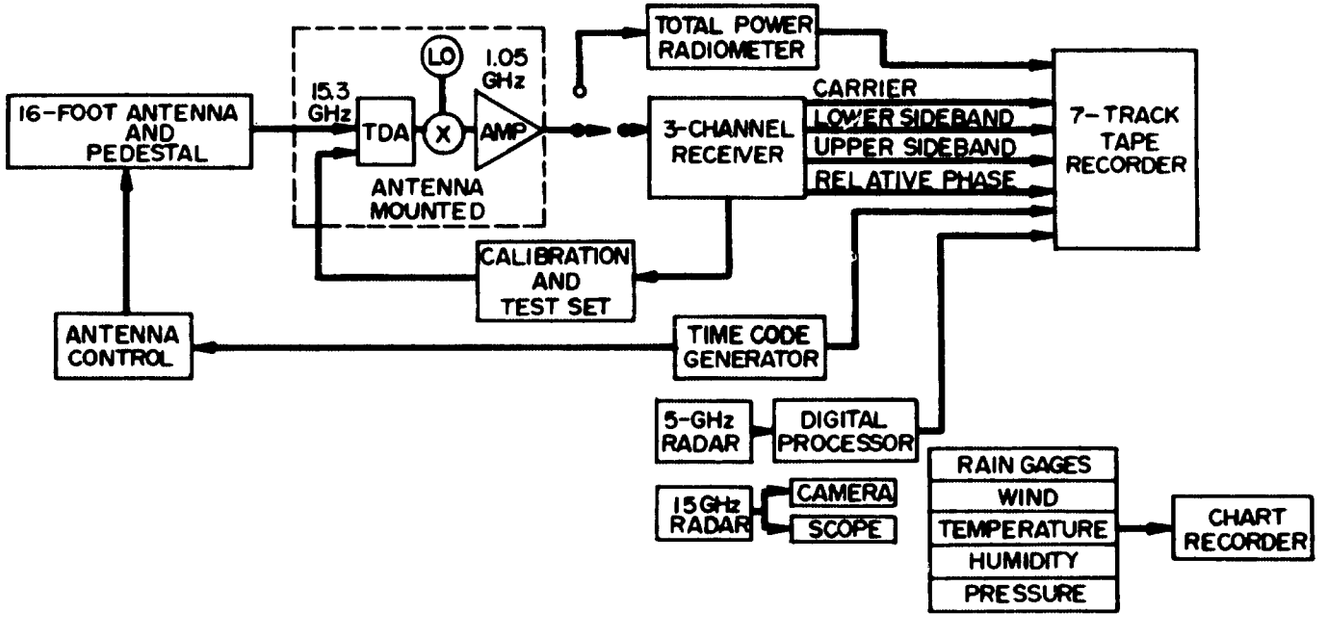

Figure 1. ATS-5 Measurement Configuration

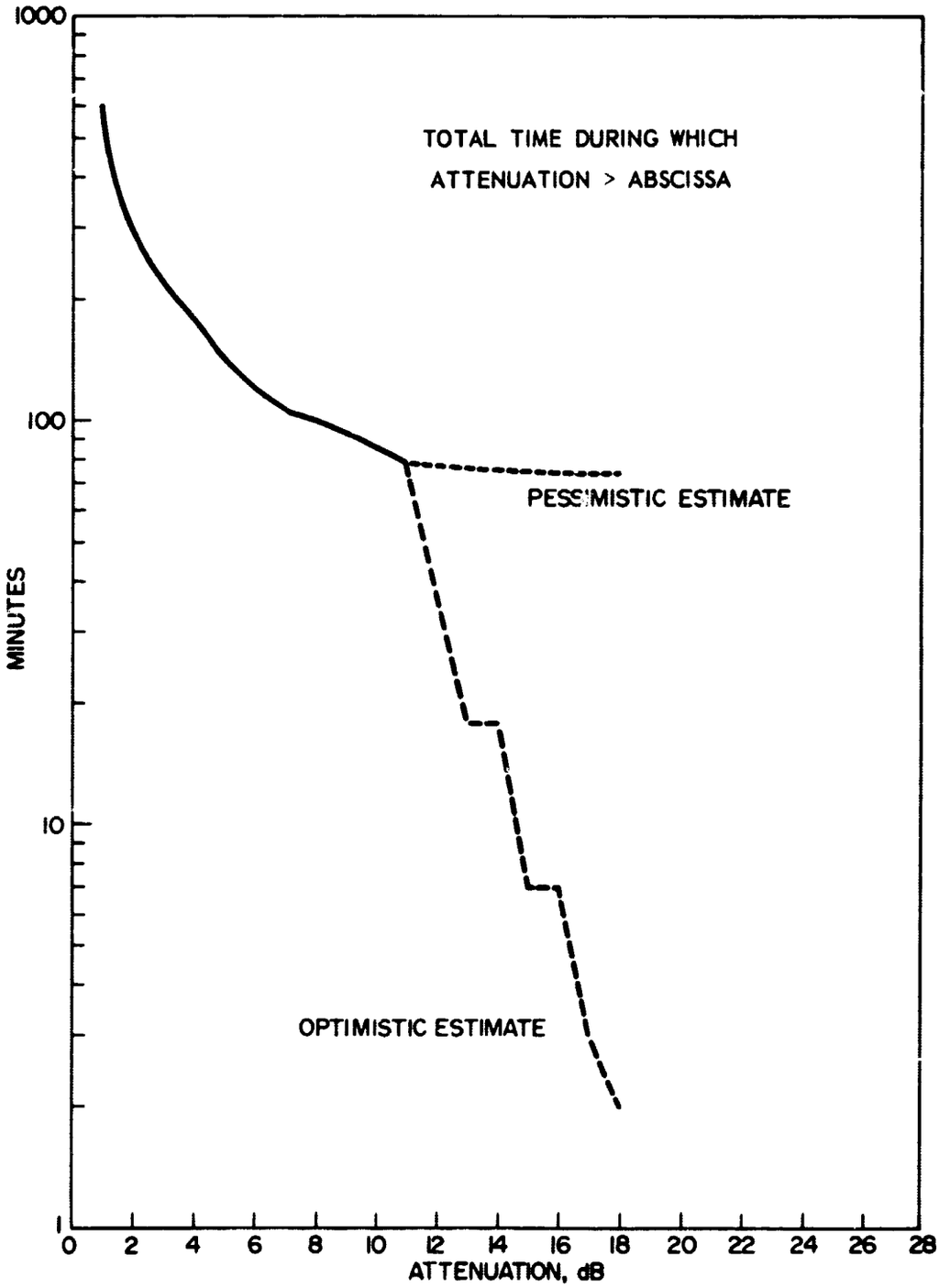

Figure 2. ATS-5 Data Nov. 1, 1969 - July 31, 1970

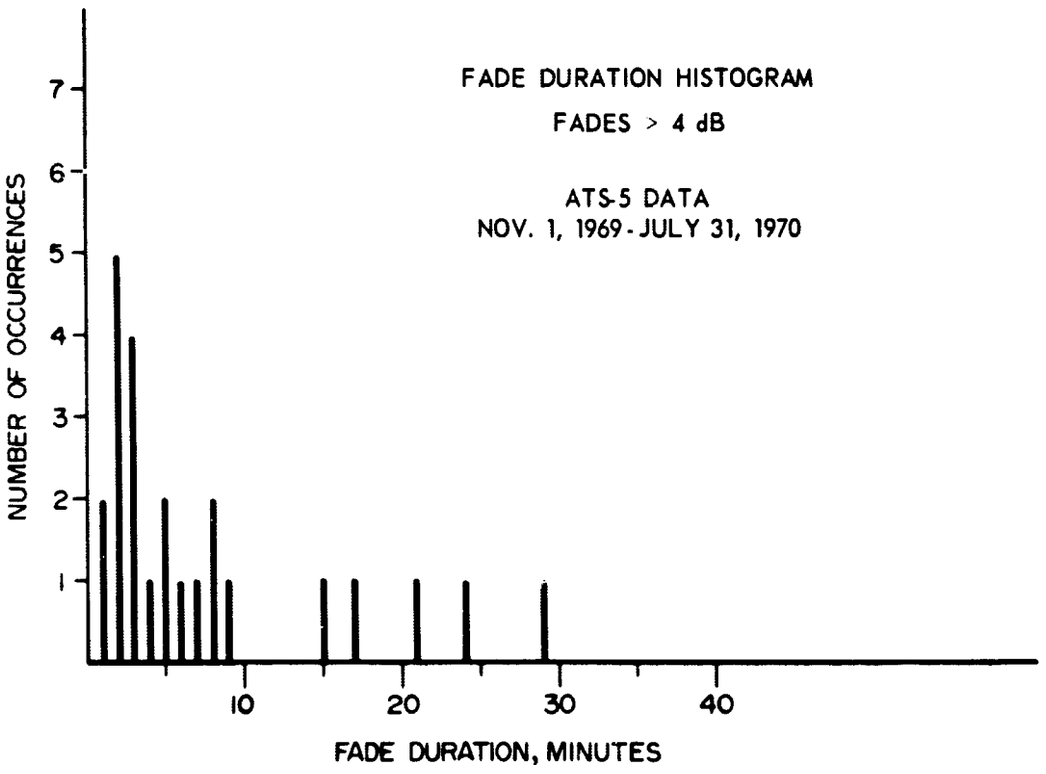
FADE DURATION HISTOGRAM
FADES > 4 dB
ATS-5 DATA
NOV. 1, 1969 - JULY 31, 1970
NUMBER OF OCCURRENCES
1
2
3
4
5
6
7
10
20
30
40
FADE DURATION, MINUTES

Figure 3

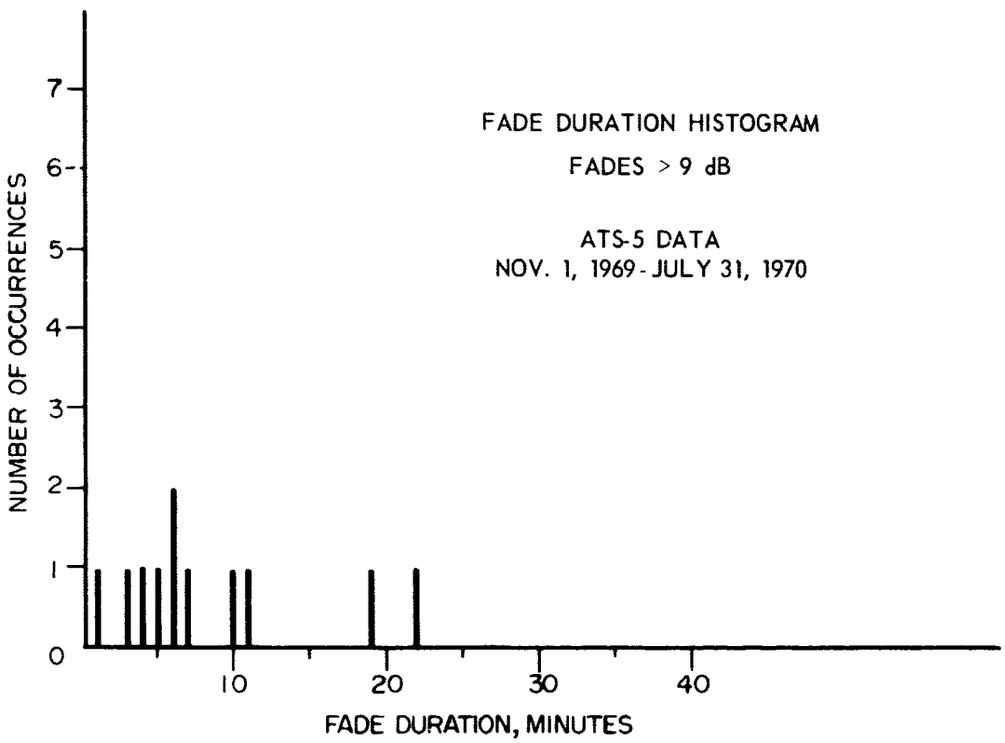
FADE DURATION HISTOGRAM
FADES > 9 dB
ATS-5 DATA
NOV. 1, 1969 - JULY 31, 1970
NUMBER OF OCCURRENCES
0
1
2
3
4
5
6
7
10
20
30
40
FADE DURATION, MINUTES

Figure 4

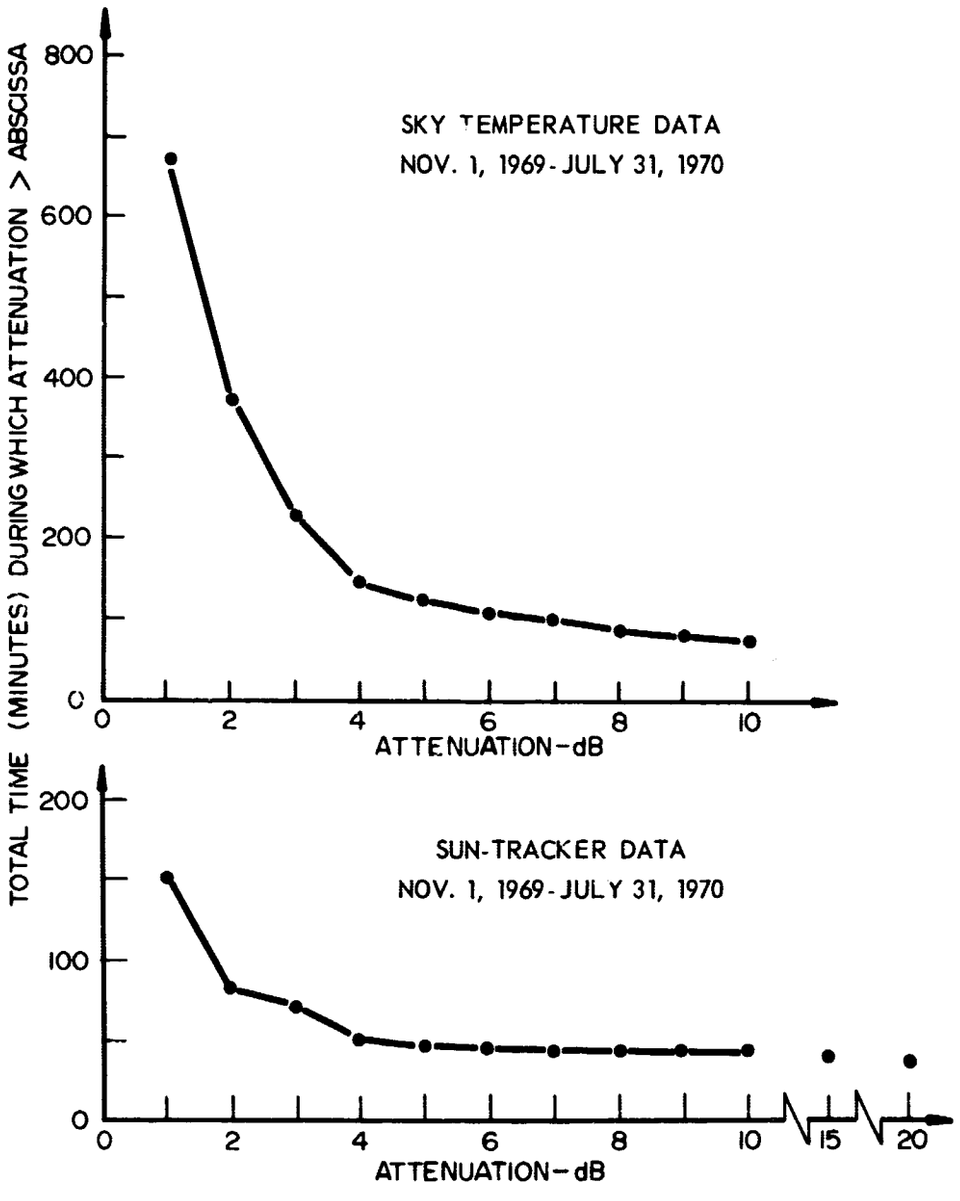
SKY TEMPERATURE DATA
NOV. 1, 1969 - JULY 31, 1970
TOTAL TIME (MINUTES) DURING WHICH ATTENUATION > ABSCISSA
800
600
400
200
0
0
2
4
6
8
10
ATTENUATION - dB
SUN-TRACKER DATA
NOV. 1, 1969 - JULY 31, 1970
200
100
0
0
2
4
6
8
10
15
20
ATTENUATION - dB

Figure 5

RADIOMETER DATA
NOV. 1, 1969 - JULY 31, 1970

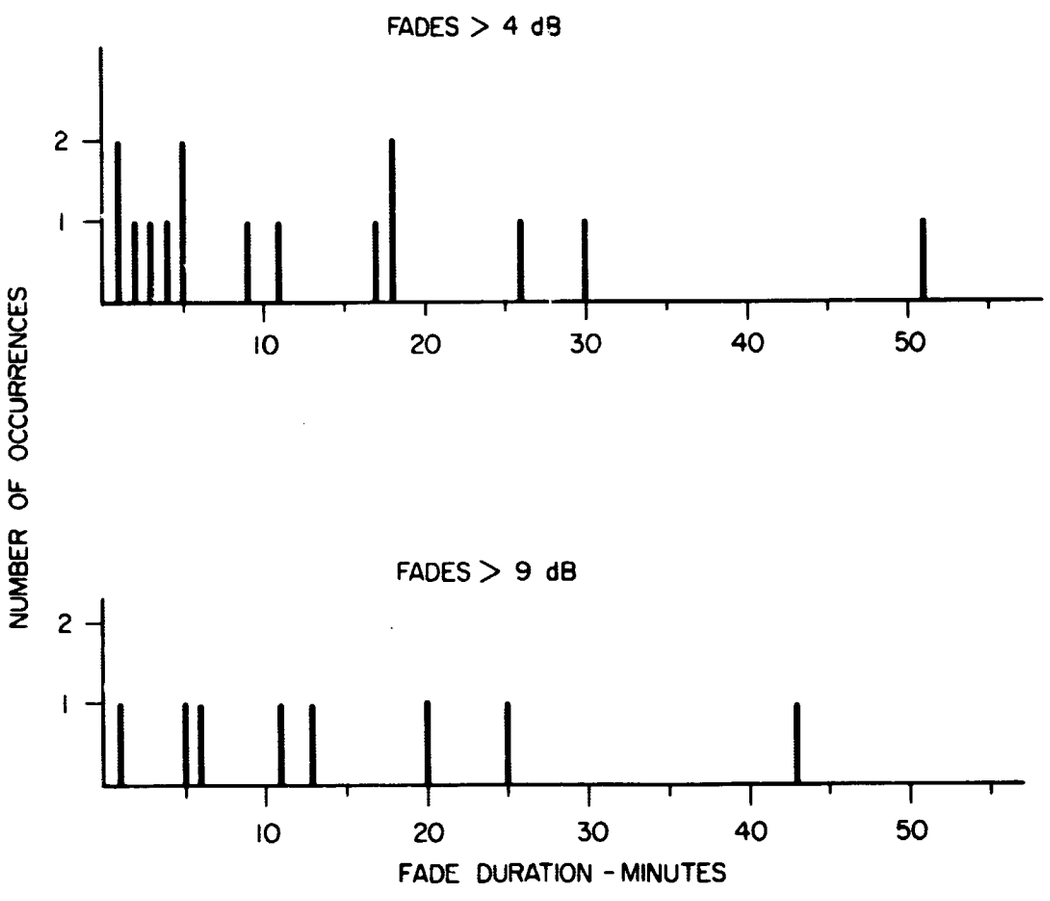

Figure 6

A MILLIMETER WAVE DIVERSITY PROPAGATION EXPERIMENT

P. Bohley, D. B. Hodge
The Ohio State University
Columbus, Ohio

ABSTRACT

This paper describes a 15.3 GHz diversity propagation experiment utilizing a transmitter on board the ATS-5 synchronous satellite. The ground-based facility consists of two complete receiving terminals, one fixed and the other transportable. Both receiving antennas are instrumented with boresight radiometers which view volumes coincident with those seen by the receiving antennas. The following meteorological parameters are recorded in addition to the received signal amplitudes and radiometer temperatures: local wind speed, wind direction, temperature, rain rate, and relative humidity.

Initial results of the analysis of diversity data collected from these two terminals are presented for a site separation of four kilometers. These data are useful in characterizing the nature of the propagation path for a satellite-to-ground millimeter wave communication link and, in particular, assessing the effect of thunderstorm cell size and structure on two separated receiving terminals. Data relating the signal attenuation and radiometric temperature are also presented.

INTRODUCTION

This paper will describe the current participation of The Ohio State University in the NASA ATS-5 Millimeter Wave Propagation Experiment. This experiment consists of the ATS-5 Satellite Millimeter Wave package and numerous ground terminals located throughout the United States and Canada. The ATS-5 synchronous satellite provides a 15.3 GHz down-link signal which can be utilized by the various ground terminals for propagation measurements. The OSU facilities for this experiment consist of two complete receiving terminals, one of which is transportable and the other fixed. These terminals provide the capability of measuring and recording the received signal level and several meteorological parameters at two spatially separated sites in a diversity configuration. In addition both terminals are equipped with narrow beam radiometers having patterns coincident with those of the receiving antennas. In the following the terminal configurations will be briefly described, sample raw data will be presented, and preliminary results of the data analyses will be discussed. More detailed descriptions of the OSU terminals may be found in References 1, 2, and 3.

EXPERIMENTAL CONFIGURATION

Both OSU 15.3 GHz terminals are equipped with 14 track magnetic tape recorders which record the following data in analog form: received signal level, radiometric temperature, time, rain rate, and several station status parameters. In addition, the transportable terminal instrumentation includes the capability for the measurement and recording of the local wind speed, wind direction, temperature, and relative humidity. A 15.5 GHz weather radar and PPI display is also available at the fixed terminal for thunderstorm cell surveillance and photography (Fig. 1). The analog data is digitized, peak detected, and recorded in digital form using a HP 2115A Digital Computer. The digitized data is then analyzed using an IBM 360-75 Computer.

The fixed receiving terminal uses one of the antennas in the ElectroScience Laboratory Satellite Communication Facility array; this antenna is a 30 ft parabolic reflector which is Cassagrainian fed by a square corrugated horn. The feed horn was designed such that approximately equal E- and H-plane patterns are produced. A polarization splitter at the input to the horn then permits the antenna to be used simultaneously in conjunction with both the receiver and the radiometer. The antenna beamwidth is approximately 0.15°. The transportable receiving terminal antenna is fed in a similar fashion; however the parabolic reflector is 15 ft. in diameter in this case which provides a beamwidth of approximately 0.3°. The receivers at both terminals are phase locked loop systems constructed by the Martin Marietta Corporation.

Top and side views of the site locations are shown in Figs. 2 and 3. All of the data presented in this paper were obtained with the transportable terminal located at Site No. 1. It is intended that measurements will be made with the transportable terminal located at Site No. 2 during the spring of 1971. In both cases the two sites in use are separated in directions both perpendicular and parallel to the ground projection of the satellite propagation path. Typical look angles for the ATS-5 satellite as viewed from Columbus, Ohio, are an elevation angle of 37° and an azimuth angle of 210°. The oblique separation of the sites with respect to the propagation path was selected in view of the facts that thunderstorm cells typically have dimensions of a few miles in both horizontal and vertical directions and that weather fronts tend to move repeatedly in similar directions. The actual site spacings are summarized in Fig. 3 with the spatial separation being the perpendicular distance between the propagation paths to the two terminals.

PRELIMINARY RESULTS

The raw data obtained during a typical spring thunderstorm is shown in Fig. 4. The upper curve on each strip chart is the radiometric temperature of the propagation path obtained using a one second integration time. The spikes which appear occasionally on these traces are a result of periodic recalibration of the radiometers. The lower trace on each strip chart is a delay-pulse recording of the received signal level;[3] the ordinate, in this case, represents a receiver calibration where 0 dB corresponds to -120 dBm at the receiver input for the fixed terminal and -124 dBm for the transportable terminal. During the time interval from approximately 1845Z to 1915Z the fixed terminal antenna was pointed toward zenith because of high wind speeds. It should also be noted that the three spikes occurring in the transportable record in the vicinity of 1915Z were apparently the result of the receiver locking onto spurious signals. The transportable terminal was located at Site No. 1 during this and the following data runs discussed in this paper.

During the passage of the main thunderstorm cell around 1900Z the peak rain rate with approximately 100 mm./hr. and the average rain rate was approximately 60 mm./hr. Note the small disturbance which was observed at the transportable terminal at about 1800Z but not at the fixed terminal. Although it is difficult to discern on this compressed representation of the data, there is a general tendency for disturbances to occur first in the view of the transportable site and approximately five minutes later at the fixed terminal. This time delay corresponds to a thunderstorm cell velocity perpendicular to the propagation paths of about 20 mi./hr. and is a consequence of the predominant motion of cells in this locale from west to east. The general behavior of the data presented in this figure is quite representative of the spring and early summer of 1970.

A rather atypical sample of data, obtained on June 15, 1970, is shown in Fig. 5. In this case several small cells were observed with relatively large time delays between their occurance in the views of the two sites. Only 0.2 mm. of rain was recorded during this entire time period. This type of behavior is associated with unstable conditions when small cells are generated locally, move slowly for a short distance, and finally dissipate.

The data shown in Fig. 6 demonstrates the extremely rapid variation in radiometric temperature and received signal level which could be produced by well defined boundaries and fine structure within the thunderstorm cell. Note particularly the slopes in the transportable data record at approximately 0545Z and 0615Z, the fade rate during the signal decline at 0545Z was approximately 1/8 dB./sec. No rain was recorded at the terminal during this event. Unfortunately the ATS-5 transmitter was turned off for a short period of time at 0300Z; and high wind speeds necessitated the raising of the fixed terminal antenna at about 0600Z.

Figure 7 shows a rather severe storm preceeded by several smaller events. A peak rain rate of 225 mm./hr. and an average rain rate of 150 mm./hr. over an eleven minute period occurred shortly after 0200Z; these intense rain rates were also accompanied by hail. The time interval from 2230Z to 2330Z is quite interesting with respect to the extended disturbances which were seen at the transportable terminal but were not observed at the fixed terminal. Again, the fixed antenna was raised from about 0115Z to 0130Z and following 0200Z due to high wind speeds. Nevertheless one can note a distinct difference in the fine structure of the signals records between 0130Z and 0200Z. This difference in structure may be due, to some extent, to the difference in antenna beamwidths at the two terminals and the fact that the cell is well within the near field of the receiving antenna. It is also interesting to note that both radiometers saturated at ambient temperatures of approximately 300°K.

Received signal level data averaged over a time period containing 10 pulses were used to obtain Fig. 8. Here the received signal level is compared with the measured radiometric temperature in order to confirm its behavior in accordance with the simple relation:

$$\alpha = \frac{T_m}{T_m - T_s} \tag{1}$$

where α is the path attenuation, T_s is the radiometric temperature, and T_m is the mean absorption temperature. In this example the mean absorption temperature was chosen empirically and three theoretical curves corresponding to

different assumed free space path losses are shown. The data spread of approximately 1 dB. in received signal level is well within the experimental tolerance determined by noise and antenna pointing error. Similar data are also presented in Fig. 9, although in this case the theoretical curves correspond to different assumed mean absorption temperatures. The data for both of these figures were obtained from rapid fade periods during the events shown in Fig. 7 in order to cover the maximum possible dynamic range with the minimum number of data points.

The fade distributions presented in Figs. 10 and 11 were also obtained from the June 17, 1970, data shown in Fig. 7. Here the durations of the received signal level below given threshold levels are given for each site independently. In addition the duration of received signal levels below given thresholds at both terminals simultaneously is also shown. This data would correspond to the output of a diversity system which simply selected the larger of the two received signals. In Fig. 10 the received signal at the fixed site experienced fades no greater than 10 dB. while the signal at the transportable site reached threshold. In Fig. 11 the received signal at both terminals dropped below threshold. In both cases, however diversity operation would have resulted in the reduction of the duration of 6 to 10 dB fades by roughly two orders of magnitude. It is also interesting to note that, although the fine structure of the received signal records during 0128Z-0201Z in Fig. 7 were quite different in nature, the resulting single site fade distributions shown in Fig. 11 are quite similar.

SUMMARY

The preliminary results of The Ohio State University's participation in the ATS-5 millimeter wave propagation experiment were presented. The narrow beam radiometer data show excellent agreement between measured attenuation and radiometric temperature for temperatures ranging up to the ambient temperature. These data also show excellent agreement with a simple theoretical model based upon the assumption that the attenuation is predominantly due to absorption rather than scattering. Further, the results of preliminary fade analyses have shown that the durations of 6 to 10 dB. fades were reduced by approximately two orders of magnitude by the use of a simple diversity system. All reported results were obtained with a ground separation of 4 Km. between terminals during spring and early summer weather conditions typical of central Ohio. The data acquisition and analysis efforts at OSU are continuing, and it is expected that measurements will be made using an 8 Km. ground separation during the spring of 1971.

REFERENCES

1. Annual Status Report, Millimeter-Wavelengths Propagation Studies, Report 2374-2, 1 November 1969, ElectroScience Laboratory, Department of Electrical Engineering, The Ohio State University; prepared under Grant Number NGR-008-080 for National Aeronautics and Space Administration.

2. Semiannual Status Report, Millimeter-Wavelengths Propagation Studies, Report 2374-3, 15 April 1969, ElectroScience Laboratory, Department of Electrical Engineering, The Ohio State University; prepared under Grant Number NGR-008-080 for National Aeronautics and Space Administration.

3. Semiannual Status Report, Millimeter-Wavelengths Propagation Studies, Report 2374-4, 30 April 1970, ElectroScience Laboratory, Department of Electrical Engineering, The Ohio State University; prepared under Grant Number NGR-008-080 for National Aeronautics and Space Administration.

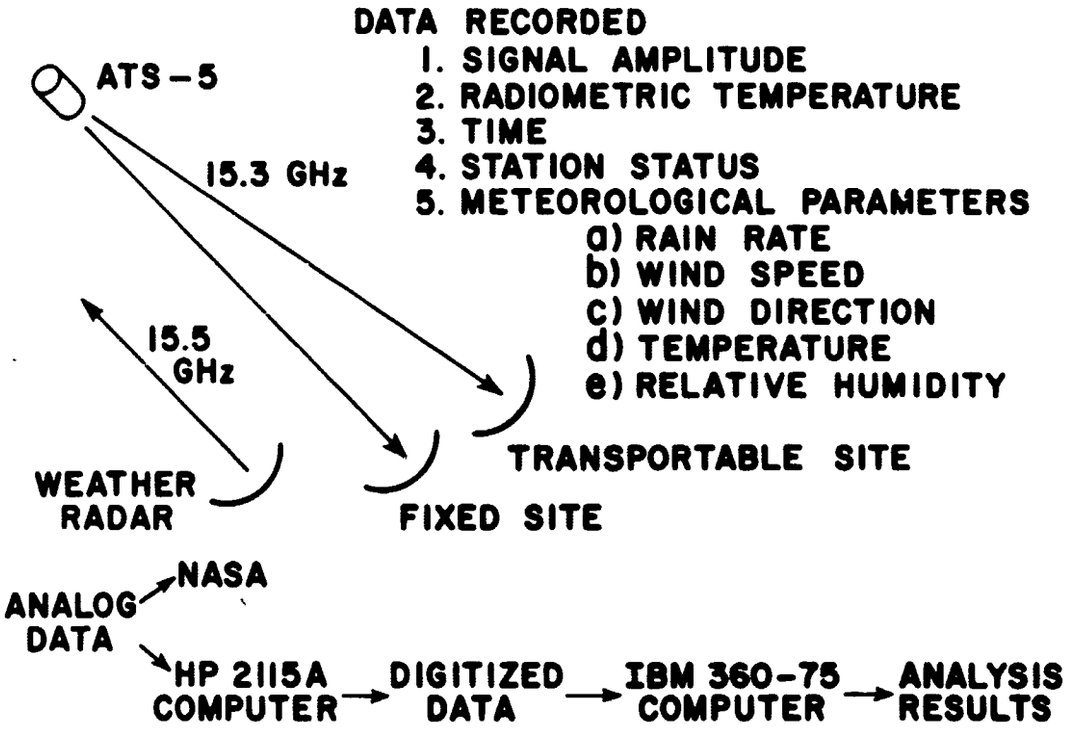

Figure 1. Diversity experiment configuration

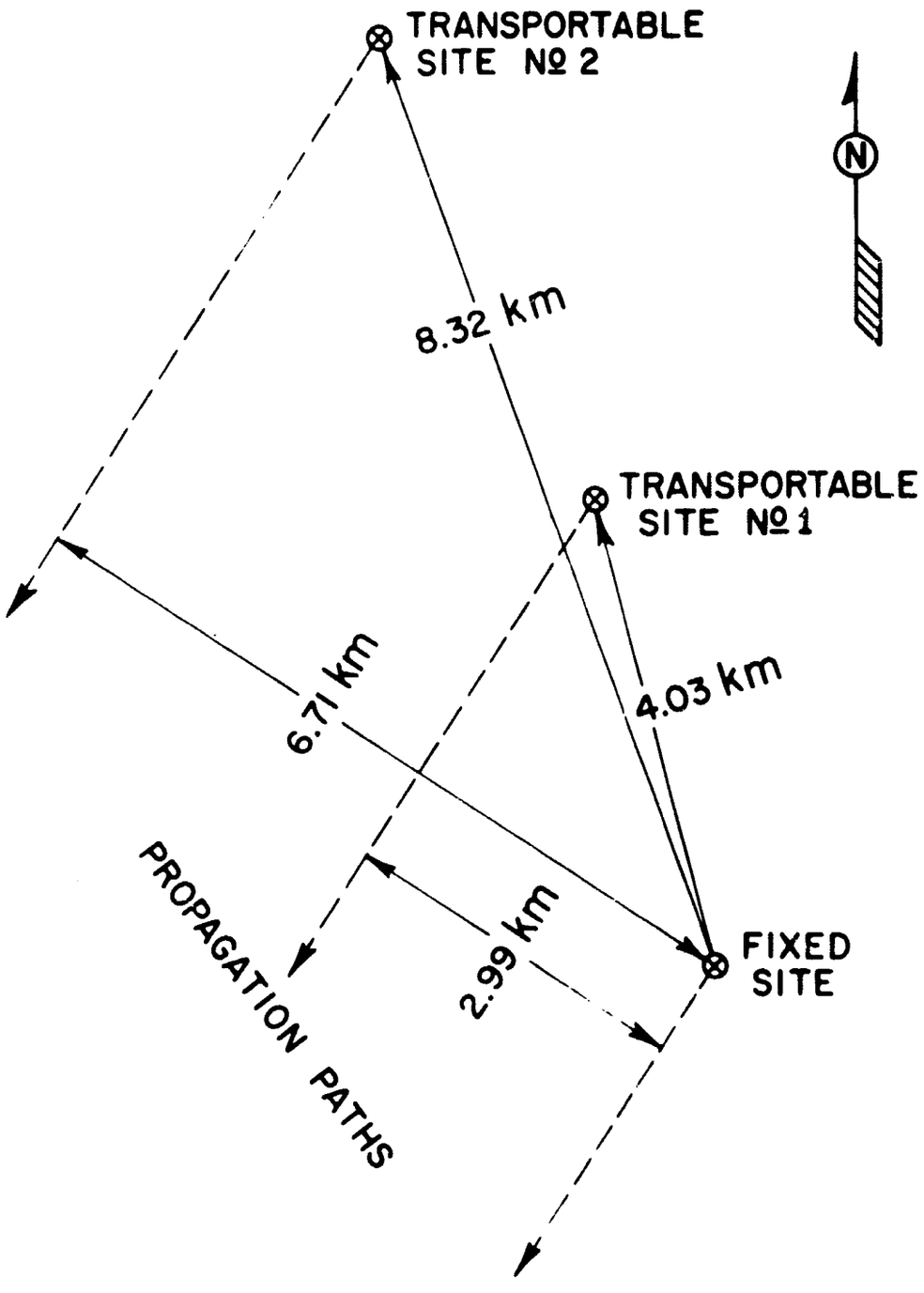

Figure 2. Top view of site locations

SIDE VIEW OF PROPAGATION PATHS

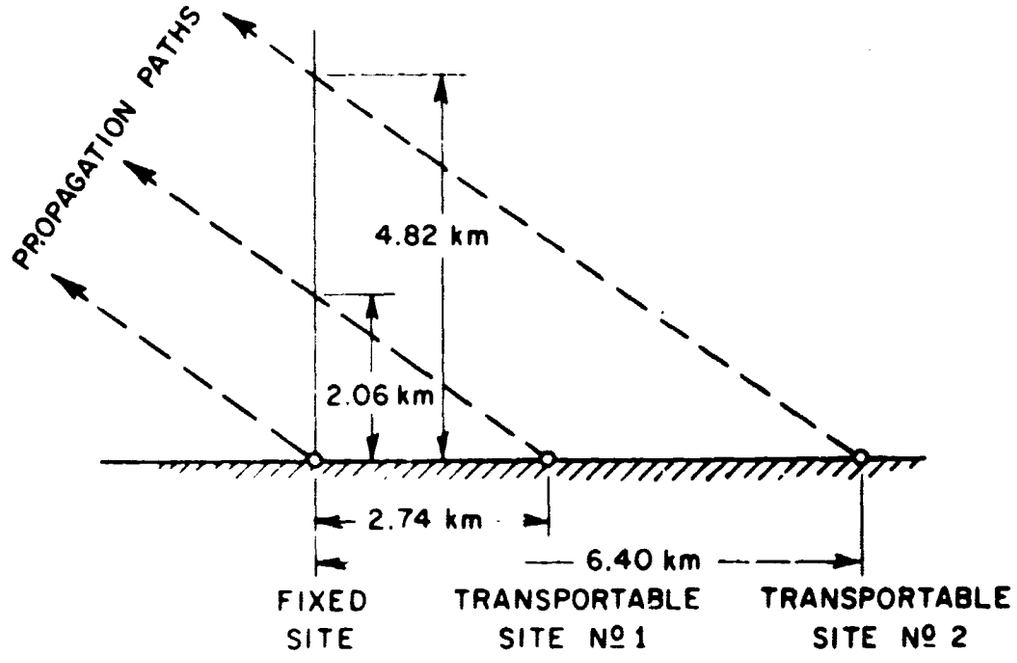

SITE	PATH SEPARATION		
	HORIZONTAL	VERTICAL	SPATIAL
Nº 1	2.99 km	2.06 km	3.41 km
Nº 2	6.71 km	4.82 km	7.73 km

Figure 3. Side view of site locations

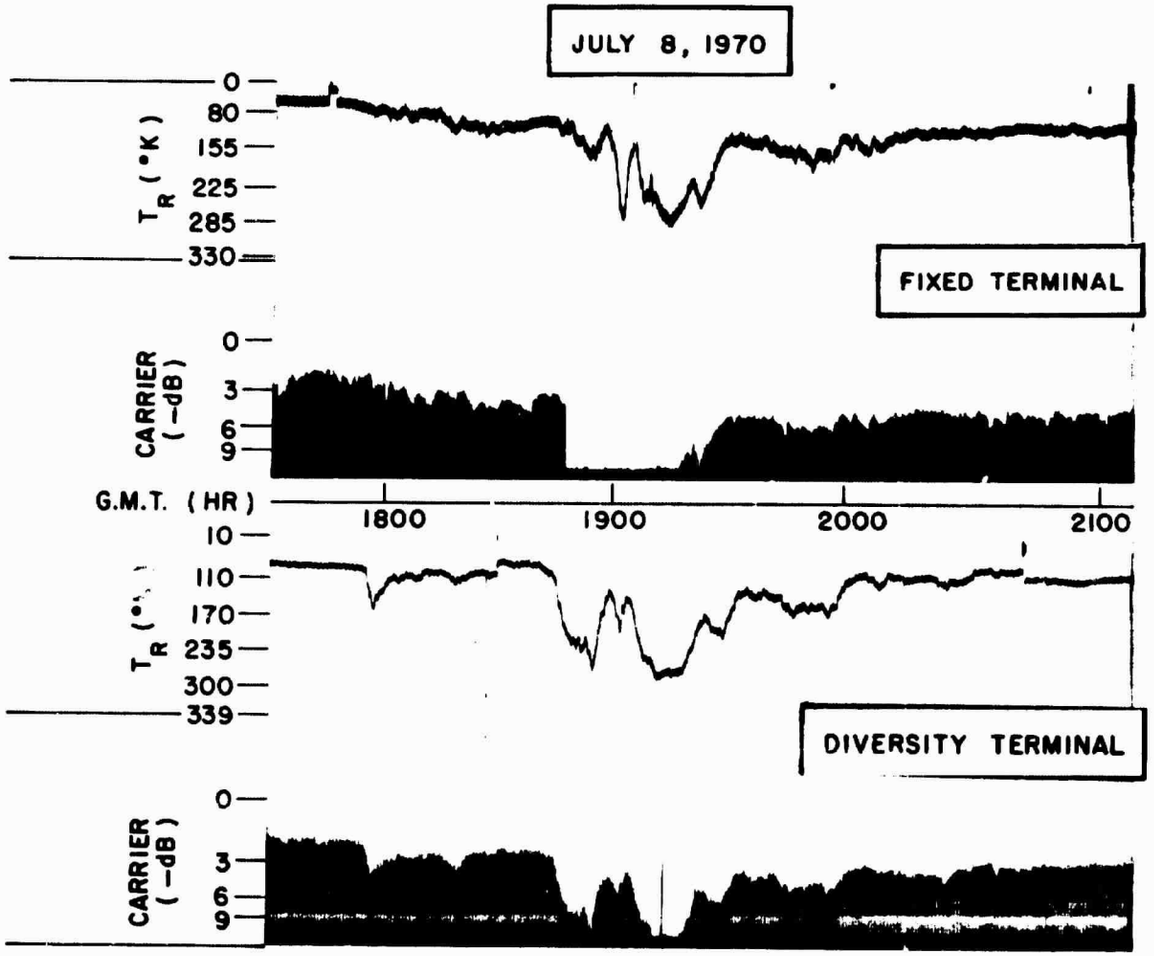

Figure 4. Radiometric temperature and received signal level on July 8, 1970

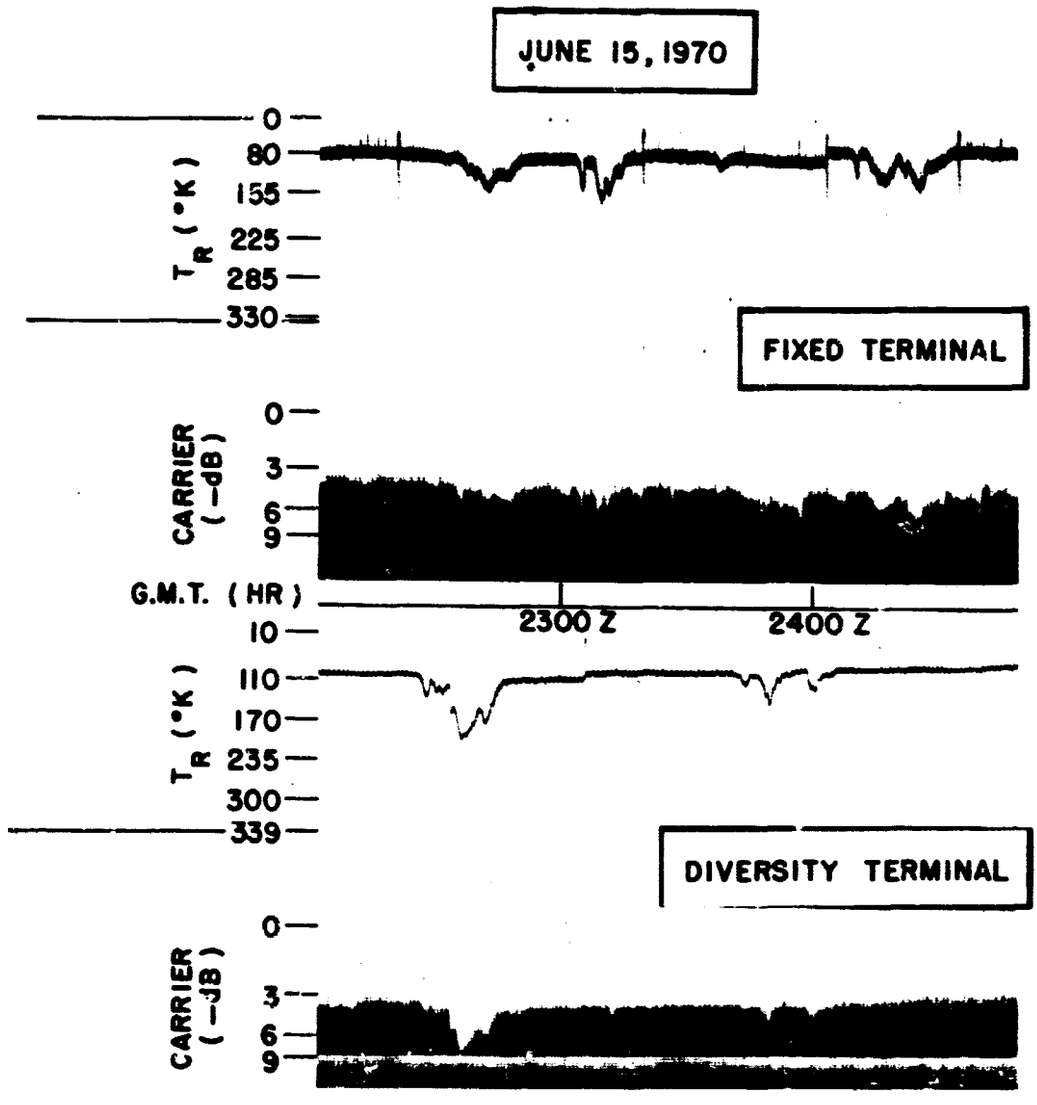

Figure 5. Radiometric temperature and received signal level on June 15, 1970

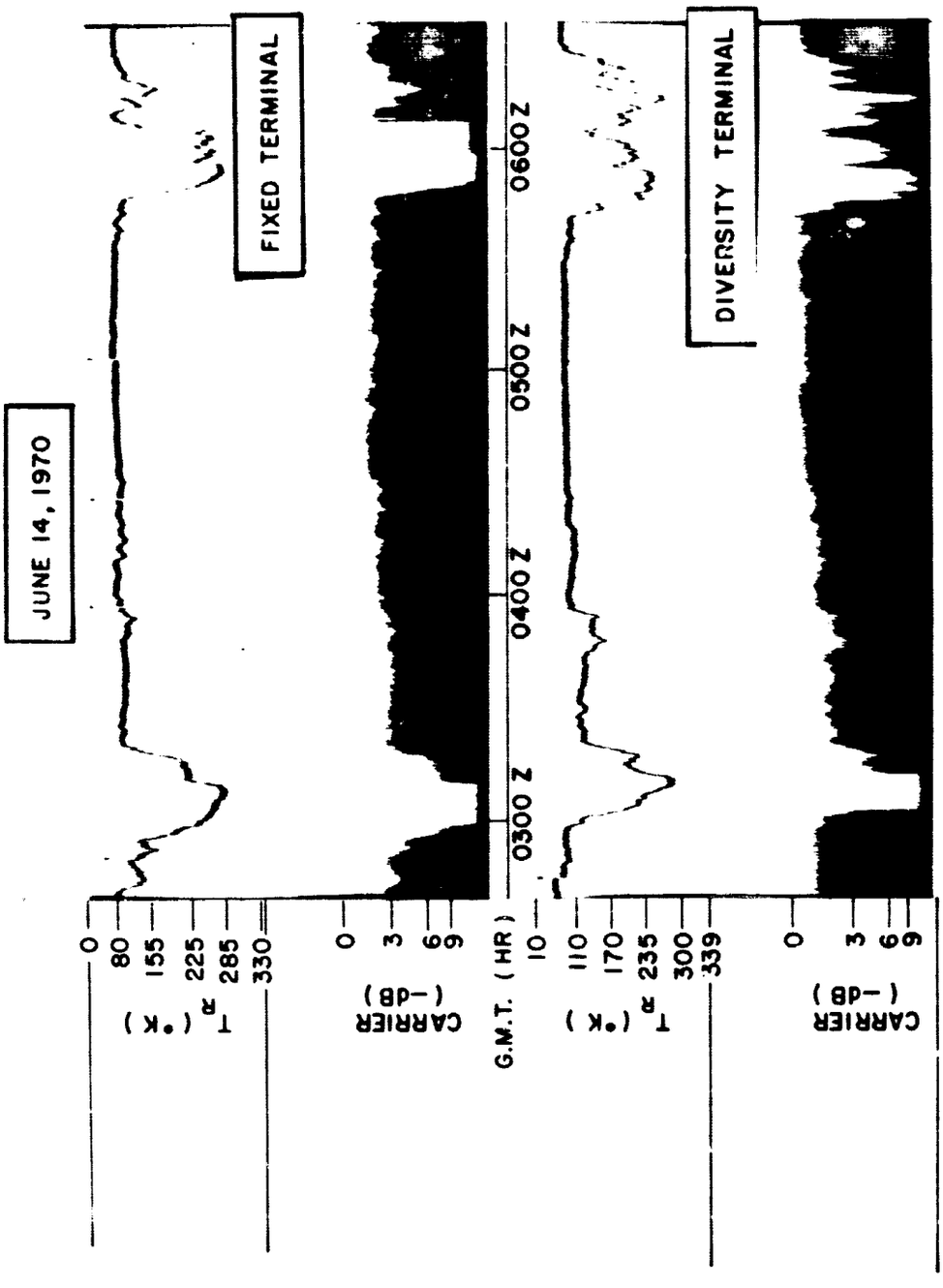

Figure 6. Radiometric temperature and received signal level on June 14, 1970

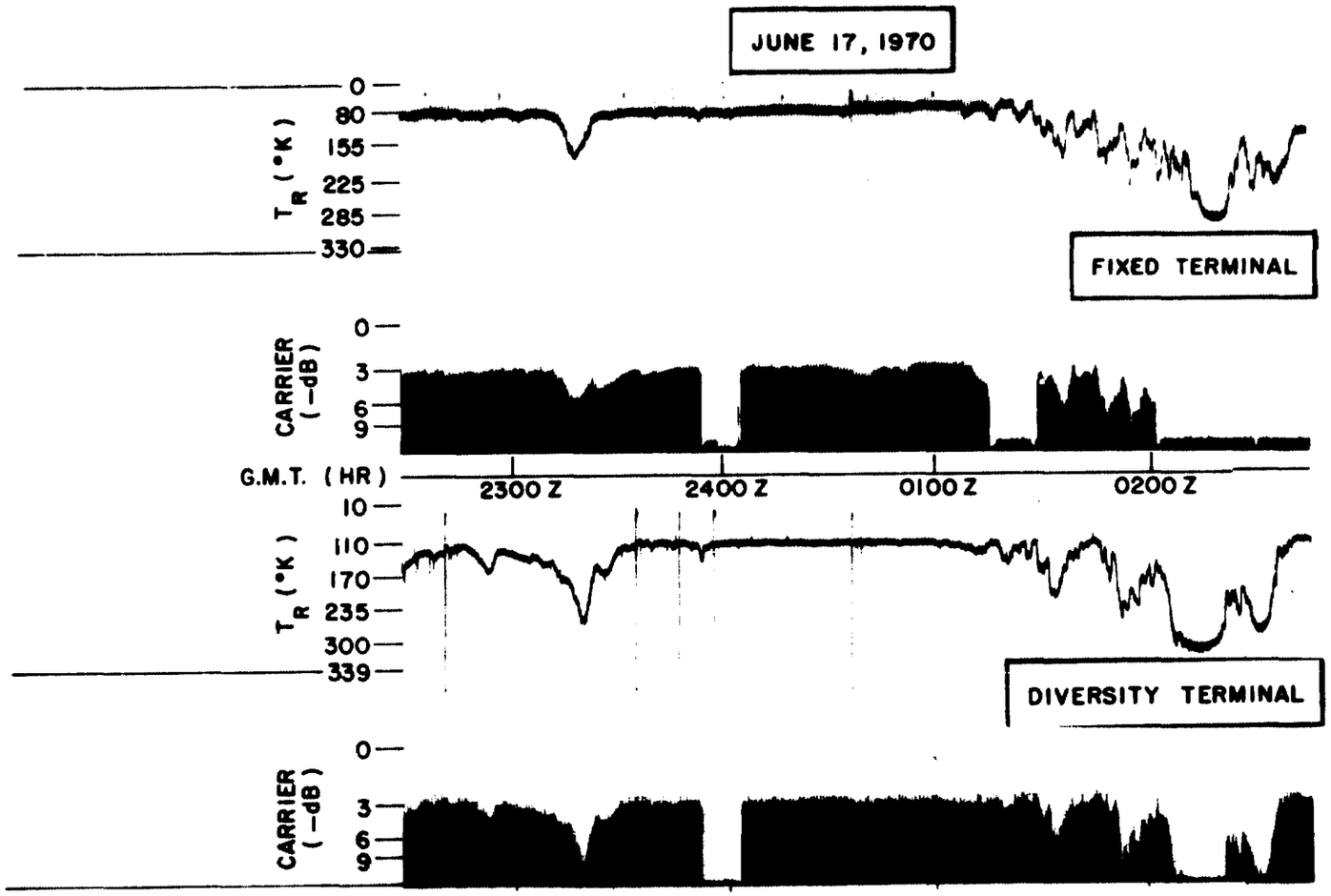

Figure 7. Radiometric temperature and received signal level on June 17, 1970

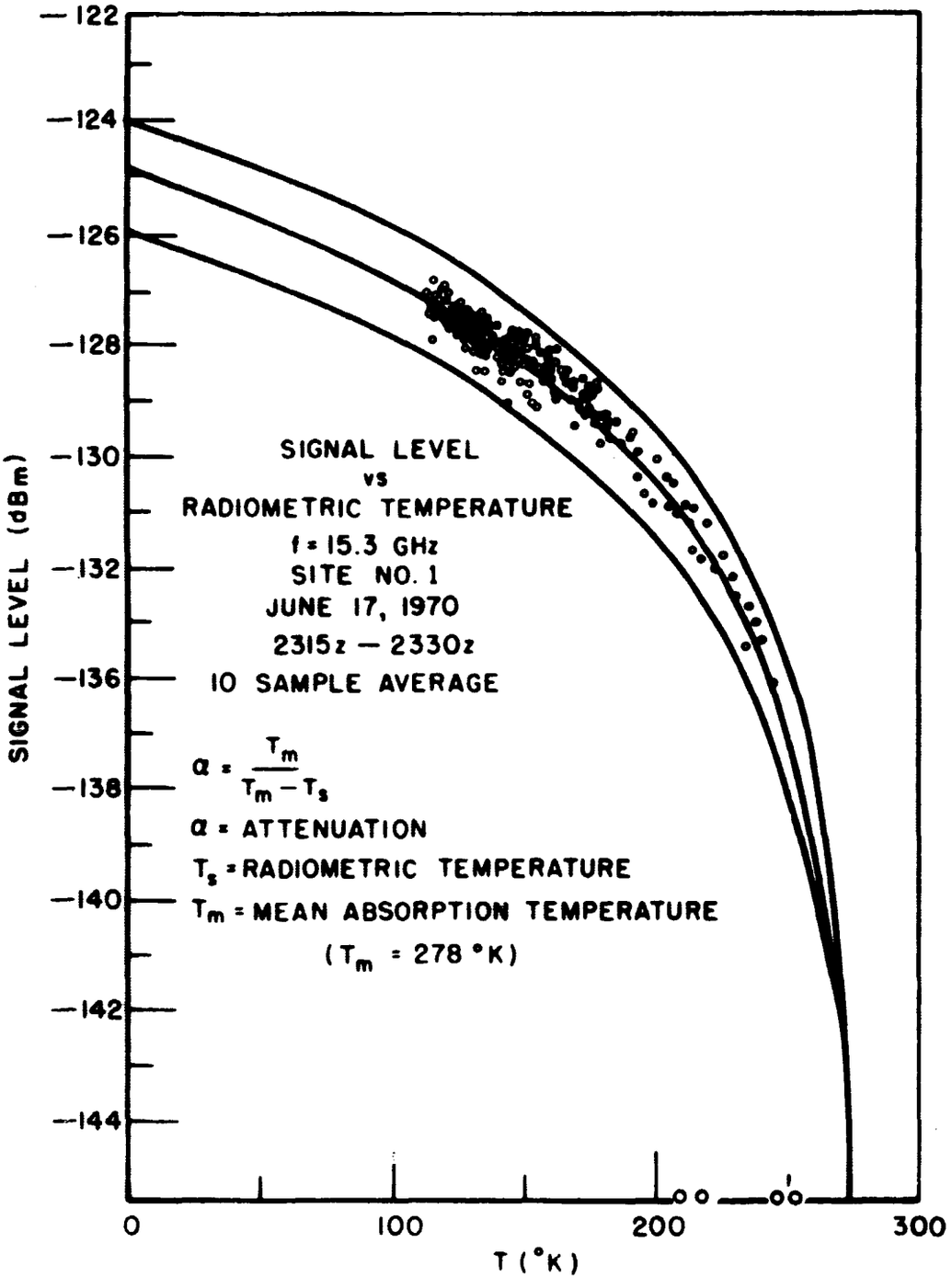

Figure 8. Received signal level vs radiometric temperature during 2315Z-2330Z on June 17, 1970

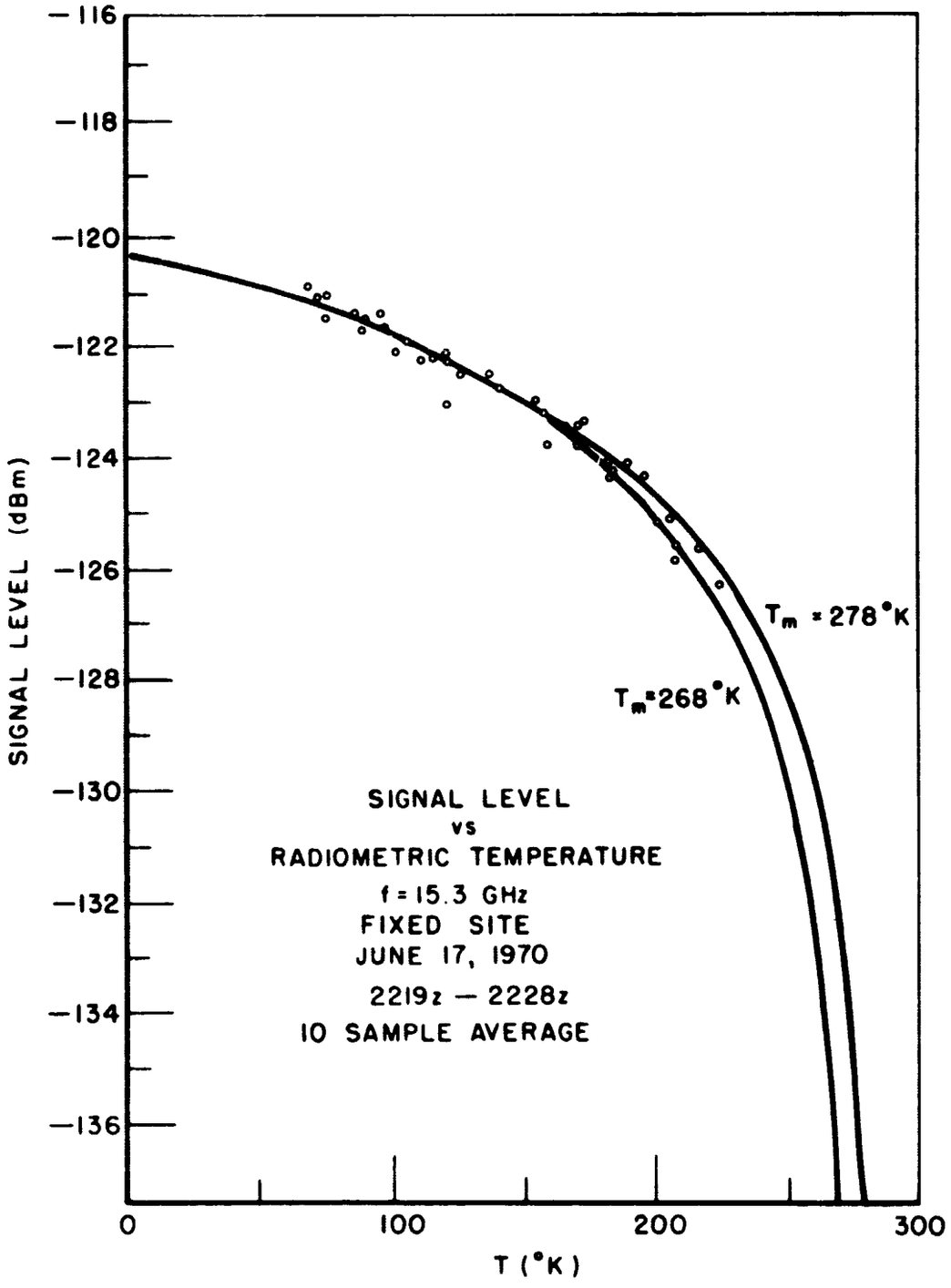

Figure 9. Received signal level vs radiometric temperature during 2219Z-2228Z on June 17, 1970

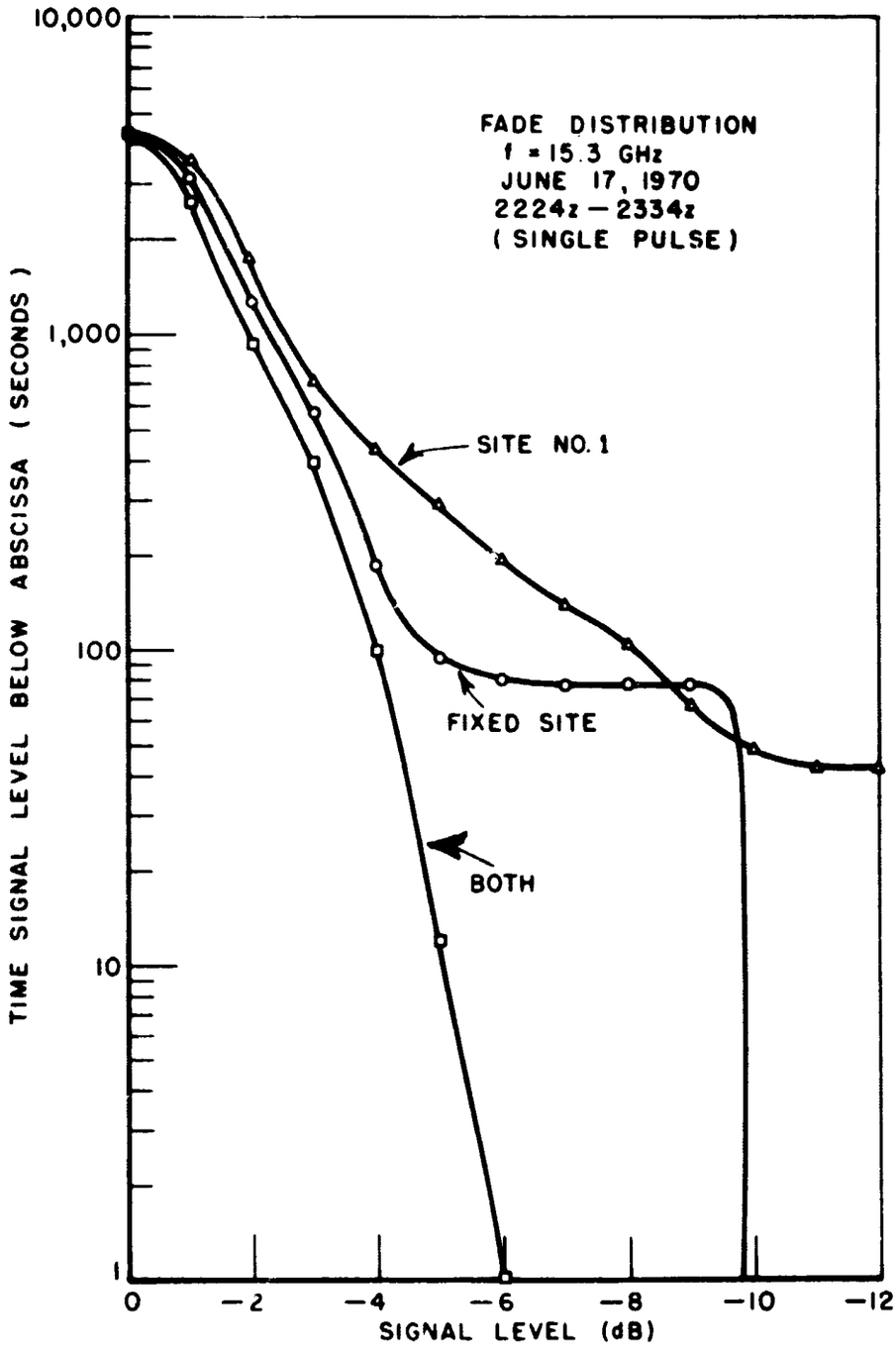

Figure 10. Fade distributions during 2224Z-2334Z on June 17, 1970

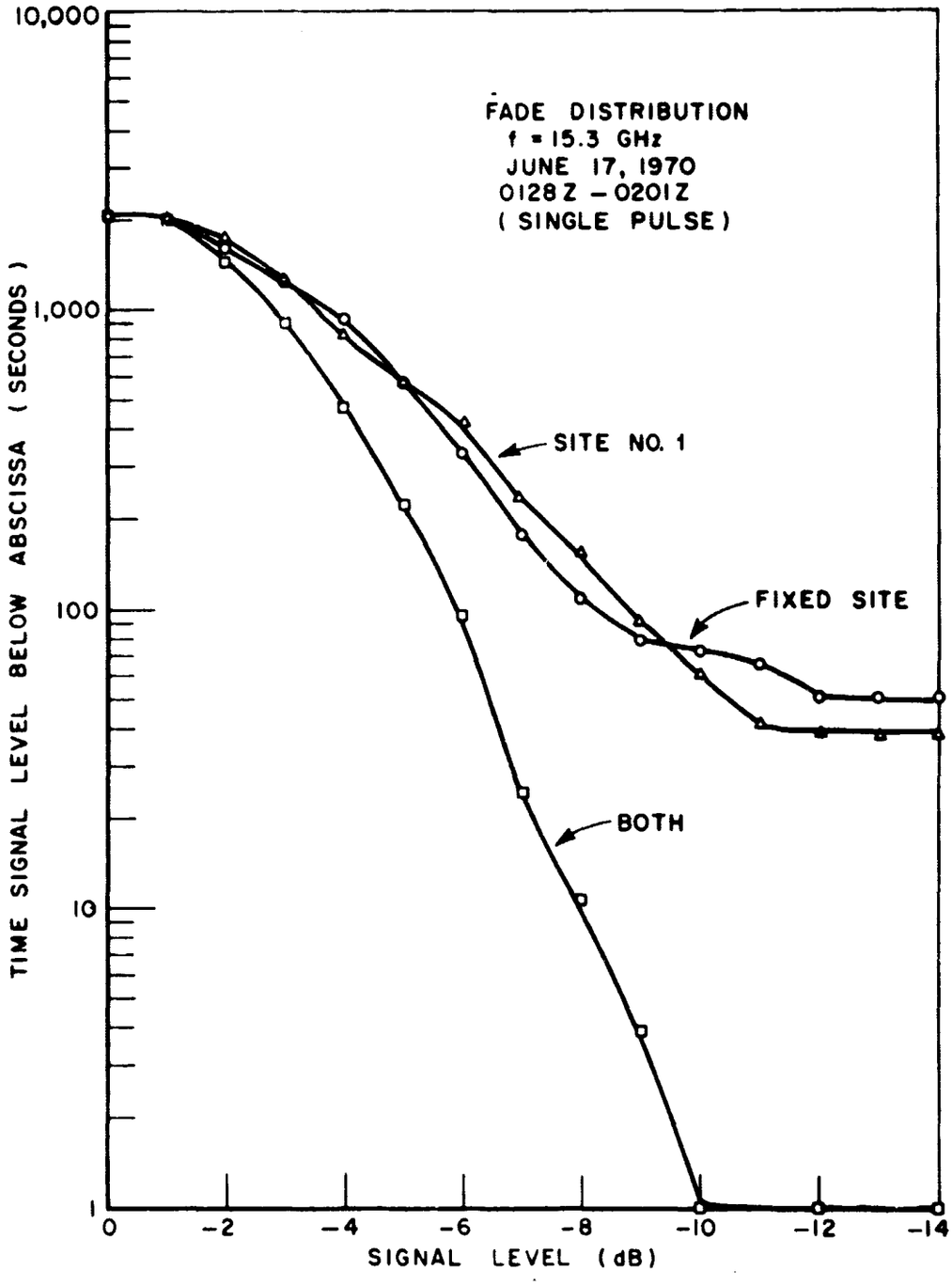

Figure 11. Fade distributions during 0128Z-0201Z on June 17, 1970

EFFECTS OF RAIN ON AN EARTH-SATELLITE PATH AT 15 GHz

B. M. Fannin, A. W. Straiton and D. N. Pate
Electrical Engineering Research Laboratory
The University of Texas at Austin

Receiving Station Features

During the early planning stages for the experiment it was anticipated The University of Texas receiver would be located at Mount Locke in West Texas using the 16-foot parabolic reflector in operation there. A change in plans, however, set the observation site as the Balcones Research Center of The University of Texas which is just north of Austin, Texas. This required a new antenna system to be devised on somewhat short notice.

The antenna system that was devised utilizes two 10-foot parabolic dishes mounted on the arms of a surplus doppler radar unit, the larger dishes replacing 6-foot ones that were in the original equipment. Figure 1 shows this antenna system. Note that although the f/D ratio for the dishes is only 0.375 they are equipped with prime focus feeds. The brick walls in evidence are those of buildings that originally housed magnesium electrolytic cells. Even though the deflectors were guaranteed by the manufacturer to operate satisfactorily in winds up to 45 mph, the system was placed in these ruins to reduce wind effects. The r-f frontend and calibration units are located on the antenna mount with the rest of the receiving and recording equipment in the shelter behind the antenna.

The new reflectors were purchased from Structural Technology, Inc. and it is estimated their surface irregularities are no greater than 0.33 mm rms. It was anticipated the two reflectors, operated as a summed interferometer, would provide 54 dB of gain and antenna pattern measurements indicate that again very close to this value has been achieved. With this antenna system, the power transmitted from the satellite, the effect of the spin, etc., the University of Texas link has operated with just about a 15 dB fade margin.

The supporting measurements made at this site include a 35 GHz radiometer with a 12-inch aperture, a 15.3 GHz weather avoidance radar, a 12.5 km low-level line-of-sight link at 15 GHz, and a set of 5 tipping bucket rain gauges.

Data for Periods of Severe Attenuation

Though Austin's average annual rainfall of 30 inches is considerably greater than that at Mount Locke, Texas, the originally planned site, it is not excessive. On only three occasions have attenuations greater than 3 dB been recorded during the almost one year of operation. During the fall and spring equipment modifications required considerable attention and, with the usual problems of getting the operation refined to the point that weekend and early morning showers could be successively recorded, it is certainly not correct to imply that some rainfall periods were not missed. Nevertheless, May 14, 1970, was the first day that attenuations as great as 3 dB were recorded.

Figure 2 gives a replot of the data recorded on May 14, 1970. The heavier curve shows the signal strength data with the dB scale to the left. The apparent sky temperature at 35 GHz is also shown, the inverted temperature scale being at the right. It is to be noted that there is reasonably good correlation between the two, the fact that the apparent sky temperature is noticeably less variable possibly being due to the averaging effe t of its 2° beamwidth. 15 GHz radar data were also obtained during this period. A plot of integrated returned power from the path exhibits general correlation with the data shown but the radar return was not corrected for range or attenuation effects so is not plotted here. Of specific note is the severe fade that occurred at the very beginning of the disturbed period. Range-gated radar data shows this was due to an isolated rain cell, with center portion no more than 1000 yds in depth, that passed across the path. In fact, the rain gauges, that were deployed up to 3000 ft. from the site, showed no tips until 2140 GMT.

Figure 3 shows data recorded on August 4, 1970. This was part of the aftermath of hurricane Celia that banged into Corpus Christi and passed inland across south Texas. The Weather Bureau had forecast rains of near 8 inches for Austin but only isolated, though intense, showers materialized. Again severe effects on the path were observed before any rain fell at the site. In fact, only a very modest shower ever reached the receiver site.

The next two figures show the scatter of data points for plots of sky temperature versus attenuation. Since the radiometer measurements were obtained at 35 GHz, the 15.3 GHz attenuation values were multiplied by 3, experience having shown this to be a reasonable value to assume for the ratio of the attenuation at these two frequencies. Also shown is the theoretical curve based on the usual assumptions of negligible scattering, side lobe and other effects and that a single value for rain temperature is appropriate.

Concluding Remarks

The conclusions to be drawn from the data obtained by The University of Texas reenforces those drawn by the other experimenters receiving the ATS-V signal. Specifically, the 15 GHz signal does occasionally get severely attenuated (in excess of 12 dB) by rain storms possessing isolated cells of unusually intense rain, these attenuations being observed even when the signal path passes through the storm cell at heights up to 4 or 5 kilometers. Rains which are relatively uniform over wide areas do not extend to such extreme heights and generally do not result in attenuations in excess of 3 dB.

The low-level, line-of-sight, 15 GHz link was not in operation during either the May 14 or August 4 rain storms so no comparison of the attenuation along this path and that from the satellite is yet possible. However, occasional pronounced fades are observed on the nearly horizontal path due to anomalous refractive-index structure when there is no hint of rain in the vicinity. Thus, if one wished to obtain statistics on expected earth-satellite attenuation by analyzing the ground-to-ground link data, the data for the no-rain periods would need to be discarded.

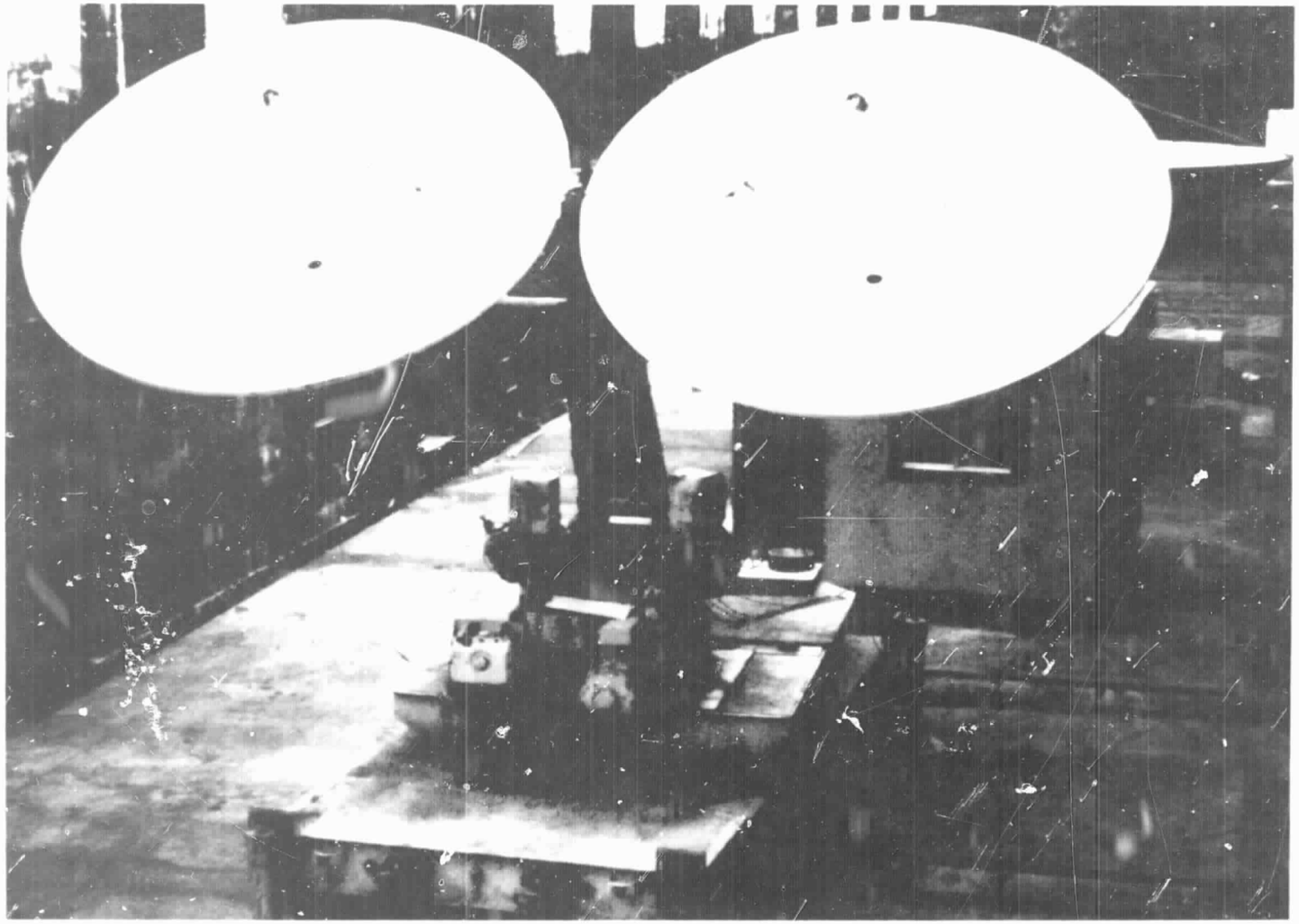

Figure 1. Dual-reflector antenna system

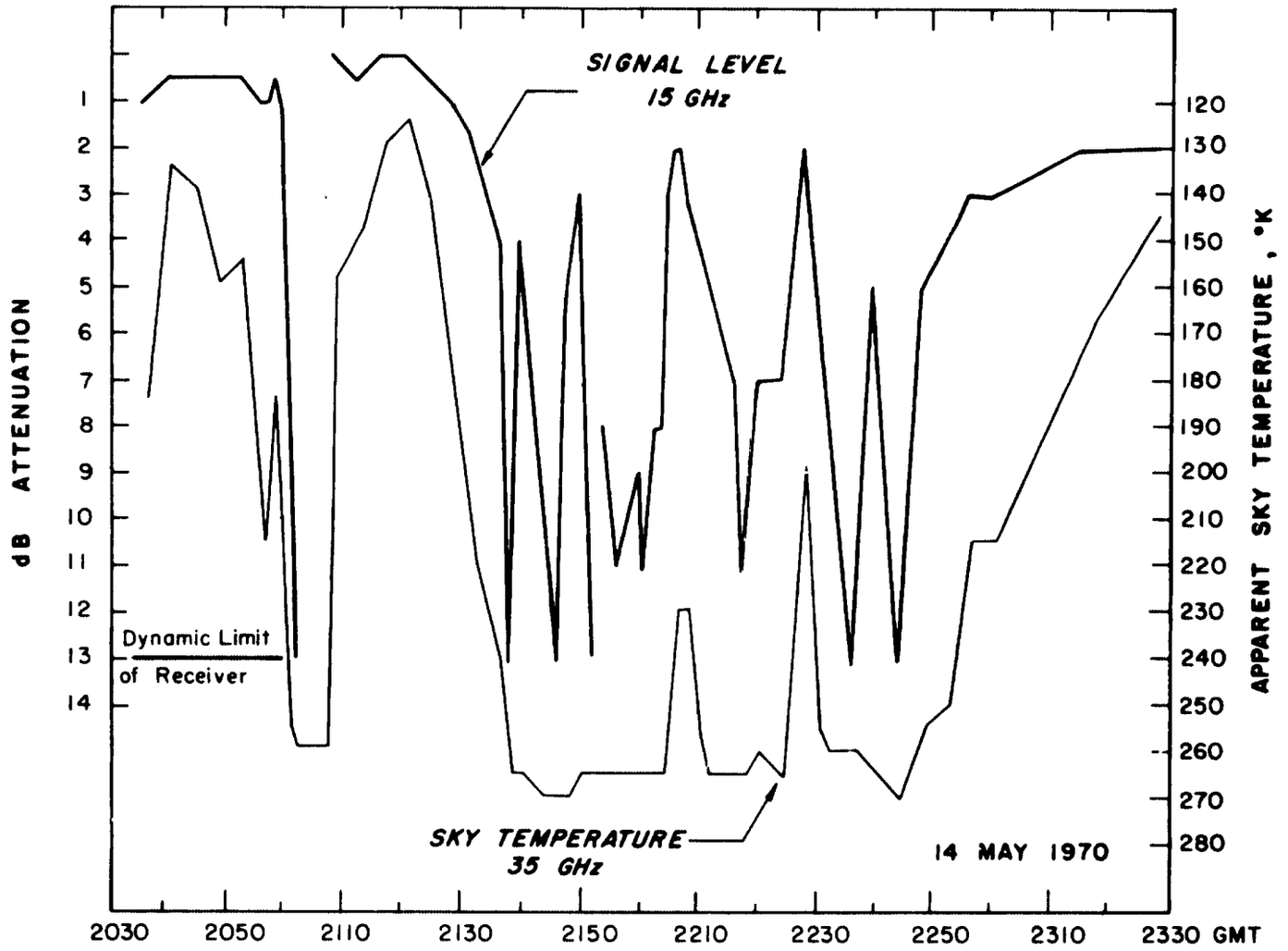

Figure 2. The University of Texas ATS-V signal and sky temperature vs. time

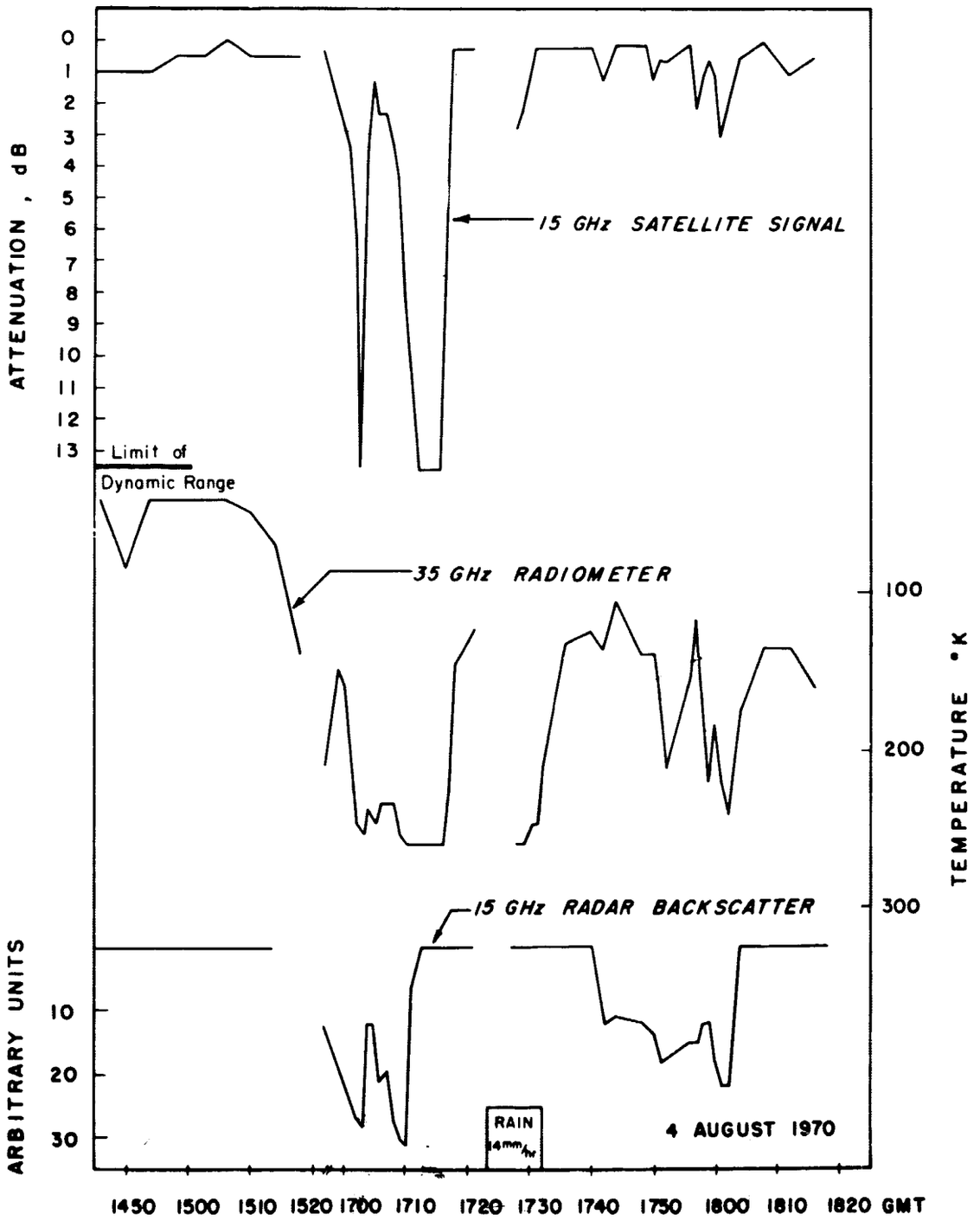

Figure 3. ATS-V signal and sky temperature vs. time

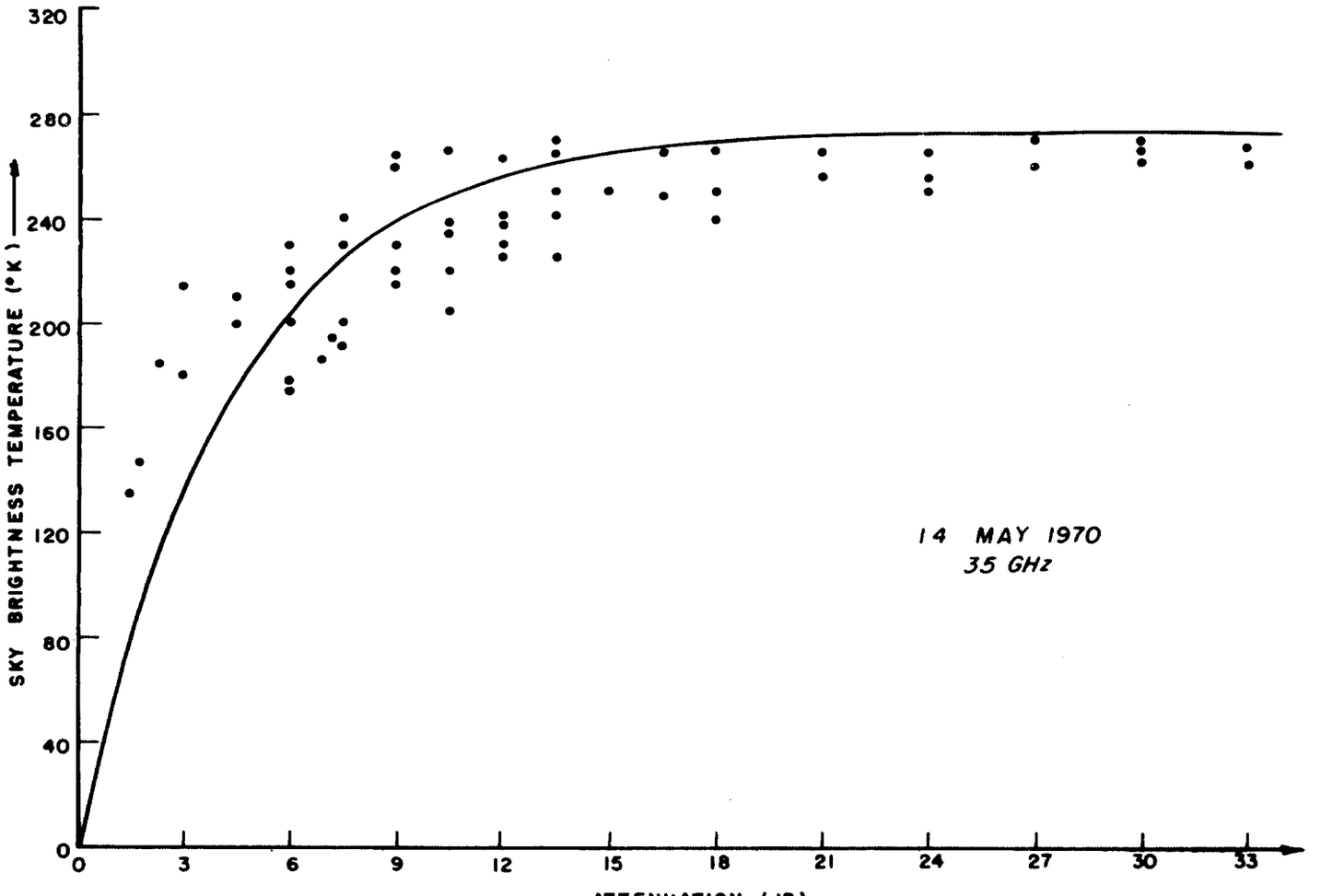

Figure 4. Sky brightness temperature vs. attenuation

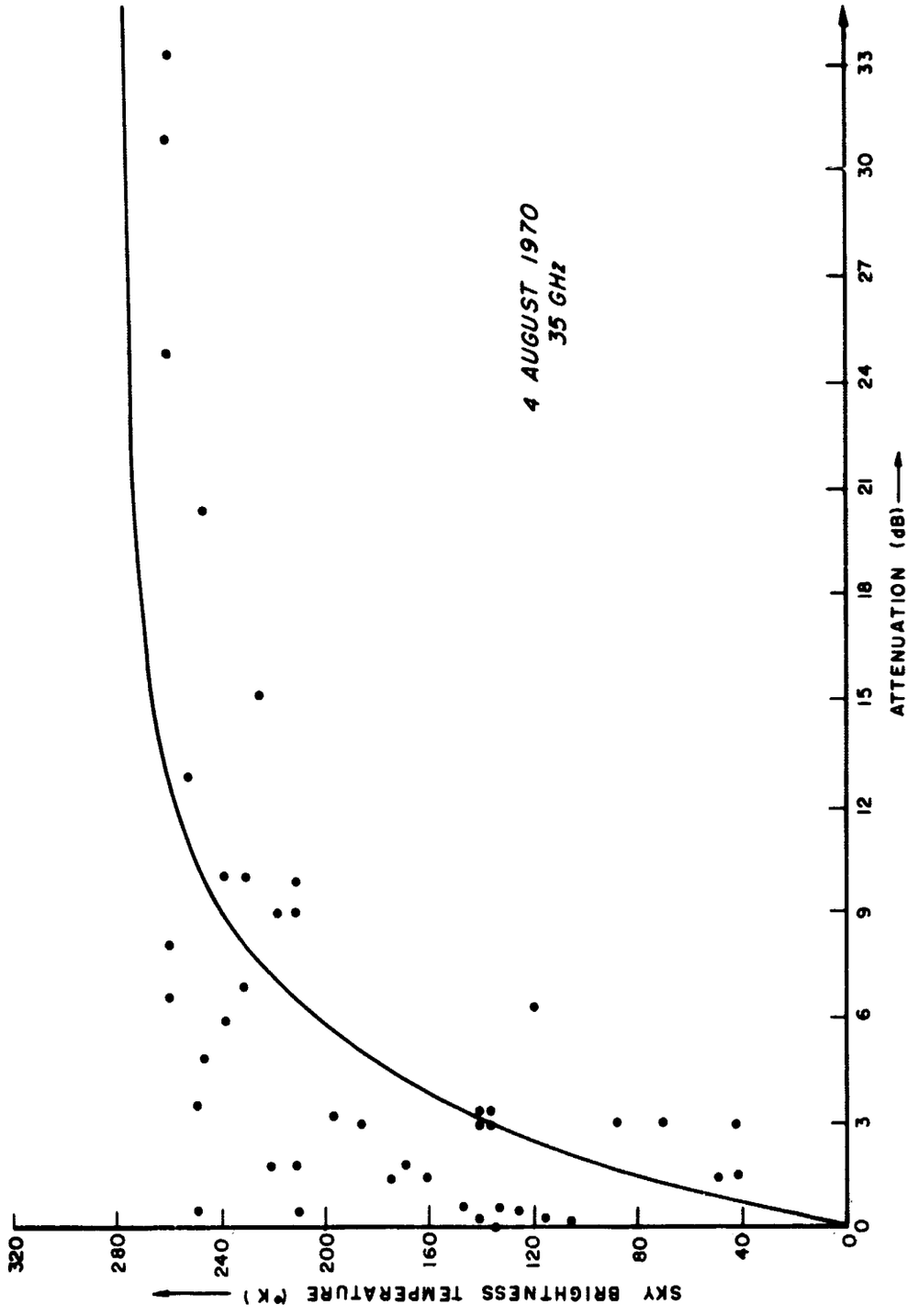

Figure 5. Sky brightness temperature vs. attenuation

APPENDIX A

DATA REPORTS ON THE ATS-5 MILLIMETER WAVE EXPERIMENT

Listed below are reports and presentations on the data results of the ATS-5 Millimeter Wave Experiment from the participating stations available through September, 1970.

I. NASA-ROSMAN, North Carolina

I-1. Ippolito, Louis J., ATS-V Millimeter Wave Experiment Data Report, October-December 1969, March 20, 1970, NASA/GSFC Report X-733-70-123.

I-2. Ippolito, Louis J., Millimeter Waves for Domestic Satellite Systems, presented at AIAA 3rd Communications Satellite Systems Conference, Los Angeles, Cal., April 7, 1970.

I-3. Ippolito, Louis J., Millimeter Waves for Space Communications, presented at the IEEE 1970 International Conference on Communications, San Francisco, Cal., June 9, 1970.

I-4. Ippolito, Louis J., Millimeter Wave Propagation Measurements from the Applications Technology Satellite (ATS-V), IEEE Trans. on Antennas and Propagation, July 1970, pg. 525-552.

I-5. Ippolito, L. J., Propagation Statistics for 15 and 32 GHz Earth-Space Transmissions from the Applications Technology Satellite (ATS-V), presented at the Fall 1970 USNC/URSI Meeting, Columbus, Ohio, Sept. 15, 1970.

I-6. Ippolito, L. J., Effects of Precipitation on 15.3 and 31.65 GHz Earth-Space Transmissions with the ATS-V Satellite, Proceedings of the IEEE, Special Issue on Space Communications, February, 1971.

II. University of Texas, Austin, Texas

II-1. Straiton, A. W., and Fannin, B. M., Comparison of 15 GHz Propagation Data from the ATS-V Satellite with Ground Based Radio and Meteorological Data, for presentation to the NATO-AGARD Electromagnetic Wave Propagation Panel, September 1970, Dusseldorf, Federal Republic of Germany.

II-2. Fannin, B. M., Straiton, A. W., Pate, D. N., Effects of Rain on Earth-Satellite Path at 15 GHz, presented at the Fall 1970 USNC/URSI Meeting, Columbus, Ohio, September 15, 1970.

III. Ohio State University, Columbus, Ohio

III-1. Bohley, P., Hodge, D. B., A Millimeter Wave Diversity Propagation Experiment, presented at the Fall 1970 USNC/URSI Meeting, Columbus, Ohio, September 15, 1970.

IV. COMSAT/INTELSAT, Clarksburg, Maryland

IV-1. Biuge, A., Levatich, J., and Robertson, E., COMSAT Laboratories, Clarksburg, Maryland, Propagation Experiment above 10 GHz for Application to Communications Satellite System, presented at the AIAA 3rd Communications Satellite Conference, April 8, 1970, Los Angeles, Calif.

IV-2. Buige, A., Craft, H. Jr., Levatich, J., Robertson, E., Millimeter Wave Propagation Measurements with ATS-5 at COMSAT Labs., presented at the Fall 1970 USNC/URSI Meeting, Columbus, Ohio, September 15, 1970.

V. Communications Research Centre, Ottawa, Canada

V-1. Strickland, J. I., Attenuation, Emission and Backscatter by Precipitation, presented at the Fall 1970 USNC/URSI Meeting, Columbus, Ohio, Sept. 15, 1970.

VI. Bell Telephone Labs, Holmdel, New Jersey

VI-1. Penzias, A. A., First Result from 15.3 GHz Earth-Space Propagation Study, The Bell System Technical Journal, July-August 1970, pg. 1242-1245.

VI-2. Penzias, A. A., Propagation Data from Crowford Hill, presented at the Fall 1970 USNC/URSI Meeting, Columbus, Ohio, September 15, 1970.

VII. NASA Participating Stations (Rosman, O.S.U., U. of T. and NELC)

VII-1. ATS Technical Data Report, Quarterly Input, July 6, 1970, prepared for NASA/GSFC by Westinghouse Electric Corp., Contract NAS 5-21129, Section 7.3.

VII-2. ATS Technical Data Report, Quarterly Input September 21, 1970, prepared for NASA/GSFC by Westinghouse Electric Corp., Contract NAS 5-21129, Section 7.3.

END

DATE

FILMED

MAR 5 1971